รายงานวิจัยฉบับสมบูรณ์

โครงการ: การศึกษาการยับยั้งปฏิกิริยาของเอนไซม์ไซโตโครมพี 450 ของยุงพาหะโดยสารสกัดจากพืช

โดย รองศาสตราจารย์ พรพิมล รงค์นพรัตน์

ภาควิชาชีวเคมี คณะวิทยาศาสตร์ มหาวิทยาลัยมหิดล

และคณะ

31 พฤษภาคม 2556

สัญญาเลขที่ BRG5380002

รายงานวิจัยฉบับสมบูรณ์

โครงการ: การศึกษาการยับยั้งปฏิกิริยาของเอนไซม์ไซโตโครมพี 450 ของยุงพาหะโดยสารสกัดจากพืช

คณะผู้วิจัย	สังกัด
รองศาสตราจารย์ พรพิมล รงค์นพรัตน์	ภาควิชาชีวเคมี คณะวิทยาศาสตร์ มหาวิทยาลัยมหิดล
ผู้ช่วยศาสตราจารย์เอกรัฐ ศรีสุข	ภาควิชาเคมี คณะวิทยาศาสตร์ มหาวิทยาลัยบูรพา
อาจารย์ทรงกลด สารภูษิต	ภาควิชาชีวเคมี คณะวิทยาศาสตร์ มหาวิทยาลัยบูรพา
ดร. นวลอนงค์ จิระกาญจนากิจ	สถาบันชีววิทยาศาสตร์โมเลกุล มหาวิทยาลัยมหิดล

สนับสนุนโดยสำนักกองทุนสนับสนุนการวิจัยและมหาวิทยาลัยมหิดล
(ความเห็นในรายงานนี้เป็นของผู้วิจัย
สกว.และมหาวิทยาลัยมหิดลไม่จำเป็นต้องเห็นด้วยเสมอไป)

ABSTRACT

Project Code: BRG5380002

Project Title: Study of inhibition activity by plant extract compounds against mosquito vector cytochrome P450 enzymes

Investigators: Pornpimol Rongnoparut, Ph.D. Principal investigator
Department of Biochemistry, Faculty of Science, Mahidol University
Email: pornpimol.ron@mahidol.ac.th
Ekaruth Srisook, Ph.D.
Department of Chemistry, Faculty of Science, Burapha University
Songklod Sarapusit, Ph.D.
Department of Biochemistry, Faculty of Science, Burapha University
Nuananong Jirakanjanakit, Ph.D.
Molecular Biosciences, Mahidol University

Project Period: 3 years (June 2010 –May 2013)

Abstract:

Insecticide resistance is a growing problem in the control of mosquito vectors. Increase in insecticide detoxification by heme-containing cytochrome P450 monooxygenases (P450s) in insects has been thought to promote resistance to insecticides, i.e. deltamethrin pyrethroid compound. Plant compounds that have both insecticidal activity and synergistic action with insecticides, due to inhibition of insect detoxification enzymes, could be a source for insect vector control. Previous investigations indicated CYP6AA3 and CYP6P7, isolated from deltamethrin-resistant *Anopheles minimus* malaria mosquito, play role in pyrethroid resistance. Enzymatic assays and 3-(4, 5-dimethylthiazol-2-y-l)-2, 5-diphenyltetrazolium bromide (MTT) cytotoxicity assays support the role of CYP6AA3 and CYP6P7 in metabolisms of pyrethroids. Thus the mosquito enzymes, CYP6AA3 and CYP6P7 could be a model for finding of natural compounds with inhibitory potential against pyrethroid detoxification enzymes. We report development of *in vitro* fluorescence-based and MTT cytotoxicity assays using P450-expressing *Spodoptera frugiperda* (Sf9) cells for rapid screening of inhibitory compounds and synergistic effect of inhibitors with pyrethroid insecticides, respectively. Since there has been no known crystal structure available for insect P450s, we have built homology model of CYP6AA3 in an attempt to increase our understanding of molecular mechanisms underlying binding site toward insecticides and inhibitors. We have screening 7 crude plant extracts including *Calotropis procera*, *Citrus reticulata*, *Stemona spp.*, *Curcuma longa* rhizomes and leaves, *Derris trifoliata*, *Andrographis paniculata* and *Rhinacanthus nasutus*. We found that *C. longa* rhizomes and leaves, *D. trifoliata*, *A. paniculata* and *R. nasutus* contained high inhibitory activities against both enzymes. Due to complexity of compounds in *C. longa*, we could not identify compounds that possess inhibition effects. Nevertheless at least three purified naphthoquinone esters isolated from *R. nasutus* and two polyoxygenated flavones specific to *Andrographis sp.* were found possessing inhibitory effect against mosquito P450 enzymes. These compounds comprising chromane ring acted synergistically with pyrethroid toxicity based on cell-based assays. Moreover preliminary results of larvicidal tests on *Aedes aegypti* mosquitoes of plant extracts were in agreement of inhibitory potency against mosquito detoxification P450 enzymes. Results obtained will thus be beneficial to implement effective resistance management of mosquito vector.

Keywords: cytochrome P450, pyrethroids, inhibition, rhinacanthins, flavones

บทคัดย่อ

รหัสโครงการ: BRG5380002

ชื่อโครงการ: การศึกษาการยับยั้งปฏิกิริยาของเอนไซม์ไซโตโครมพี 450 ของยุงพาหะโดยสารสกัดจากพืช

คณะผู้วิจัยและสังกัด

รองศาสตราจารย์ พรพิมล รงค์นพรัตน์ ภาควิชาชีวเคมี คณะวิทยาศาสตร์ มหาวิทยาลัยมหิดล
ผู้ช่วยศาสตราจารย์เอกรัฐ ศรีสุข ภาควิชาเคมี คณะวิทยาศาสตร์ มหาวิทยาลัยบูรพา
อาจารย์ทรงกลด สารภูษิต ภาควิชาชีวเคมี คณะวิทยาศาสตร์ มหาวิทยาลัยบูรพา
ดร นวลอนงค์ จิระกาญจนากิจ สถาบันชีววิทยาศาสตร์โมเลกุล มหาวิทยาลัยมหิดล

ระยะเวลาโครงการ: มิถุนายน 2553 – พฤษภาคม 2556

บทคัดย่อ

ปัจจุบันการดื้อยาฆ่าแมลงในยุงพาหะเป็นปัญหาสำคัญต่อการควบคุมประชากรของยุง เนื่องจากยุงมีการแสดงออกของเอนไซม์ Cytochrome P450 monooxygenase (P450s) ที่กำจัดยาฆ่าแมลงจากยุงเพิ่มขึ้น ส่งผลทำให้ยุงเกิดการดื้อต่อยาฆ่าแมลง เช่น สารเดลต้าเมทริน (deltamethrin) และ สารไพรีทรอยด์ (pyrethroid) การใช้สารประกอบจากพืชซึ่งมีฤทธิ์เป็นทั้งยาฆ่าแมลง และมีฤทธิ์ในการเพิ่มประสิทธิภาพแก่ยาฆ่าแมลง สามารถใช้ในการควบคุมยุงที่ดื้อต่อยาฆ่าแมลงโดยสารเหล่านี้จะไปยับยั้งการทำงานของเอนไซม์ที่เกี่ยวข้องกับการกำจัดสารพิษออกจากแมลง ดังนั้น สารประกอบเหล่านี้สามารถนำมาใช้ในการควบคุมยุงที่ดื้อต่อยาฆ่าแมลงได้ จากการศึกษาก่อนหน้านี้ระบุว่า เอนไซม์ CYP6AA3 และ CYP6P7 ซึ่งเป็นเอนไซม์ที่ได้จากยุงก้นปล่อง (*Anopheles minimus*) พาหะนำโรคมาลาเรียที่ดื้อต่อยาฆ่าแมลงเดลต้าเมทรินเกี่ยวข้องกับการดื้อยาฆ่าแมลงในยุง นอกจากนี้ยังมีข้อมูลที่ได้จากการศึกษากลไกการทำงานของเอนไซม์ทั้งสอง และผลจาก 3-(4, 5-dimethylthiazol-2-y-l)-2, 5-diphenyltetrazolium bromide (MTT) cytotoxicity assays สนับสนุนหน้าที่ของเอนไซม์ CYP6AA3 และ CYP6P7 ในการกำจัดไพรีทรอยด์ จากข้อมูลข้างต้น เอนไซม์ CYP6AA3 และ CYP6P7 จึงสามารถนำมาเป็นต้นแบบในการศึกษากลไกการกำจัดสารพิษ และค้นหาสารประกอบจากธรรมชาติที่มีฤทธิ์ในการยับยั้งการทำงานของเอนไซม์ที่เกี่ยวข้องกับการกำจัดไพรีทรอยด์ เทคนิคในการค้นหาสารประกอบจากธรรมชาติที่มีฤทธิ์ในการยับยั้งการทำงานของเอนไซม์ ได้ถูกพัฒนาขึ้น 2 วิธีคือใช้เทคนิค in vitro fluorescence-based ซึ่งเป็นวิธีที่สะดวก รวดเร็ว และเทคนิคในการศึกษาการเสริมฤทธิ์ของตัวยับยั้งร่วมกับไพรีทรอยด์ ด้วยเทคนิค MTT cytotoxicity assay โดยใช้เซลล์ *Spodoptera frugiperda* (Sf9) ซึ่งเป็นเซลล์ของแมลงที่มีการแสดงออกของเอนไซม์ P450s เป็นต้นแบบในการศึกษา เนื่องจากไม่มีข้อมูลเกี่ยวกับโครงสร้างของเอนไซม์ P450s ของแมลง ดังนั้นแบบจำลองของ CYP6AA3 และ CYP6P7 จึงได้ถูกสร้างขึ้น เพื่อศึกษากลไกการทำงานของเอนไซม์ในการกำจัดยาฆ่าแมลง ตลอดจนศึกษากลไกการยับยั้งการทำงานของตัวยับยั้งต่อเอนไซม์ นอกจากนี้ การศึกษานี้ได้ทำการค้นหาสารประกอบซึ่งมีฤทธิ์ในการยับยั้งการทำงานของทั้ง 2 เอนไซม์จากสารสกัดของพืช 7 ชนิด ได้แก่ ต้นรัก (*Calotropis procera*), ส้มโชกุน (*Citrus reticulate*), หนอนตายอยาก (*Stemona spp.*), ขมิ้นชัน (*Curcuma longa*) ในส่วนของเหง้า และใบ, ถอบแถบ (*Derris trifoliata*), ฟ้าทะลายโจร (*Andrographis paniculata*) และ ทองพันชั่ง (*Rhinacanthus nasutus*) จากการศึกษาพบว่า สารสกัดจากเหง้าและใบของขมิ้นชัน, ถอบแถบ, ฟ้าทะลายโจร และทองพันชั่ง ประกอบไปด้วยสารประกอบที่มีฤทธิ์ในการยับยั้งการทำงานของทั้งสองเอนไซม์ ผลจากการศึกษานี้ทำให้ได้สารบริสุทธิ์ที่มีฤทธิ์ในการยับยั้งการทำงานของเอนไซม์ P450s ในยุงได้สารอย่างน้อย 3 ชนิด ได้แก่ naphthoquinone esters ซึ่งแยกได้จากทองพันชั่ง และpolyoxygenated flavones ซึ่งเป็นสารประกอบที่มีความจำเพาะกับพืชตระกูล *Andrographis* สารเหล่านี้ประกอบด้วย chromane ring ซึ่งทำหน้าที่ในการเสริมฤทธิ์ให้กับไพรีทรอยด์ เนื่องจากขมิ้นชันประกอบด้วยสารประกอบที่ซับซ้อน จึงไม่สามารถระบุโครงสร้างของสารประกอบที่มีฤทธิ์ในการยับยั้งการทำงานของเอนไซม์ทั้งสองได้ นอกจากนี้ ผลการศึกษาเบื้องต้นเกี่ยวกับประสิทธิภาพในการกำจัดลูกน้ำของยุงลาย (*Aedes aegypti*) ด้วยสารสกัดจากพืชสอดคล้องกับประสิทธิภาพในการยับยั้งการกำจัดสารพิษของเอนไซม์ P450s ซึ่งข้อมูลที่ได้จากการศึกษานี้จะเป็นประโยชน์ต่อการนำไปใช้ในการควบคุมยุงที่ดื้อต่อยาฆ่าแมลงต่อไป

คำหลัก *ไซโตโครมพี* 450 *ไพรีทรอยด์ การยับยั้งเอนไซม์* ไรน่าแคนทิน ฟลาโวน

Executive Summary

Insecticide resistance is a growing problem in the control of mosquito vectors. Increase in insecticide metabolisms by heme-containing cytochrome P450 monooxygenases (P450s) in insects has been thought to promote resistance to insecticides, i.e. deltamethrin pyrethroid compound. While medicine and effective vaccine are not yet available, a method to control vector-borne diseases including malaria, dengue fever and recently the re-emerging Chikungunya infection, has been using space-spraying with synthetic chemical insecticides (such as organophosphates and pyrethroids) to control mosquito vectors. Long-term insecticide use has caused insecticide resistance in mosquitoes. Plant compounds that have both insecticidal activity and synergistic action with insecticides, due to inhibition of insect detoxification enzymes, could be a source for resistance management of mosquito vector control.

Previous investigations indicated CYP6AA3 and CYP6P7, isolated from deltamethrin-resistant *Anopheles minimus* malaria mosquito, play role in pyrethroid resistance. Enzymatic assays, homology modeling of enzymes, and 3-(4, 5-dimethylthiazol-2-y-l)-2, 5-diphenyltetrazolium bromide (MTT) cytotoxicity assays support the role of CYP6AA3 and CYP6P7 in metabolisms of pyrethroids. Thus the objective of this study is to investigate the inhibitory effect, mode of inhibition, and structure of plant compounds against mosquito P450s activities using *An. minimus* CYP6AA3 and CYP6P7 as model enzyme. In this study we developed *in vitro* fluorescence-based and MTT cytotoxicity assays using P450-expressing *Spodoptera frugiperda* (Sf9) cells for rapid screening of inhibitory compounds and synergistic effect of inhibitors with pyrethroid insecticides, respectively. Since there has been no known crystal structure available for insect P450s, we have built homology model of CYP6AA3 to increase our understanding of molecular mechanisms underlying binding site toward insecticides and inhibitors. Plants that possess insecticidal/mosquitocidal activity are chosen and used in this study. Upon accomplishment of screening 7 crude plant extracts including *Calotropis procera*, *Citrus reticulata*, *Stemona spp.*, *Curcuma longa* rhizomes and leaves, *Derris trifoliata*, *Andrographis paniculata* and *Rhinacanthus nasutus*, we found that *C. longa* rhizomes and leaves, *D. trifoliata*, *A. paniculata* and *R. nasutus* contained high inhibitory activities (LD_{50} value within 20 μg/ml range) against both enzymes. Further successful purification of plant compounds revealed that at least three purified naphthoquinone esters of *R. nasutus* and two polyoxygenated flavone compounds specific to *Andrographolide sp.* were found inhibitory effect against both mosquito P450 enzymes and act synergistically with pyrethroid toxicity based on cell-based assays. These compounds shared chromane ring with hydrophobic nature that could efficiently inhibited mosquito P450 enzymes. Results of *Ae. aegypti* larvicidal tests with plant extracts were in agreement with inhibitory effects on mosquito enzymes. Knowledge gained on these plant compounds and structure, and on inhibition against P450 mosquito enzyme will thus be beneficial to implement effective control and resistance management of mosquito vectors.

TABLE OF CONTENT

LIST OF TABLES

LIST OF FIGURES

Figures **Page**

INTRODUCTION

Mosquito-borne diseases such as dengue fever and recently the re-emerged Chikungunya infection, and malaria caused by *Aedes aegypti* and *Anopheles sp.* mosquito vectors remain important diseases in the tropical countries including Thailand. For instance 50 to 100 million dengue infections are reported, while medicine and efficient vaccine are not yet available (WHO, 2006). In Thailand, 40% increased dengue infections were found from 2006 to 2007, and an additional 16% increase found from 2007 to 2008 (WHO, 2008). A strategy is to control the mosquito vectors by use of synthetic chemical insecticides. However, insecticide resistance to chemical insecticides is on the rise. One of the resistance mechanisms has been suggested to be due to the insects' increased metabolism of insecticides through bio-transformation by detoxification enzymes (Marcombe et al, 2009). While organophosphate resistance has been shown linked to elevated nonspecific esterases and P450s activities (Feyereisen, 1999), pyrethroid resistance is suggested to be primarily conferred by elevated cytochrome P450 enzymes (P450s) activities (Feyereisen, 1999). A strategy of resistant management control could be the targeting on resistance mechanism to overcoming resistance first, followed by use of existing insecticides. The compound that can inhibit P450s activities will be of interest for use as synergist of pyrethroid insecticide which has been widely used via household spraying in resistance management. The synergist such as piperonyl butoxide (PBO), P450 inhibitor, has been tested as mixture with pyrethroids and showed synergistic action against *Ae. aegypti* (Fakoorziba et al, 2009; Kumar et al, 2002; Vijayan et al, 2007). But toxicity test has shown that it is acutely toxic to rodents (Piyachaturawat et al. 1983, Scott 1996, Daware et al. 2000, Bhardwaj et al. 2002). The synergist that also contains insecticidal activity, particularly with different mode of action from insecticide could be used more effectively in dealing with mosquito resistant populations and at the same time could kill mosquitoes. Botanical compounds have been discovered to comprise insecticidal activity, but the kinetics and mechanism of inhibition on mosquito detoxifying enzymes have not been comprehensively investigated. Nowadays, numerous plants have been reported that possess insecticidal activities (Kamaraj et al 2009; Kuppusamy and Murugan 2010; Govindarajan and Sivakumar 2012; Komalamisra et al 2005; Rongsriyam et al, 2006; Shaalan et al, 2005). Plants commonly found in Thailand and comprise insecticidal/mosquitocidal activities include *Calotropis procera* (Rak), *Citrus reticulata* (Som Keaw Wan), *Curcuma longa* (Khamin Chan), *Derris trifoliata* (Tao Thob Thab),

Rhinacanthus nasutus (Thong Phan Chang), *Andrographis paniculata* (Phah Talai Jone) and *Stemona sp.* (Non Tai Yak) have shown insecticide activities with high potency.

In this study we used the CYP6AA3 and CYP6P7 isolated from pyrethroid-resistant *Anopheles minimus* mosquito strain that have been shown ability to metabolize deltamethrin (Boonseupsakul et al, 2008; Kaewpa et al, 2007) as model mosquito P450 enzyme in this study. The cytochrome P450 monooxygenases (P450s) constitute a superfamily of membrane-bound heme-containing enzymes that are involved in metabolisms of endogenous compounds such as pheromones and exogenous compounds such as insecticides. This study is to test botanical compounds, found distributed in Thailand and have shown insecticidal activity that inhibit CYP6AA3 and CYP6P7 P450 activity. Homology models of both CYP6AA3 and CYP6P7 were to be constructed to increase an understanding of the pyrethroid metabolisms and inhibition. In order to increase the effectiveness of synergism, the inhibitory mechanism of compounds that inhibit P450s in mechanism-based manner (irreversible inhibition) is essential. Mechanism-based P450 inactivation usually involves covalent modification of heme and/or the active site amino acid residue of enzyme, thus inhibiting the enzyme irreversibly and rendering the enzyme inactive. For P450 enzymes to be active after being inhibited, P450 enzymes must be replaced by newly synthesized protein and thus making mechanism-based inhibition more efficient than reversible inhibition (Kalgukar et al, 2007). Thus this study also determined mode of inhibition of inhibitory compounds obtained. Knowledge of inhibition activity of different compound structure on the two CYP6s will lead to understanding of P450s that involve in pyrethroid metabolism. Information gained from this study can be applied in vector resistant management program and vector control in Thailand. Since most plant extracts are degradable, thus use of botanical insecticide as insecticide synergist may reduce use of chemical insecticides without introduction of new risk to human health. Eventually, botanical blends that contain both synergistic action and different modes of insecticidal action could be used safely for mosquito control program in the future.

The goal of this project is to obtain plant compounds that has inhibitory effects against CYP6AA3 and CYP6P7 and could be used as insecticide synergist in control of mosquito vectors using *Spodoptera frugiperda* (Sf9) insect cell model. The objectives of this study are:

1. Development of system to determine inhibition of test compounds against CYP6AA3 and CYP6P7 using *in vitro* fluorescence-based reconstitution enzymatic assays
2. Development of cell-based inhibition assay to determine synergism of plant compounds with insecticide toxicity using Sf9 insect cell model
3. Construction of CYP6AA3 and CYP6P7 homology models
4. Determination of plant extracts *in vitro* that have inhibitory effects on CYP6AA3 and CYP6P7 enzymes
5. Determination of the extracts that show inhibition effect on CYP6AA3 and CYP6P7
6. Purification and determination of the chemical structure of the compounds with inhibitory effect

MATERIALS AND METHODS

1. Chemicals

Benzyloxyresorufin, cypermethrin, leupeptin, nicotinamide adenosine diphosphate reduced form (NADPH), 1,2-dilauroyl-rac-glycero-3-phosphocholine (DLPC), phenylmethylsulfonyl fluoride (PMSF), dimethyl sulfoxide (DMSO), α-naphthoflavone, piperonyl butoxide (PBO) were purchased from Sigma-Aldrich (St. Louis, MO), and 3-(4, 5-dimethylthiazol-2-y-l)-2, 5-diphenyltetrazolium bromide (MTT) from USB (Cleveland, OH). Analytical grade hexane, ethyl acetate (EtOAc), ethanol, methanol, diethyl ether and high performance liquid chromatography (HPLC) grade acetonitrile were supplied by RCI Labscan (Bangkok, Thailand).The *Spodoptera frugiperda* (Sf9) insect cell line and SF-900 II SFM culture media were provided by Invitrogen (Carlsbad, CA).

2. Expression of Anopheles minimus CYP6AA3, CYP6P7 and NADPH-dependent cytochrome P450 reductase (CPR) enzyme

Expression of CYP6AA3 and CYP6P7 were carried out using baculovirus-mediated insect cell expression system in Sf9 cells as previously described (Kaewpa et al., 2007). The recombinant P450-baculovirus was produced by insertion of either CYP6AA3 or CYP6P7 cDNA into pBacPAK8 transfer plasmid vector (BD Biosciences, Palo Alto, CA), and co-transfected with a linearized BacPAK6 viral DNA into Sf9 cells. The resulting recombinant virus was used for expression of enzymes. To express CYP6AA3 and CYP6P7 enzymes, Sf9 cells were infected with recombinant P450-baculovirus containing either CYP6AA3 or CYP6P7 at multiplicities of infection (MOI) of 3 and cells were cultured in SF900-II medium (Invitrogen) at 28°C. Heme-albumin was added at 24 h post-infection and cells were harvested at 70-80 h post-infection. Cells were resuspended in sodium phosphate buffer pH 7.2 containing 1 mM EDTA, 0.5 mM PMSF, 5 μg/ml leupeptin, 0.1 mM DTT, and 20% glycerol, and subjected to microsome preparation using differential centrifugation as described (Boonseupsakul et al., 2008). The microsomal pellet was resuspended in buffer containing 150 mM KCl and 1% Triton X-100, prior to centrifugation at 10,000 x g for 10 min. The solubilized microsomal proteins from membrane fraction was collected and kept at -80°C.

For a P450 enzyme to function, it requires the membrane-bound NADPH-dependent cytochrome P450 reductase (CPR) enzyme as redox partner by passing a pair of electrons

from NADPH through CPR to P450. Thus in the P450 enzymatic assays *in vitro*, assay system comprise a reconstitution assay reaction comprising P450 enzyme and CPR, and DLPC is served as lipid support. The double mutant membrane-bound CPR enzyme (L86F/L219F-fnAnCPR) that could efficiently increased CYP6AA3-mediated enzymatic activity (Sarapusit et al., 2010) was used for P450 reconstitution enzyme assays in this study. The double mutant membrane-bound CPR was expressed in *Escherichia coli* XL1-blue cells under the same condition as the wild-type enzyme described by Kaewpa et al. (2007). The expression of enzyme was induced by addition of IPTG, and the cultured were grown for 64 h at 28°C, 160 rpm. Cells were harvested and resuspended in 50 mM sodium phosphate buffer pH 8.0 containing 300 mM NaCl, 0.2 mM PMSF and 20% glycerol. Cells were disrupted by sonication, before subjected to centrifugation at 10,000 x g for 30 min and 100,000 ×g for 90 min to separate membrane fraction. The pellet of membrane protein was resuspended in buffer containing 0.5% CHAPS and subjected to purification using Ni^{2+}-NTA metal affinity chromatography. The fraction containing purified protein with 6xHis-tagged were pooled, dialyzed, and concentrated with Centriprep YM-30 centrifugal filter devices (Millipore, Billerica, MA) for further use in the reconstitution assay with P450 enzyme.

To improve electron transfer from CPR to cytochrome P450 enzyme, we recently have tested the use of rat CPR in place of mosquito CPR in the reconstitution reaction. Mutations of the *An. minimus* CPR enzyme have also been constructed during the granting period and tested for reconstitution enzymatic assays of mosquito CYP6AA3 enzyme. The results revealed that the rat CPR enzyme could more effectively transfer electron to CYP6AA3 and CYP6P7 enzymes than any *An. minimus* CPR mutant constructs. The results have also been published (Sarapusit et al, 2013 in **Appendix**). We thus have used rat CPR in the screening of plant extracts.

3. Construction of CYP6AA3 homology model

Amino acid sequences of CYP6AA3 (GenBank ID: AAN05727.1), CYP6P7 (GenBank: AAR88141.1) were aligned against protein structures deposited in Brookhaven Protein Data Bank (PDB) [Berman et al, 2000] using PSI-BLAST. Crystal structures of ligand-free CYP3A4 (1TQN), CYP2C8 (1PQ2), and CYP2C9 (1OG2) were templates and their sequences were top-ranked identical to target P450. Comparative modeling of the three enzymes was performed using restrained-based approach implemented in MODELLER9v6 (Sali and Blundell, 1993). Multiple amino acid sequence alignment of template structures

was performed using SALIGN module in MODELLER9v6, and subsequently aligned individually with target enzyme. Heme coordinate of the constructed model was obtained from CYP3A4 (1TQN) and positioned in target as in 1TQN template. The resulting three-dimensional models of CYP6AA3 and CYP6P7 were sorted according to scores of discrete optimized protein energy scoring function (Shen and Sali, 2006). The knowledge-based conditional probabilities for the residue specific all-atom probability discriminatory function (RAPDF) in RAMP suite was used to discriminate native structure from incorrectly-folded structures (Samudrala and Moult, 1998). The refined model was determined their distribution of phi and psi angles using ProSAII (Sippl, 1993; Wiederstein and Sippl, 2007) and Procheck (Laskowski et al, 1993).

4. Plant materials and preparation of crude plant extracts

Derris trifoliata (leaves & stems), *Rhinacanthus nasutus* (leaves & stems), *Curcuma longa* (rhizomes), *Citrus reticulate* (seeds), *Andrographis paniculata* (leaves & stems), and *Stemona spp* (roots) were purchased from traditional medicine market (Bangkok, Thailand). *Curcuma longa* leaves were collected from Samutsakorn province and leaves of *Calotropis procera* were collected from Nongkhai province, Thailand. Plants were extracted as previously described (Komalamisra et al., 2005) with some modification. Briefly dried plant parts were cut into small pieces and ground in homogenizer. Ground material from each plant was macerated in 900 ml of 95% ethanol at room temperature. The ethanol extract of each plant was filtered through filter paper (Whatman no.1), and filtrate was extracted twice using the same procedure. All filtrates from extractions were combined and solvent removed by evaporation at 45°C under reduced pressure using rotary evaporator. Crude ethanol extracts and aliquots of 200 mg/ml stock solution of crude ethanol extract of each plant (dissolved in DMSO) were kept at -20°C until used.

5. Purification of plant compounds.

***R. nasutus* extract:** The dry *R. nasutus* material was homogenized, macerated in 95% ethanol to obtain ethanol extract, and further partitioned with *n*-hexane and ethyl acetate (EtOAc), yielding *n*-hexane, EtOAc and aqueous extracts. Stepwise gradient elution of each *n*-hexane extract was conducted in a chromatography column containing silica gel using a *n*-hexane/EtOAc/ methanol solvent system (see Pethuan et al 2012 in **Appendix** for yields). Fractions that showed potent inhibition activities were subjected to analysis by high

performance liquid chromatography (HPLC) and thin layer chromatography (TLC) as described (Pethuan et al 2012). The three purified compounds were subjected to NMR analyses and their chemical structures elucidated by comparing ^{1}H- and ^{13}C-NMR spectral data with those previously reported (Sendl et al. 1996, Wu et al. 1998).

***A. paniculata* extract:** Extraction was preformed according to Rao et al (2004) with modification. Briefly, air-dried parts of *A. paniculata* were ground, macerated in ethanol at room temperature, filtered, and fractionated with *n*-hexane and EtOAc. Among these fractions, only *n*-hexane contained potent inhibition activity against CYP6AA3 and CYP6P7. The residue from chloroform was separated by silica gel column chromatography using *n*-hexane-EtOAc stepwise gradient elution to give five fractions 1-5. Fraction 1: *n*-hexane, Fraction 2: *n*-hexane-EtOAc (8.5:1.5), Fraction 3: *n*-hexane-EtOAc (7:3), Fraction 4: *n*-hexane-EtOAc (1:1), Fraction 5: EtOAc. Among these, fraction 4 showed potent inhibition and was subjected to TLC using *n*-hexane-diethyl ether (4:6, vol:vol) as mobile phase.

The sub-fractions from TLC which showed inhibitory effect on P450 enzymes were subjected to analysis by HPLC. HPLC gradient was initiated from 50% acetonitrile (ACN) in water (vol:vol) to 60% ACN over 5 min, 60% ACN was held for 10 min, followed by 100% ACN for 10 min before returning to 50% ACN over 10 min and final equilibration with 50% ACN for 30 min with flow rate of 1.5 ml per min. Two purified compounds, namely AP-hex 1 and AP-hex 2, were obtained and are in the process of chemical structural determination by NMR analyses. However preliminary identification by electrospray ionization source equipped with tandem mass spectrometer (ESI-MS/MS) suggested that both compounds are polyoxygenated and methoxylated flavones based on patterns of ionized mass fragmentation previously described (Kuroyanagi et al, 1987; Jayakrishna et al, 2001; Rao et al, 2004.)

***D. trifoliata* extract:** The dry *D. trifoliata* material was homogenized, macerated in 95% ethanol to obtain ethanol extract, and further partitioned with *n*-hexane and EtOAc, yielding *n*-hexane, EtOAc and aqueous extracts. Purification of compounds from *n*-hexane and EtOAc fractions through silica gel column chromatography, TLC and HPLC followed conditions described with *R. nasutus* extract.

6. Fluorescence-based inhibition assay of CYP6AA3 and CYP6P7

Fluorescence-based assay was first developed by screening for fluorescent compounds that act as substrate of both enzymes. Fluorescent substrates dissolved in dimethylsulfoxide were benzyloxyresorufin, ethoxyresorufin, methoxyresorufin, and penthoxyresorufin. The assay was performed in 50 mM Tris-HCl buffer pH 7.5, in a total volume of 500 µl. The reaction was initiated by addition of NADPH to a final concentration of 1 mM. Resorufin production was measured for 5 min at λ_{ex} = 530 and λ_{em} = 590 nm using RF-5301 PC spectrofluoro-photometer (Shimadzu, Kyoto, Japan). The amount of resorufin product was calculated referring to the resorufin standard curve. Results revealed that benzyloxyresorufin could best be used as substrate probe for inhibition assays.

Inhibitory effect of crude plant extracts against the metabolic activities of CYP6AA3 and CYP6P7 was determined by performing *in vitro* reconstitution assays using benzyloxyresorufin as substrate probe. The membrane fraction containing either CYP6AA3 or CYP6P7 were incubated with the purified CPR, benzyloxyresorufin substrate at the concentration approximately K_m value (2 µM for CYP6AA3 and 0.5 µM for CYP6P7), and different concentrations of plant extracts/compounds dissolved in DMSO (1% final concentration). The IC_{50} values of plant extracts/fractions/compounds were determined graphically by nonlinear regression analysis of logarithm of test compound concentrations against the relative residual enzyme activity using GraphPad Prism 5 (GraphPad Co. Ltd., USA). Enzyme activities in the presence of test compounds were compared to reaction with DMSO as vehicle control. When tested with silica and HPLC eluted fractions, inhibition of CYP6AA3 and CYP6P7 was performed with a final concentration of 10 µg/ml of each fraction.

7. NADPH and time-dependent inhibition assay

NADPH-dependent inhibition of P450 activity was investigated to preliminarily determine whether plant extracts exhibit mechanism-based inhibition characteristic. Assays were performed by preincubating various concentrations of each plant extract/compound with enzyme in the presence of NADPH for 30 minute, prior to addition of benzyloxyresorufin substrate. After pre-incubation, aliquots of the incubated mixture were withdrawn and diluted 5-fold with fresh reaction mixture followed by determination of enzymatic activities. IC_{50} values of each extract/compound were calculated and were compared between reactions pre-incubating with and without NADPH. An indication of

mechanism-based inhibition is the IC_{50} shift to lower range in the assay pre-incubation with NADPH (Fowler and Zhang, 2008).

Time-dependent inhibition of P450 activity was investigated to determine mechanism-based inhibition by plant extracts/compounds. Assays were performed by pre-incubation of various concentrations of each extract with P450 enzyme for 20, 40, 60 min in the presence of NADPH or absence of NADPH prior to addition of benzyloxyresorufin substrate, and IC_{50} values of extracts were calculated. The indication of mechanism-based inhibition is the IC_{50} shift to lower range in pre-incubation with inhibitor in the presence of NADPH compared with co-incubation assay (Fowler and Zhang 2008).

8. Inhibition of NADPH-dependent Cytochrome P450 reductase (CPR) enzymatic activity by plant extract

Inhibition effect of plant extracts against CPR activity was assayed by determining cytochrome *c* reduction activity of CPR in the presence of different concentrations of plant extracts. The reaction was performed as previously described (Sarapusit et al., 2010). The reaction was initiated by addition of saturated amount of NADPH and cytochrome c. The NADPH-dependent cytochrome c reduction was measured as a change in absorbance at 550 nm (extinction coefficient of 21 $mM^{-1}cm^{-1}$) using HP8453 UV-visible spectrophotometer (Agilent Technologies, Palo Alto, CA). Cytochrome c reduction rate of the reaction treated with vehicle control (DMSO) was arbitrary set as 100% activity. CPR activities in the presence of plant crude extracts were expressed as relative percent activity of vehicle control reaction.

9. NADPH oxidation

Several 1,4-naphthoquinone derivatives are known to stimulate oxidation of NADPH as 1,4-naphthoquinones undergo reduction by CPR, possibly forming superoxide radical (Kumagai et al 2012), and could modulate mosquito CYP6AA3 and CYP6P7. To see this effect, test of reduction of rhinacanthins which are 1,4-naphthoquinone esters by CPR was performed in the presence of CPR and was measured by the decrease in absorbance at 340 nm, based on oxidation of NADPH, using an extinction coefficient of 6.26 $mM^{-1}cm^{-1}$ as described (Kostrzewa-Nowak et al 2012).

10. Determination of Inhibition Kinetics

Apparent K_i values and modes of inhibition were determined from enzymatic assays with various concentrations of benzyloxyresorufin substrate (0.75, 1.5, 3, or 4.5 μM for CYP6AA3 and 0.25, 0.5, 1, or 2 μM for CYP6P7) conducted with different concentrations of purified plant compounds. Mode of inhibition on each enzyme activity of each purified compound was estimated graphically from a double reciprocal plot of velocity against substrate concentrations (Lineweaver-Burk plot), K_i values were calculated via second plots of the slopes from Lineweaver-Burk plots versus inhibitor concentrations.

The kinetics constant for mechanism-based inhibition of plant compounds was determined from time-dependent assay by varying compound concentrations and pre-incubation times. A logarithm of the percentage of the remaining activity was plotted against pre-incubation time and the slope of the lines was obtained from linear regression analysis. The apparent inactivation rate constants (k_{obs}) were taken from the slope of the line ($-k_{obs}$). The maximal inactivation rate constant (k_{inact}) and the inhibitor concentration required for half-maximal rate of inactivation (K_I) were calculated from double reciprocal plots of k_{obs} versus inhibitor concentrations by linear regression analysis using GraphPad Prism 5.

11. Evaluation of cytotoxicity of plant extracts/compounds by MTT assays and cell-based inhibitory effects of plant extract against P450s

This assay was developed to test whether pyrethroid cytotoxicity could be determined and whether cells expressing pyrethroid metabolizing P450s could protect insect cells from pyrethroid toxicity. CYP6P7- or CYP6AA3-expressing cells and control Sf9 cells were used and cell-based inhibition assays were performed as reported (Duangkaew et al 2012b and Pethuan et al 2012 in **Appendix**). The 50% lethal concentration (LC_{50}) was evaluated from the plot of percentage of cell viability against different concentrations of each pyrethroid. To determine inhibitory activity of plant extracts/compounds, MTT assays were performed with cypermethrin pyrethroid insecticide in the presence of each plant extract. Control Sf9 cells, CYP6AA3-, and CYP6P7-expressing cells were treated with selected doses of each extract/compound followed by treatment with various concentrations of cypermethrin (12.5-500 μM). Concentration of extracts causing 10-20 percent mortality in Sf9 control cells was used. Cytotoxicity of cypermethrin was determined by MTT assay and LC_{50} values compared between cells treated with cypermethrin alone and presence of plant extract, after normalization with cells treated with DMSO vehicle. Data was statistically

analyzed using a one-way analysis of variance (ANOVA) with Tukey's multiple comparison tests. Results with $P \leq 0.05$ were considered to be significantly different.

12. Larvicidal bioassay

Larvicidal activity of plant crude extracts was evaluated using batches of 20 third instar lavae in 100 ml water. Five replicates were set up for each concentration. Mortality rate was obtained after overnight exposure at room temperature LC_{50} values were obtained using log-probit software.

RESULTS AND DISCUSSION

1. Development of inhibition assays against CYP6AA3 and CYP6P7

CYP6AA3 and CYP6P7 cytochrome P450 proteins and NADPH-cytochrome P450 reductase (CPR), the P450 redox partner were expressed and used in enzymatic assays. Fluorescence-based enzymatic activities of both CYP6AA3 and CYP6P7 were developed for ease of further inhibition study using fluorescence substrate rather than pyrethroid substrate that require HPLC analysis. We tested the assay system to determine mode of inhibition against both enzymes using known inhibitors including α-naphthoflavone, β-naphthoflavone, xanthotoxin, bergapten, piperonyl butoxide and piperine. We found that compounds we chose for inhibition studies exhibited all types of inhibitions, such as mechanism-based inhibition, uncompetive inhibition, and mixed-type inhibition (see detail in Duangkaew et al 2012b, **Appendix**).

1.1. Expression of CYP6AA3, CYP6P7 and CPR proteins

The enzyme assay system relies on measurement of cytochrome P450 (P450) activity through reconstitution assay system. The catalytic activities of all P450s require CPR as their redox partner enzyme. Both CYP6AA3 and CYP6P7 expression was carried out using baculovirus-mediated *Spodoptera frugiperda* (Sf9) insect cell expression system as previously described in Boonsuepsakul et al (2008). The baculovirus containing either CYP6AA3 and CYP6P7 cDNA were used to infect Sf9 insect cells for production of CYP6AA3 and CYP6P7 enzymes. The P450 proteins with the expected molecular weight of 58.8 kDa were detected by SDS-PAGE analysis in the microsome of Sf9 cells infected with baculovirus-P450s compared to the parent Sf9 cells.

The membrane-bound CPR enzyme was expressed in *E. coli* XL1-blue and the membrane fraction was separated by ultracentrifugation and subjected to purification with Ni^{2}+-NTA affinity column and analyzed by SDS-PAGE analysis

1.2. In vitro reconstitution of CYP6AA3 and CYP6P7 enzymatic activities with fluorescence substrates

To characterize for potential fluorogenic substrate probe and for use in inhibition studies of CYP6AA3 and CYP6P7, four resorufin fluorogenic substrates containing different alkyl groups including benzyloxyresorufin, ethoxyresorufin, methoxyresorufin, and

penthoxyresorufin were screened. Result revealed that both CYP6P7 and CYP6AA3 could metabolize benzyloxyresorufin and ethoxyresorufin, with higher specific activities toward benzyloxyresorufin than ethoxyresorufin, while there was absence of activities against methoxyresorufin and penthoxyresorufin (Figure 1, Duangkaew et al 2012b). Thus benzyloxyresorufin (BzR) was selected for use as substrate in further inhibition assays.

The kinetic parameters (K_m and V_{max}) were investigated in order to determine the concentration range of BzR that will be used in inhibition assays. By performing steady-state kinetic study of CYP6P7- and CYP6AA3-mediated benzyloxyresorufin *O*-benzylation (BROD) reaction, results showed that K_m value of CYP6P7 and CYP6AA3 against BzR was 0.49±0.1 µM and 1.92±0.24 µM, respectively.

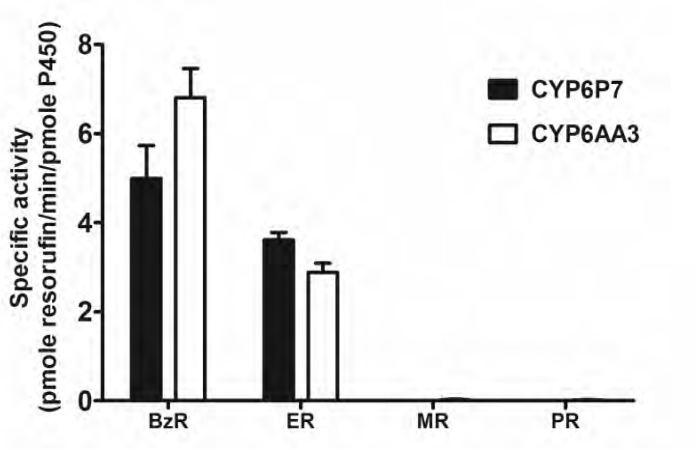

Figure 1. Specific activities of CYP6AA3 and CYP6P7 toward resorufin derivatives: benzyloxyresorufin (BzR), ethoxyresorufin (ER), methoxyresorufin (MR), and penthoxyresorufin (PR). Data are mean ± SD of triplicates.

2. Construction of CYP6AA3 and CYP6P7 homology models

We have successfully built on model structures of CYP6AA3 and CYP6P7. The model was constructed based on crystal structures of CYP3A4 (1TQN), CYP2C8 (1PQ2) and CYP2C9 (1OG2) human P450s that involve in pyrethroid metabolism using multiple amino acid sequence alignment strategy. Candidate predicted models of both mosquito P450s were selected based on the consensus judgment of DOPE and RAPDF scores that discriminate native structures from those misfolded. ProSA z-score and Ramachandran plot analysis support reasonable quality of CYP6AA3 model. Figure 2 shows overall conserved P450 folds found in CYP6AA3 and CYP6P7 models, such as helices D, E, I, J, K and L, and cysteine-pocket attaching heme. But both model structures are different in geometry of their active-site cavities and differences in their substrate access channels are prominent (Figure 2,

Lertkiatmongkol et al, 2011). The CYP6AA3 model has a large active site while CYP6P7 has a restrained narrow opening to the heme prosthetic group (Figure 2).

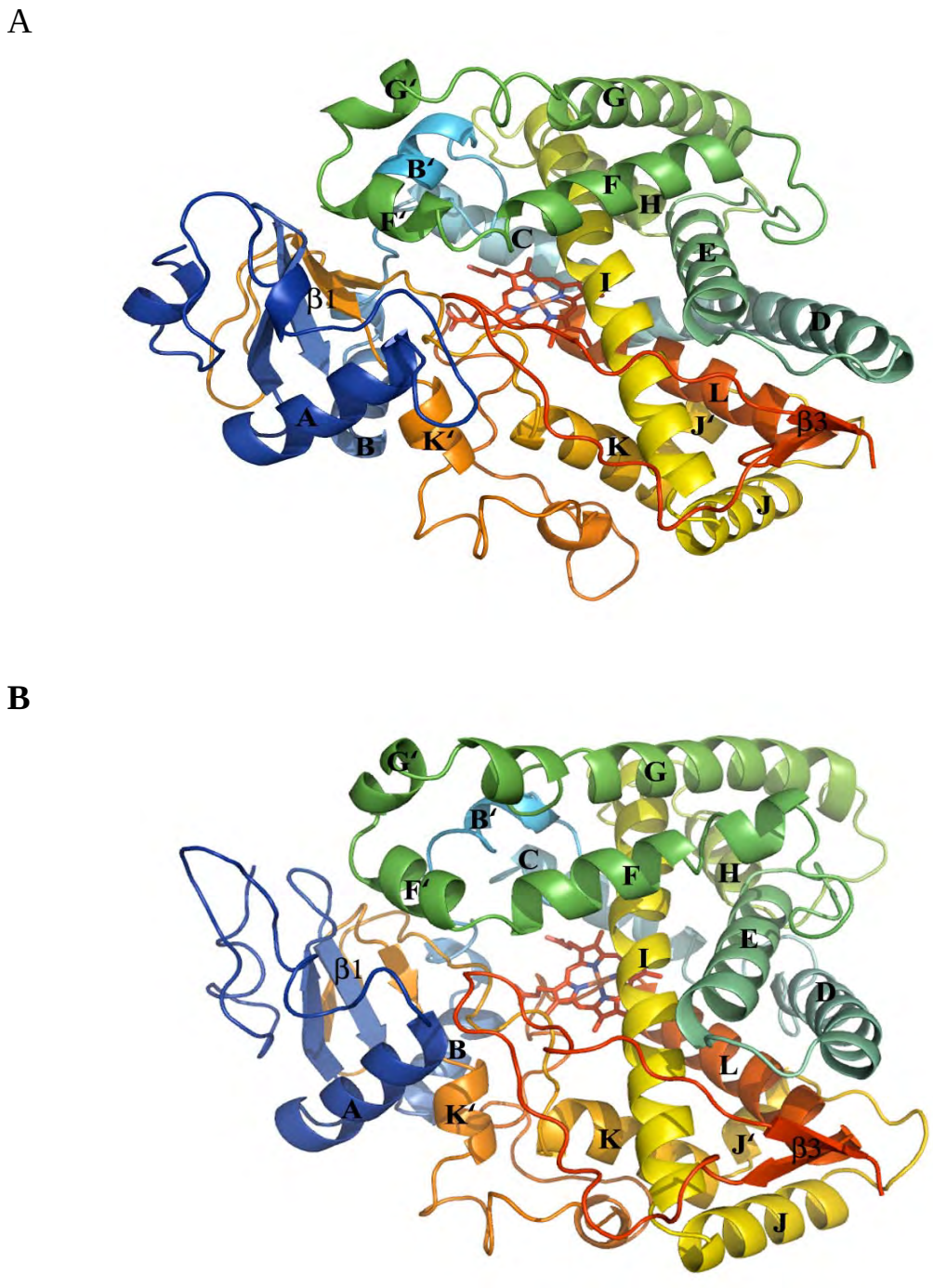

Figure 2. Overall fold of CYP6AA3 (A) and CYP6P7 (B) homology models. Each α-helices and β-sheets are labeled. The heme group is in the middle of the structure.

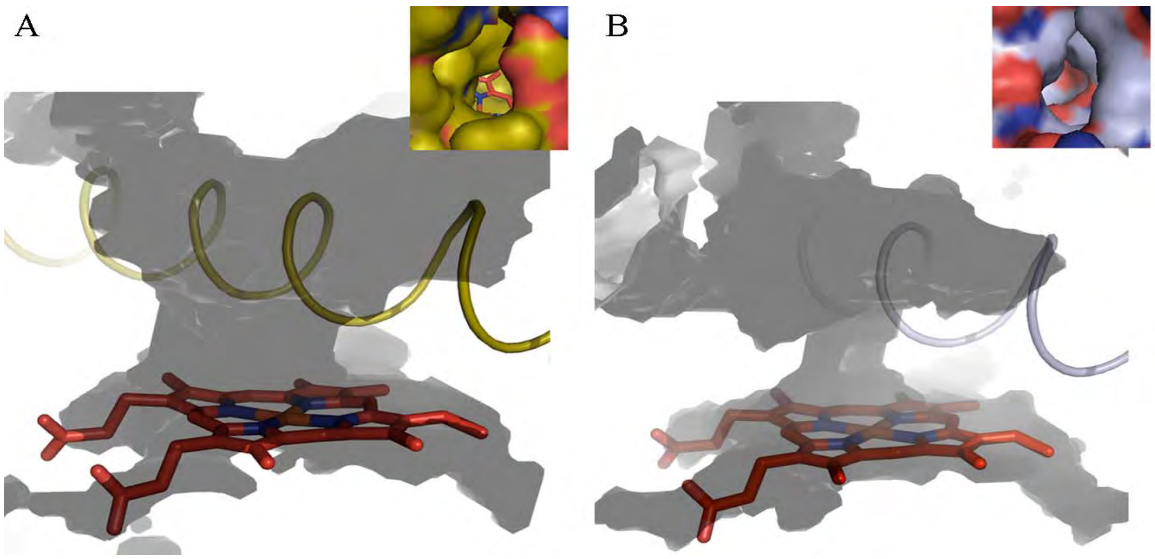

Figure 3. Predicted active sites extending to enzyme surface of CYP6AA3 (A), CYP6P7 (B). Active sites were calculated using VOIDOO. I-helices of CYP6AA3, CYP6P7 are depicted in cartoon, spanning across heme. Caption in each figure corresponds to molecular surface view of each access channel. CYP6AA3 and CYP6P7 both display oval shape of access opening.

The predicted enzyme model structures were used for molecular docking with insecticides (including pyrethroids, carbamate and organophosphate shown in figure 4) and compared with results of *in vitro* enzymatic assays reported by Duangkaew et al, 2011a. The large active site of CYP6AA3 allows the enzyme to accommodate multiple conformations of pyrethroids such as deltamethrin (figure 5) resulting in multiple products as previously detected (Boonseubsakul et al, 2008). The constrained pocket of CYP6P7 is consistent with that CYP6P7 shows restricted substrate access toward pyrethroids than CYP6AA3. For example, with CYP6P7 model we could explain that the limited ability of CYP6P7 to metabolize λ-cyhalothrin due to its bulky trifluoromethyl group and unable to fit into the restrained pocket of CYP6P7. In contrast λ-cyhalothrin can fit in large CYP6AA3 cavity, consistent with detected CYP6AA3 activity toward λ-cyhalothrin (Duangkaew et al, 2011a). Moreover the predicted hydrophobic interface in the active-site cavities of CYP6AA3 and CYP6P7 may contribute to their substrate selectivity against carbamate and organophosphate insecticides that are more hydrophilic than pyrethroids (figure 5), as both enzymes could not metabolize carbamate and organophosphate (Duangkaew et al, 2011a).

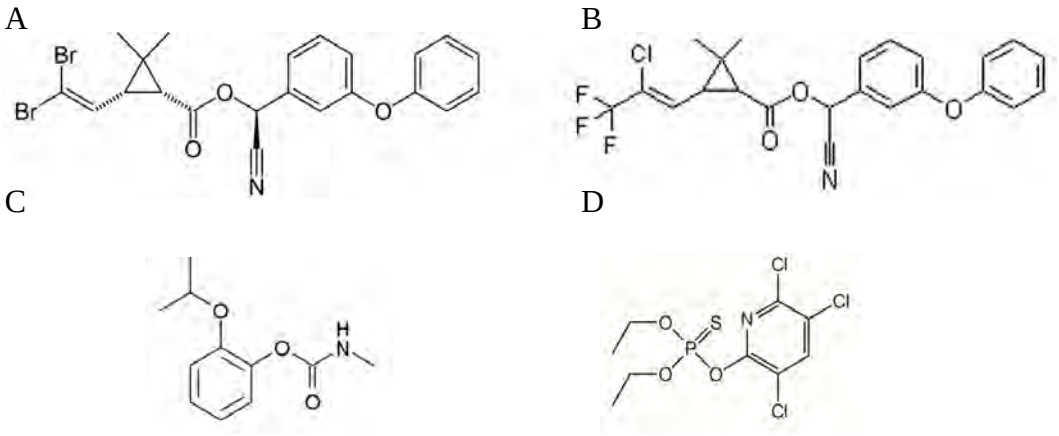

Figure 4 Insecticide chemical structures. Substrate pyrethroids shown are deltamethrin (A) and λ-cyhalothrin (B). Non-substrate insecticides docked in this study are: propoxur, a type of carbamate insecticide (C); chlopyrifos, a type of organophosphate insecticide (D)

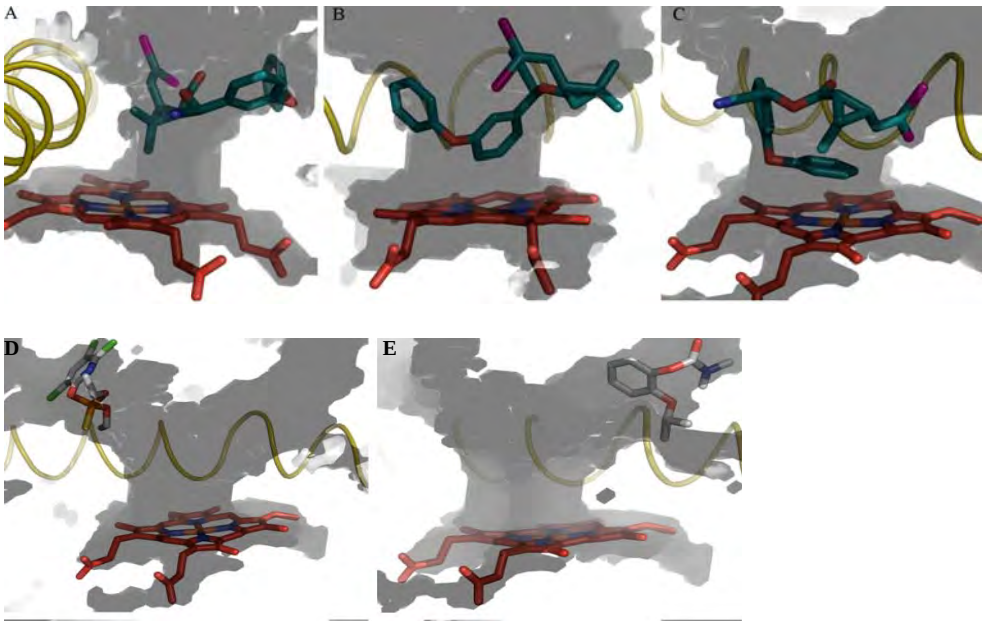

Figure 5. Binding modes of deltamenthrin, chlorpyrifos and propoxur in active site of CYP6AA3. CYP6AA3 exhibited multiple binding modes of deltamethrin positioning close to heme iron: geminal-dimethyl group (A), 5-phenoxybenzyl carbon (B), 4′-phenoxybenzyl carbon (C). In contrast chloripyrifos (D, organophosphate) and propoxur (E, carbamate) non-substrate insecticides move away from CYP6AA3 heme center.

All together the model structures of CYP6AA3 and CYP6P7 generated in this study have allowed us to better understand the different substrate preferences between these P450 enzymes and the predictions based on our docking studies are consistent with experimental results of pyrethroid metabolism mediated by P450 enzymes. The differences in size also corresponded to K_i values of inhibitory compounds such as rhinacanthin B (see Section 3.3)

in that CYP6AA3 may better accommodate rhinacanthin B than CYP6P7 resulting in metabolites through catalysis process that inhibit both enzyme in a mechanism-based irreversible inhibition pattern. These models should have the potential to be used in the investigation of candidate P450 inhibitors that have potential for use in the control of the mosquito vector and the spread of malaria.

3. Fluorescence-based CYP6P7 and CYP6AA3 inhibition assay and CPR inhibition assay

3.1. Selection of plant extracts possessing inhibitory effects against CYP6AA3 and CYP6P7

Plant materials were extracted by maceration with 95% ethanol to obtain crude ethanolic extracts. Yields of plant extract ranged from 3.25 to 22.93% w/w of dried starting materials. To investigate the effect of plant ethanol extracts on catalytic activity of CYP6AA3 and CYP6P7, P450-mediated BROD was conducted with various concentrations of extracts. Assays were performed by incubating enzyme mixture with BzR substrate together with each plant extracts. P450 activities were calculated as percentage of the remaining activity and plotted against concentrations of extract and IC_{50} value for each of plant extracts determined. The results shown in Table 1 indicated that of the extracts, rhizome of *C. longa* showed the strongest inhibition effect with IC_{50} value of 1.9 µg/ml for CYP6AA3 and 0.89 µg/ml for CYP6P7. Extracts from *A. paniculata, C. longa* leave, *R. nasutus* and *D. trifoliata* inhibited both P450s nearly in the same range of IC_{50} values (4-20 µg/ml). CYP6AA3 was inhibited by *Stemona spp.* and *C. procera* extract efficiently than CYP6P7 (1.6- to 2-fold lower of IC_{50} value, respectively). Much less inhibitory effect against BROD activity mediated by CYP6AA3 and CYP6P7 was observed with extract from seed of *C. reticulata* with $IC_{50} > 100$ µg/ml.

NADPH-dependent inhibition assay was performed by pre-incubating each crude extract with the enzyme mixture for 30 minutes in the presence of NADPH before addition of BzR substrate prior to start of reactions. Inhibition effects of each plant extract in the assay against CYP6AA3 and CYP6P7-BROD activity are summarized in Table 1. Upon comparison of IC_{50} values between incubation with and without NADPH, the *D. trifoliata* extract showed NADPH-dependent inhibition activities against both enzymes indicating a typical mechanism-based inhibition characteristic. The remaining plant extract shown in

Table 1 did not exhibit mechanism-based inhibition pattern. It could be noted that *C. longa* (leave and rhizome), *D. trifolata, A. paniculata* and *R. nasutus* comprise high inhibitory activities against both CYP6AA3 and CYP6P7, with low LC_{50} values (within range of <20 μg/ml). Thus *D. trifoliata, A. paniculata* and *R. nasutus* were further chosen for inhibition studies. Further study was not performed with *C. longa* leaves and rhizomes due to complication of numerous compounds/ and or the inhibitory candidates were existed in tiny amount.

Table 1. IC_{50} values for NADPH-dependent inhibition of P450s-mediated BROD activities by plant extracts

Plant extracts/ pure compounds	CYP6AA3 (ug/ml)		CYP6P7 (ug/ml)	
	Co-incubation	Pre-incubation	Co-incubation	Pre-incubation
Calotropis procera	25.3 ± 3.1	22.8 ± 0.9	38.0 ± 6.2	30.0 ± 3.1
Citrus reticulata	136.2 ± 17.7	243.1 ± 57.7	143.2 ± 32.2	123.0 ± 29.7
Curcuma longa-leave	14.8 ±1.7	12.4 ± 1.6	11.5 ± 2.5	12.7 ± 4.4
Curcuma longa-rhizome	1.9 ± 0.4	1.6 ± 0.2	0.89 ± 0.16	0.95 ± 0.23
Derris trifoliata	18.9 ± 2.6	6.7 ± 0.8	14.4 ± 3.1	10.5 ± 0.79
Rhinacanthus nasutus	18.8 ± 2.44	21.4 ± 3.3	14.7 ± 0.29	13.8 ± 0.79
Stemona spp.	66.3 ± 9.7	59.5 ± 8.6	107.0 ± 21.4	69.1 ± 9.9
Andrographis paniculata	8.08±0.02	6.05±0.03	10.32±0.23	10.26±0.26

ND: Not determined

3.2. Inhibition of CPR enzymatic activity by crude plant extracts

Inhibition study of CYP6AA3 and CYP6P7 by plant crude extracts revealed that all extracts have inhibition effect toward both CYP6AA3 and CYP6P7 activities. However, it is possible that P450s inhibition could be due to inhibition of CPR enzyme that plays an important role in P450-mediated reaction. Therefore, the effect of plant crude extracts toward CPR activity was evaluated. As shown in Figure 6, there was no apparent inhibition effect toward CPR activity observed for all plant crude extracts. Effect of crude extract from *C. longa* rhizome could not be determined because it absorption spectrum was interfered with spectrum of reduced cytochrome c. Thus it could be summarized that inhibitory effects of crude plant extracts were due to inhibition on CYP6AA3 and CYP6P7 enzymes.

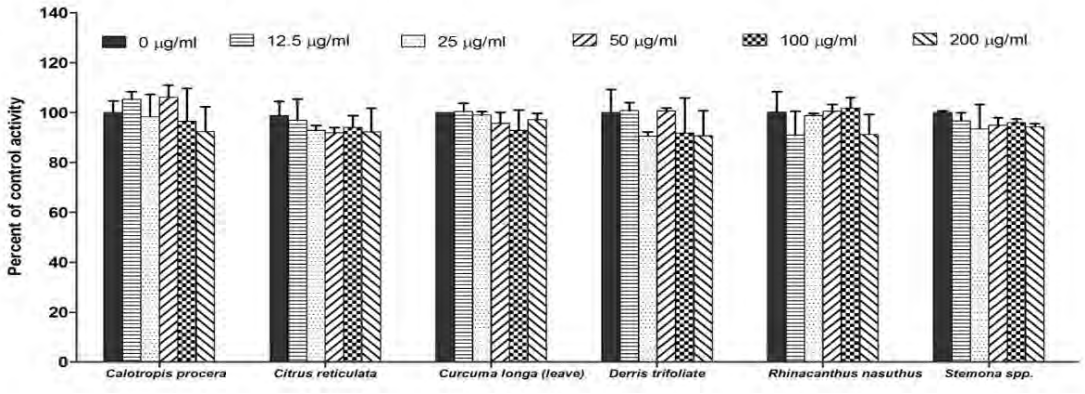

Figure 6. Inhibition of CPR enzymatic activity by plant extracts at concentrations of 0 µg/ml (■), 12.5 µg/ml (▤), 25 µg/ml (▥), 50 µg/ml (▨), 100 µg/ml (▩), and 200 µg/ml (▧).Values are means ± SD of two replicated experiments.

3.3. Inhibition of CYP6AA3 and CYP6P7 by R. nasutus, A. paniculata and D. trifoliata compounds

R. nasutus: To obtain *R. nasutus* plant compounds, stepwise gradient elution of each *n*-hexane extract was conducted in a silica gel chromatography column using an hexane/EtOAc/ methanol solvent system. This provided six fractions; fr. 3 and fr. 4 showed potent inhibition activities and were subjected to analysis by HPLC. Four major absorption peaks at 254 nm were obtained. The two peaks at retention time, 18.3 min and 19.3 min, (figure 7) that were associated with inhibition effect were identified by NMR analysis as rhinacanthn-B and rhinacanthin-C, respectively.

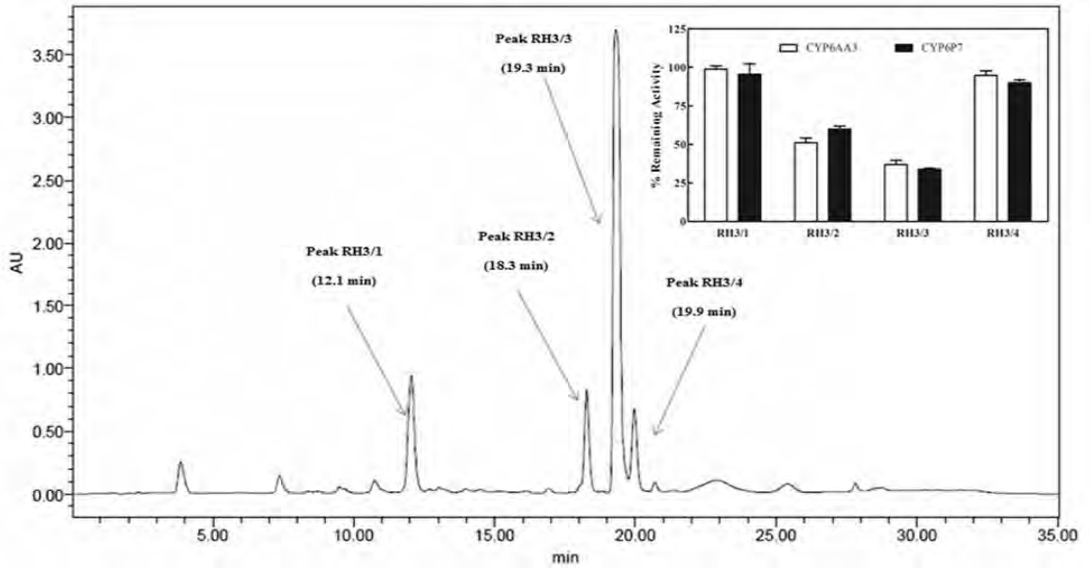

Figure 7. HPLC chromatogram of silica fraction from *R. nasutus* hexane (RH) fraction, the eluate was monitor at 254 nm. The inlet figure represents inhibition of CYP6AA3 and CYP6P7 by the HPLC peaks at concentration 10µg/ml of each peak. Each column represents the means ± SD of duplicate experiments.

Inhibition assays employed fluorescent-based reconstitution enzymatic assay using benzyloxyresorufin fluorescent compound as substrate. Both rhinacanthin-B and –C compounds ran on thin layer chromatography (TLC) using *n*-hexane-diethyl ether (6:4, v/v) as mobile phase at retardation factor (R_f) values of 0.59 and 0.7 respectively. The ethyl acetate fraction (400 mg) was separated by TLC and HPLC. The compound collected from HPLC at retentime 10.01 min and showed inhibitory effect against both P450s was identified as rhinacanthin-A. The structural formula of rhinacanthin-A, -B, and -C are shown in figure 8.

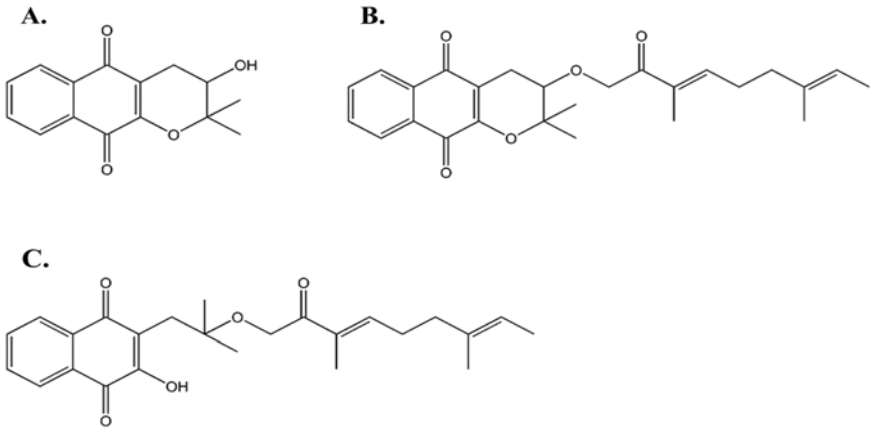

Figure 8. Chemical structures of rhinacanthin-A (A), rhinacanthin-B (B), and rhinacanthin-C (C).

Inhibition studies using time-dependent inhibition assay, by means of pre-incubation of enzyme mixture with each test extract/compound for 0 and 30 min in the presence of NADPH prior to addition of benzyloxyresorufin substrate, was performed with CYP6AA3 and CYP6P7 expressed in baculovirus-insect cell expression system. This was to primarily determine whether inhibition of *R. nasutus* extracts/constituents followed a mechanism-based inhibition pattern. Inhibition of crude ethanol extract of *R. nasutus* did not differ dramatically against BROD mediated by mosquito CYP6AA3 and CYP6P7 enzymes (Table 2). However, significant increase in inhibition by the *n*-hexane fraction against both enzymes occurred when pre-incubation time was increased to 30 min, a characteristic of mechanism-based inactivation. The ethyl acetate fraction inhibited CYP6AA3 with higher potency than CYP6P7 with the IC_{50} for the latter shifting to a lower range. It should be noted that there was no inhibitory activity against enzymatic activity of CPR-mediated cytochrome *c* reduction to 200 µg/ml of crude ethanolic extract (data not shown), suggesting inhibition effect was not attributable to CPR redox partner enzyme.

Table 2. IC_{50} values of purified compounds, fractions and ethanol extract of *R. nasutus* and test compounds in inhibition against BROD of CYP6AA3 and CYP6P7

Sample	IC_{50}[a] (μg/ml)			
	CYP6AA3		CYP6P7	
	Co-incubation	Pre-incubation	Co-incubation	Pre-incubation
Ethanol extract	18.78 ± 2.44	21.44 ± 3.30[b]	14.63 ± 0.29	13.82 ± 0.79[b]
n-hexane fraction	12.25 ± 0.98[c]	6.33 ± 0.54[c]	15.44 ± 2.43[c]	6.74 ± 1.52[c]
EtOAc fraction	6.20 ± 0.14[b]	5.89 ± 0.46[b]	14.70 ± 1.07[b,c]	7.75 ± 0.49[b,c]
Aqueous fraction	>100	N.D.[e]	>100	N.D.[e]
Rhinacanthin-A (μM)	9.15 ± 0.23[b]	8.59 ± 0.21[b]	35.14 ± 0.91[b,c]	6.41 ± 0.91[b,c]
Rhinacanthin-B (μM)	2.39 ± 0.28[b,c]	0.29 ± 0.05[c]	3.69 ± 0.07[b,c]	0.67 ± 0.01[c]
Rhinacanthin-C (μM)	10.64 ± 0.84	10.10 ± 0.76	9.56 ± 0.27	8.92 ± 0.10
α-Naphthoflavone (μM)	0.37 ± 0.06[d]	0.38 ± 0.06[d]	2.90 ± 0.27[d]	3.03 ± 0.45[d]
PBO (μM)	9.91 ± 0.81[c,d]	4.04 ± 0.31[c,d]	31.77 ± 3.21[c,d]	16.22 ± 1.81[c,d]

[a] Each value represents mean ± SD of triplicate tests
[b] Significant differences between enzymes, $P < 0.05$
[c] Significant differences between co-incubation and pre-incubation, $P < 0.05$
[d] Values obtained from Duangkaew et al. 2011a
[e] N.D., not determined

Mosquito enzymes, CYP6AA3 and CYP6P7, were inhibited by rhinacanthin-A, -B and –C, but differed in their modes of action. Rhinacanthin-B inhibited both enzymes in a mechanism-based manner, while rhinacanthin-A reversibly inhibited CYP6AA3 in the mixed-type manner with K_i values of 5.11 μM (table 2) and irreversibly inhibited CYP6P7 (Figures 9 and 10). In contrast, rhinacanthin-C noncompetitively inhibited CYP6AA3 with a K_i value of 7.95 μM, and competitively inhibited CYP6P7 with a K_i value of 7.32 μM (Figure 11). In particular the mechanism-based inhibition of rhinacanthin-A and rhinacanthin-B is time-, concentration-, and NADPH-dependent irreversible pattern. Efficiency of enzyme inactivation from the ratio of k_{inact} to K_I by rhinacanthin-A was 3.71 $min^{-1}{\cdot}nM^{-1}$ for inhibition of CYP6P7, and efficiency by rhinacanthin-B on CYP6AA3 was 96.07 $min^{-1}{\cdot}nM^{-1}$ and on CYP6P7 was 32.94 $min^{-1}{\cdot}nM^{-1}$, indicating that rhinacanthin-B has higher inhibition potency than rhinacanthin-A. *R. nasutus* extracts do not possess inhibition activity on CPR-mediated cytochrome c reduction, suggesting the inhibition effect was on mosquito P450 enzymes

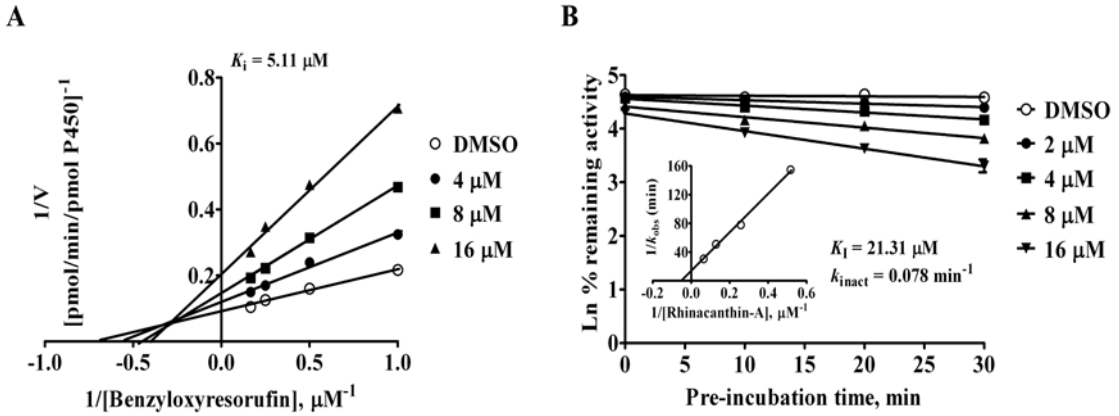

Figure 9. Inhibition of CYP6AA3 and CYP6P7 by rhinacanthin-A. (A) Lineweaver-Burk plot of inhibition on CYP6AA3. (B) Plot of natural log percentage of remaining CYP6P7 activity in the presence of rhinacanthin-A *versus* preincubation times. Inlet in (B) is a plot of reciprocal of the k_{obs} values against the reciprocal of rhinacanthin-A concentrations. Each fitted line was produced by linear regression analysis of each point. Each point represents the mean ± SD of triplicate experiments.

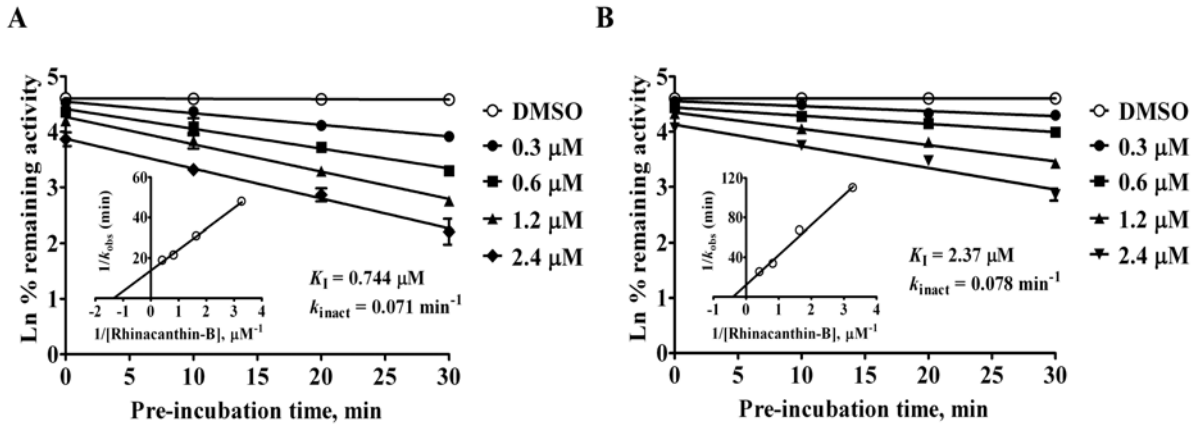

Figure 10. Kinetic analysis of CYP6AA3 and CYP6P7 inhibition by rhinacanthin-B. Plots of inhibition on CYP6AA3 (A) and CYP6P7 (B) were performed as described in Fig. 2B. Each point represents the mean ± SD of triplicate experiments.

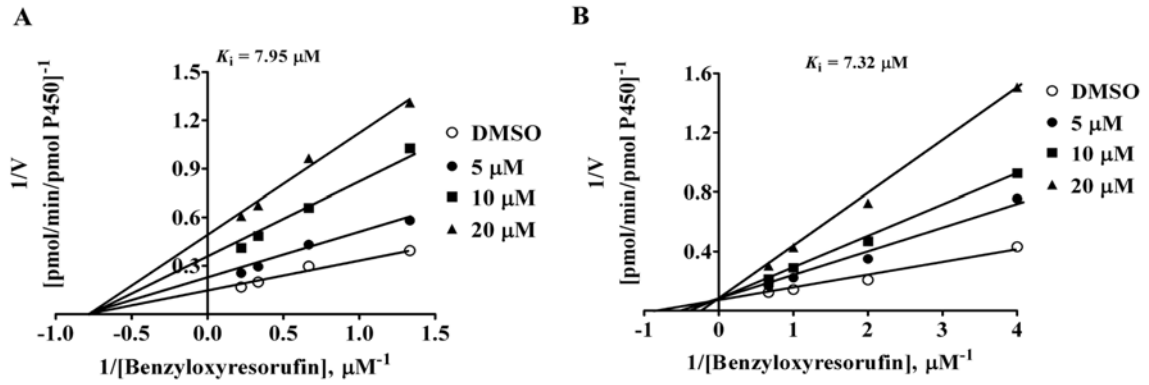

Figure 11. Lineweaver-Burk plots of CYP6AA3- or CYP6P7-mediated BROD in the presence of rhinacanthin-C. Inhibitions of CYP6AA3 (A) and CYP6P7 (B) are shown. Each point represents the mean ± SD of triplicate experiments.

NADPH oxidation: Rhinacanthins A, B, C are 1,4-naphthoquinone esters and thus might stimulate oxidation of NADPH as 1,4-naphthoquinones undergo reduction by CPR, possibly forming superoxide radical (Kumagai et al 2012), and could modulate CYP6AA3 and CYP6P7. To see this effect, CPR in the presence of NADPH and each of 40 µM rhinacanthins A-C was carried out and molar absorption change of NADPH oxidation was measured. The results revealed that rhinacanthins B and C did not accelerate NADPH oxidation by CPR, suggesting no interference of electron transfer from CPR to CYP6AA3 and CYP6P7 by both compounds. Hence inhibition by rhinacanthin B and C was due to inhibitory effect of CYP6AA3 and CYP6P7 enzymes. In contrast rhinacanthin A evidently showed accelerated NADPH oxidation by CPR with a high K_m value of 33.65 µM, suggesting no interference with electron transfer to mosquito P450s.

A. paniculata: Among fractions, crude ethanol and hexane fractions of *A. paniculata* showed the largest inhibitory effect on CYP6P7 and CYP6AA3 with IC_{50} values of 2 µg/ml for CYP6P7 and 10 µg/ml for CYP6AA3. There was no inhibition activity in EtOAc and aqueous fractions. The *n*-hexane fraction was further subjected to silica column chromatography using *n*-hexane-EtOAc step gradients to give five fractions, with fraction 4 comprised potential inhibition activity. Further purification suggested that compounds AP-hex1 and 2 exerted potent inhibition effects against both mosquito P450s. The efficacy of each compound was determined by IC_{50} value shown in Table 3. Identification of AP-hex1 and 2 is underway via NMR. However primary ESI/MS data suggested that both compounds have the polyoxygenated flavone structures as shown in Figure 12. Since *A. paniculata*

comprises andrographolide as major component, we thus tested inhibition with this compound. The IC_{50} value suggest that andrographolide does not inhibit both mosquito P450s (unreported data).

Table 3. IC_{50} values of extracts and compounds from *A. paniculata*

Sample	**IC_{50} (µg/ml)**			
	CYP6P7		CYP6AA3	
	Co-incubation	Pre-incubation	Co-incubation	Pre-incubation
Ethanol extract	10.32±0.23	10.26±0.26	8.08±0.02	6.05±0.03
Hexane fraction	6.20±0.15	5.75±0.07	5.02±0.26	2.57±0.05
EtOAc fraction	42.07±0.57	35.94±0.59	16.57±0.09	15.01±0.33
Aqueous fraction	>100	ND	>100	ND
AP-hex-1	2.61±0.17	2.40±0.14	2.16±0.56	0.89±0.14
AP-hex-2	2.99±0.05	2.68±0.23	2.31±0.02	1.18±0.04

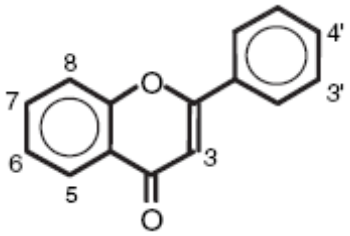

Figure 12. Core structure of polyoxygenated flavone with methyl groups being attached at various positions in *A. paniculata*

As shown in Table 3, both AP-hex-1 and AP-hex-2 apparently exhibited mechanism-based inhibition against CYP6AA3. The mechanism-based inhibition against CYP6AA3 was confirmed as both compounds inhibited in time-, concentration-, and NADPH-dependent manner (data not shown). Inhibition against CYP6AA3 by AP-hex-1 and AP-hex-2 was irreversible. of 5.8 and 6.7 µM, respectively. Conversely inhibition by AP-hex-1 and AP-hex-2 was reversible with apparent K_i values against CYP6P7 of 6.81 and 5.5 µM, respectively, corresponding to the approximately equal IC_{50} values shown for CYP6P7 in Table 3.

D.trifoliata: Bioassay-guided fractionation suggested that the *n*-hexane and EtOAc fractions contained potent inhibition activity, however further purification suggested that inhibition might be due to rotenone and derivatives (data not reported). Further investigations are underway.

4. Cytoxicity assays

4.1. Development of MTT cytoxicity assays

We have established cell-based MTT cytotoxicity assays to further determine inhibitory effects of compounds on CYP6AA3-mediated or CYP6P7-mediated detoxification activity using Sf9 cells that express CYP6AA3 or CYP6P7. The method is based on the rationale that a deltamethrin insecticide is cytotoxic to Sf9 cells (i.e. inhibition of mitochondrial complex I) causing cell mortality. Thus treatment of cells with cytotoxic insecticide compounds in cytotoxicity assays can cause cell mortality unless cells possess ability to detoxify insecticides, which in this case the mosquito CYP6AA3 and CYP6P7 enzymes could protect insect cells from deltamethrin cytotoxicity. Further addition of plant compounds that are CYP6AA3 and CYP6P7 inhibitors might abolish their cytoprotective capability.

As shown in Figure 13, MTT assays revealed capabilities of both enzymes in specifically protecting Sf9 cells against test pyrethroids (permethrin, cypermethrin, and deltamethrin) but not other insecticide groups such as chlorpyrifos (organophosphate insecticide) and propoxur (carbamate). These results comply with results of enzymatic assays. The MTT assay system could thus be used as a cell-based screening of plant inhibitory compounds against both P450s.

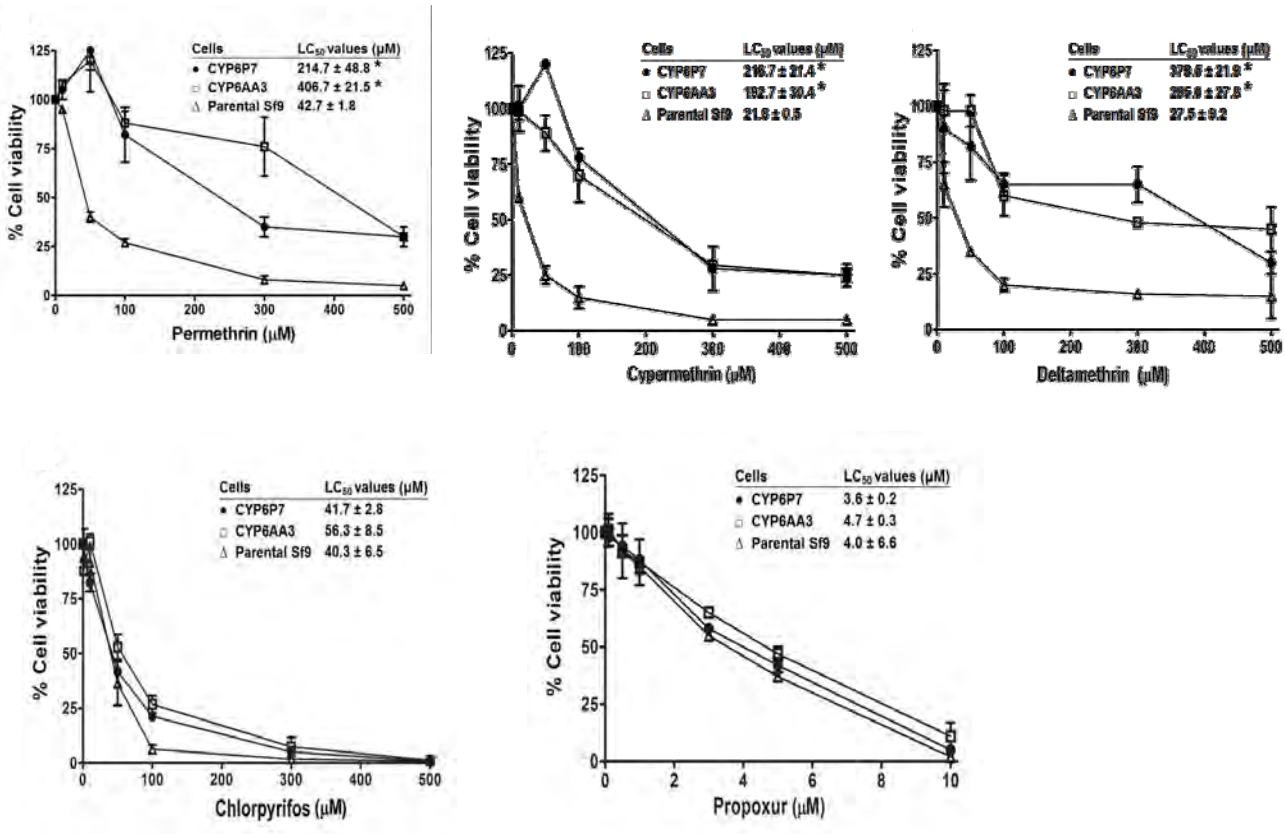

Figure 13. Viability of CYP6P7-expressing Sf9 cells (●), CYP6AA3-expressing Sf9 cells (□) and parental Sf9 cells (Δ) upon incubation with various insecticides. The LC50 values of *C. procera*, *C. reticulata*, *C. longa*, *D. trifoliate*, *R. nasutus*, *A. paniculata* and *Stemona spp* were 55.02, 454.8, 11.67, 2.86, 7.56, 18.43 µg/mL, respectively

4.2. Effect of rhinacanthin-A, -B, and -C on susceptibility to cypermethrin in P450-expressing cells

Crude ethanol extract, rhinacanthin-A,-B, and -C significantly decreased cypermethrin LC_{50} values in cells expressing mosquito P450s (Table 4), as a result of synergistic action of *R. nasutus* compounds with cypermethrin cytotoxicity. Two compounds, α-naphthoquinone and PBO, that showed high inhibitory potency against CYP6AA3 and CYP6P7 were also used for comparison with rhinacanthins.

Table 4. Effect of *R. nasutus* extract and compounds on cypermethrin susceptibility of Sf9, CYP6AA3- and CYP6P7-expressing cells

Cells	Treatment	LC_{50} [a] (μM)	SR[b]	Ratio[c]
Sf9 cells	Cypermethrin	130.7 ± 8.13[d,e]	-	-
	+ Ethanol extract	173.4 ± 13.7[d,e]	0.79	NA
	+ Rhinacanthin-A	123.0 ± 5.52[e]	1.06	NA
	+ Rhinacanthin-B	107.6 ± 3.89[e]	1.21	NA
	+ Rhinacanthin-C	20.3 ± 0.01[d,e]	6.44	NA
	+ α-Naphthoflavone	162.4 ± 9.42[d]	0.80	NA
	+ PBO	144.9 ± 11.3[e]	0.90	NA
CYP6AA3-expressing cells	Cypermethrin	397.9 ± 16.7[d,e]	-	-
	+ Ethanol extract	61.8 ± 2.30[d,e]	6.44	8.15
	+ Rhinacanthin-A	125.2 ± 3.08[d]	3.18	2.99
	+ Rhinacanthin-B	46.1 ± 0.19[d,e]	8.63	7.13
	+ Rhinacanthin-C	9.3 ± 0.95[d,e]	42.78	6.64
	+ α-Naphthoflavone	162.7 ± 1.08[d]	2.45	3.06
	+ PBO	182.7 ± 13.2[d,e]	2.17	2.4
CYP6P7-expressing cells	Cypermethrin	402.4 ± 42.5[d,e]	-	-
	+ Ethanol extract	126.1 ± 6.10[d,e]	3.19	4.04
	+ Rhinacanthin-A	137.9 ± 4.45[d,e]	2.92	2.75
	+ Rhinacanthin-B	33.3 ± 2.37[d,e]	12.08	9.98
	+ Rhinacanthin-C	11.0 ± 0.63[d,e]	36.58	5.68
	+ α-Naphthoflavone	178.5 ± 14.5[d]	2.25	2.80
	+ PBO	209.6 ± 14.3[d,e]	1.92	2.13

[a] Each value is mean ± SD of triplicate experiments.
[b] Synergism ratio: LC_{50} cypermethrin alone/LC_{50} cypermethrin in the presence of inhibitors.
[c] Synergism ratio for P450-expressing cells after normalization with Sf9 cells.
[d] Significant difference between cypermethrin alone and with inhibitors, $P < 0.05$
[e] Significant difference of each treatment between Sf9 and P450-expressing cells, $P < 0.05$
NA, not applicable

It should be noted that rhinacanthin-C has a synergistic effect on cypermethrin cytotoxicity in the control uninfected Sf9 cells, but this was not prominent for rhinacanthin-A and rhinacanthin-B. We thus normalized percent cell viability of P450-expressing cells upon treatment with cypermethrin and each of rhinacanthin compounds with that of Sf9 parent cells. Synergistic ratios of rhinacanthin-B and rhinacanthin-C with cypermethrin cytotoxicity on P450-expressing cells was approximately 6-10 folds higher than Sf9 cells

and 2-4 folds higher than those obtained from α-naphthoflavone and PBO inhibitors. This is consistent with results of *in vitro* inhibition assays in that rhinacanthin-B possessed higher inhibitory effect than rhinacanthin-C. Synergism of rhinacanthin-A with cypermethrin cytotoxicity was much less than that with rhinacanthin-B and C and was comparable to those of α-naphthoflavone and PBO inhibitors.

4.3. Effect of AP-H1 and AP-H2 isolated from A. paniculata on susceptibility to cypermethrin in P450-expressing cells

As shown in Table 5, hexane and ethyl acetate, including the two purified compounds significantly decreased cypermethrin LC_{50} values in cells expressing mosquito P450s, as a result of synergistic action of *A .paniculata* compounds with cypermethrin cytotoxicity.

Table 5. Effect of *A .paniculata* extracts and compounds on cypermethrin susceptibility of Sf9, CYP6P7-, and CYP6AA3-expressing cells

Cells	Treatment	LC_{50} [a] (μM)	SR[b]
Sf9 cells	Cypermethrin	150.3±0.57	-
	+Hexane extract	99.6±0.23	1.5
	+EtOAc extract	49.66±1.15	3
	+AP-hex-1	149.6±0.57	1
	+AP-hex-2	140.3±1.15	1
CYP6P7-expressing cells	Cypermethrin	442.0±2.28	-
	+Hexane extract	93.4±0.57	4.73
	+EtOAc extract	148.3±2.88	2.98
	+AP-hex-1	93.0±5.19	4.75
	+AP-hex-2	120.3±0.50	3.68
CYP6AA3-expressing cells	Cypermethrin	393.3±5.77	-
	+Hexane extract	50.0±1.73	7.86
	+EtOAc extract	81.0±1.52	4.85
	+AP-hex-1	74.16±1.04	5.30
	+AP-hex-2	46.0±1.73	8.55

[a] Each value is mean ± SD of triplicate experiments.

[b] Synergism ratio: LC_{50} cypermethrin alone/LC_{50} cypermethrin in the presence of inhibitors.

Together data of in vitro enzymatic inhibition assays, cell-based assays and larvicidal studies (Section 4.4) suggest that *rhinacanthus nasutus* and *A .paniculata* could be potential candidate for development of synergistic compounds for mosquito control in the future.

4.4. Larvicidal bioassays

Larvicidal assays showed that crude extracts of C. longa showed significant larvicidal activity with IC50 value of 79.24 mg/L, while *A. paniculata* of 213 mg/L. *D. trifoliata* showed 11% mortality at 500 mg/L, *C. procera* at 5% mortality at 500mg/L. *C. reticulata* and *Stemona spp*. appeared no detectable larvicidal activity up to 300 mg/L. The data are correlated to the cytotoxicity of crude extracts against insect cells and enzymatic inhibition results, except *D. trifoliata* and *Stemona spp*. Due to insufficient amount of purified compounds obtained we did not perform tests with inhibitory compounds.

CONCLUSION

We have developed *in vitro* fluorescence-based and MTT cytotoxicity assays using P450-expressing *Spodoptera frugiperda* (Sf9) cells for rapid screening of inhibitory compounds and synergistic effect of inhibitors with pyrethroid insecticides, respectively. We have built homology model of CYP6AA3 in an attempt to increase our understanding of molecular mechanisms underlying binding site toward insecticides and inhibitors. Screening of 7 crude plant extracts including *Calotropis procera*, *Citrus Reticulata*, *Stemona spp.*, *Curcuma longa* rhizomes and leaves, *Derris trifoliata*, *Andrographis paniculata* and *Rhinacanthus nasutus*, we found that *C. longa* rhizomes and leaves, *D. trifoliata*, *A. paniculata* and *R. nasutus* contained high inhibitory activities against both enzymes. Due to complexity of compounds in *C. longa*, we could not identify compounds that possess inhibition effects. Nevertheless at least three purified naphthoquinone esters isolated from *R. nasutus* and two polyoxygenated methoxylated flavones specific to *Andrographis sp.* were found possessing inhibitory effect against mosquito P450 enzymes. Judging from the purified inhibitory compounds obtained it could be concluded that naphthoquinone ring or chromane ring could contribute significantly to inhibition against mosquito P450 enzymes. These compounds acted synergistically with pyrethroid toxicity based on cell-based assays. Moreover preliminary results of larvicidal tests on *Aedes aegypti* mosquitoes of plant extracts were in agreement of inhibitory potency against mosquito detoxification P450 enzymes. Results obtained will thus be beneficial to implement effective resistance management strategies of mosquito vector control. However, further studies on insecticidal mode of action and effects on other non-target organisms and environment of these plant compounds are needed for practical use as mosquito control.

REFERENCES

1. Berman H.M., Westbrook J., Feng Z., Gilliland G., Bhat T.N., Weissig H., Shindyalov I.N., Bourne P.E. (2000). The Protein Data Bank. *Nucleic Acids Res* 28:235-242.
2. Bhardwaj, R. K., H. Glaeser, L. Becquemont, U. Klotz, S. K. Gupta, and M. F. Fromm. (2002). Piperine, a major constituent of black pepper, inhibits human P-glycoprotein and CYP3A4. *J Pharmaco. Exp Ther* 302: 645‰650.
3. Boonsuepsakul S., Luepromchai E., Rongnoparut P. (2008). Characterization of *Anopheles minimus* CYP6AA3 expressed in a recombinant baculovirus system. Arch *Insect Biochem Physiol* 63: 13-21
4. Daware, M. B., A. M. Mujumdar, and S. Ghaskadbi. (2000). Reproductive toxicity of piperine in Swiss Abino mice. *Planta Med* 66: 231-236.
5. Duangkaew, P., Kaewpa D., and Rongnoparut P. (2011a). Protective efficacy of *Anopheles minimus* CYP6P7 and CYP6AA3 against cytotoxicity of pyrethroid insecticides in *Spodoptera frugiperda* (Sf9) insect cells. *Trop Biomed* 28: 293-301.
6. Duangkaew, P., Pethuan S., Kaewpa D., Boonsuepsakul S., Sarapusit S., and Rongnoparut P. (2011b) Characterization of mosquito CYP6P7 and CYP6AA3: differences in substrate preference and kinetic properties. *Arch Insect Biochem Physiol* 76: 236-248.
7. Fakoorziba, M.R., Eghbal, F., Vijayan, V.A. (2009) Synergist efficacy of piperonyl butoxide with deltamethrin as pyrethroid insecticide on *Culex tritaeniorhynchus* (Diptera: Culicidae) and other mosquito species. *Environ Toxicol* 24: 19-24.
8. Feyereisen R. (1999). Insect P450 enzymes. *Annu Rev Entomo*l 44: 507-533
9. Fowler, S. and Zhang, H. (2008). In vitro evaluation of reversible and irreversible cytochrome P450 inhibition: current status on methodologies and their utility for predicting drug–drug interactions. *AAPS J* 10:410–424.
10. Jayakrishna G., Harikishore P., Rao C.V., Gunasekar D., Blond A. and Bodo B. (2001). Two new 2'-oxygenated flavones from Andrographis elongate. *Chem Pharm Bull* 49: 1555-1557.
11. Kaewpa, D., Boonsuepsakul, S., Rongnoparut, P. (2007). Functional expression of mosquito NADPH-cytochrome P450 reductase in *Escherichia coli*. *J Econ Entomol* 100: 946-953.
12. Kalgukar, A. S., Obach, R.S., Maurer, T.S. (2007). Mechanism-based inactivation of cytochrome P450 enzymes: chemical mechanisms, substrate-activity relationships and relationship to clinical drug-drug interaction and idiosyncratic adverse drug reaction. *Curr Drug Met* 8: 407-447

13. Kamaraj, C., Bagavan A., Rahuman A., Abduz Zahir A., Elango G., and Pandiyan G. (2009) Larvicidal potential of medicinal plant extracts against *Anopheles subpictus* Grassi and *Culex tritaeniorhynchus* Giles (Diptera: Culicidae). Parasitol Res 104: 1163-1171.
14. Komalamisra, N., Trongtokit Y., Rongsriyam Y., and Apiwathnasorn C. (2005) Screening for larvicidal activity in some Thai plants against four mosquito vector species. *Southeast Asian J Trop Med Public Health* 36:1412-1422.
15. Kostrzewa-Nowak, D., Bieg, B., Paine, M.J.I., Wolf, C.R. and Tarasiuk, J. (2012). Role of structural factors of antitumour anthraquinone derivatives and analogues in the ability to undergo bioreductive activation by NADPH cytochrome P450 reductase. Implications for increasing the activity against sensitive and multidrug-resistant leukemia HL60 cells. *Anti-Cancer Drug* 23: 393–405
16. Kumar. S., Thomas, A., Sahgal, A., Verma, A., Samuel, T., Pillai, M.K. (2002) Effect of the synergist, piperonyl butoxide, on the development of deltamethrin resistance in yellow fever mosquito, *Aedes aegypti* L. (Diptera: Culicidae). *Arch Insect Biochem Physiol* 50:1-8.
17. Kuppusamy C. and Murugan K. (2010) Effects of *Andrographis paniculata* Nees on growth, development and reproduction of malarial vector *Anopheles stephensi* Liston (Diptera: Culicidae). *Trop Biomed* 27: 509-516.
18. Kuroyanagi M., Sato M., Ueno A. and Nishi K. (1987) Flavonoids from *Andrographis paniculata*. *Chem Pharm Bull* 35: 4429-4435.
19. Laskowski R.A., MacArthur M.W., Moss D.S., Thornton J.M. (1993) PROCHECK: a program to check the stereochemical quality of protein structures. *J Appl Cryst* 26:283-291.
20. Lertkiatmongkol P., Jenwitheesuk E., Rongnoparut P. (2011) Homology modeling of mosquito cytochrome P450 enzymes involved in pyrethroid metabolism: insights into differences in substrate selectivity. *BMC Research Notes* 4: 321.
21. Marcombe S., Carron S., Etienne M., Agnew P., et al (2009) Reduced efficacy of pyrethroid space sprays for dengue control in an area of Martinique with pyrethroid resistance. *Am J Trop Med Hyg* 80: 745-751.
22. Govindarajan M. and Sivakumar R. (2012) Adulticidal and repellent properties of indigenous plant extracts against *Culex quinquefasciatus* and *Aedes aegypti* (Diptera: Culicidae). *Parasitol Res* 110: 1607-1620.
23. Piyachaturawat, P., Glinsukon, T. and Toshulkao C. (1983) Acute and subacute toxicity of piperine in mice, rat and hamsters. *Toxicol Lett* 16: 351ꟷ359

24. Rao YK, Vimalamma G, Rao CV and Tzeng YM (2004) Flavonoids and andrographolides from *Andrographis paniculata*. *Phytochemistry* 65: 2317-2321.
25. Rongsriyam, Y., Trongtokit Y., Komalamisra N., Sinchaipanich N., Apiwathnasorn C., and Mitrejet A. (2006) Formulation of tablets from the crude extract of *Rhinacanthus nasutus* (Thai local plant) against *Aedes aegypti* and *Culex quinquefasciatus* larvae: a preliminary study. *Southeast Asian J Trop Med Public Health* 37: 265-271.
26. Sali A. and Blundell TL. (1993) Comparative protein modelling by satisfaction of spatial restraints. *J Mol Biol* 234:779-815.
27. Samudrala R. and Moult J. (1998) An all-atom distance-dependent conditional probability discriminatory function for protein structure prediction. *J Mol Biol* 1998, 275:895-916.
28. Sarapusit S, Lertkiatmongkol P, Duangkaew P and Rongnoparut P (2013) Modeling of *Anopheles minimus* mosquito NADPH-cytochrome P450 oxidoreductase (CYPOR) and mutagenesis analysis. *Int J Mol Sci* 14: 1788-1801.
29. Sarapusit S., Pethuan S., Rongnoparut P. (2010) Mosquito NADPH-cytochrome P450 oxidoreductase: kinetics and role of phenylalanine amino acid substitutions at Leu86 and Leu219 in CYP6AA3-mediated deltamethrin metabolism. *Arch Insect Biochem Physiol* 73:232-244.
30. Scott, JG (1996) Inhibitors of CYP6D1 in house fly microsomes. *Insect Biochem Mol Biol* 26: 645-649.
31. Sendl, A., Chen J. L., Jolad S. D., Stoddart C., Rozhon E., Kernan M., Nanakorn W., and M. Balick. (1996) Two new naphthoquinones with antiviral activity from *Rhinacanthus nasutus*. *J Nat Prod* 59: 808-811.
32. Shaalan EA-S, Canyon D., Wagdy M., Younes F., Abdel-Wahab H., and Mansour A.H. (2005) A review of botanical phytochemicals with mosquitocidal potential. *Environ Int* 31: 1149- 1166.
33. Shen M.Y. and Sali A. (2006) Statistical potential for assessment and prediction of protein structures. *Protein Sci* 2006, 15:2507-2524.
34. Sippl M.J. (1993) Recognition of errors in three-dimensional structures of proteins. *Proteins* 17:355-362.
35. WHO (2006) Report of the Scientific Working Group on dengue. Document WHO/TDR/SWG/08 Geneva, Switzerland. World Health Organization.
36. WHO (2008) Dengue Status in South East Asia Region: An Epidemiological Perspective. Document WHO/TDR/SWG/08 Geneva, Switzerland. World Health Organization.

37. Wiederstein M. and Sippl M.J. (2007) ProSA-web: interactive web service for the recognition of errors in three-dimensional structures of proteins. *Nucleic Acids Res* 35:W407-410.
38. Wu, T. S, Hsu H. C., Wu P. L., Teng C. M., and Wu Y. C. (1998) Rhinacanthin-Q, a naphthoquinone from *Rhinacanthus nasutus* and its biological activity. Phytochemistry 49: 2001-2003.
39. Vijayan V.A., Sathish Kumar B.Y., Ganesh K.N., Urmila J., Fakoorziba M.R., Makkapati A.K. (2007) Efficacy of piperonyl butoxide (PBO) as a synergist with deltamethrin on five species of mosquitoes. *J Commun Dis* 39:159-63.

ผลงานวิจัย (OUTPUT)

1. ผลงานวิจัยที่ตีพิมพ์ในวารสารวิชาการระดับนานาชาติ (International Peer-reviewed Publications):

1. Pethuan, S., Duangkaew, P., Sarapusit, S., Srisook, E., and Rongnoparut, P. (2012). Inhibition against mosquito cytochrome P450 enzymes by rhinacanthin-A, -B, and –C elicits synergism on cypermethrin cytotoxicity in *Spodoptera frugiperda* cells. Journal of Medical Entomology 49: 993-1000.

2. Rongnoparut P, Pethuan S, Sarapusit S, Lertkiatmongkol P (2012) “Metabolism of pyrethroids by mosquito cytochrome P450 enzymes: impact on vector control” in Pest Engineering, InTech, Croatia, 265- 284.

3. Sarapusit S, Lertkiatmongkol P, Duangkaew P and Rongnoparut P (2013) Modeling of *Anopheles minimus* mosquito NADPH-cytochrome P450 oxidoreductase (CYPOR) and mutagenesis analysis. Int. J. Mol. Sci. 14: 1788-1801.

4. Duangkaew P, Pethuan S, Kaewpa D, Sarapusit S, and Rongnoparut P (2011). Characterization of mosquito CYP6P7 and CYP6AA3: differences in substrate preference and kinetic properties. Archives of Insect Biochemistry and Physiology. vol. 76: 236–248.

5. Lertkiatmongkol, P, Jenwitheesuk E, and Rongnoparut, P (2011). Homology modeling of mosquito cytochrome P450 enzymes involved in pyrethroid metabolism: insights into differences in substrate selectivity. BMC Research Notes vol 4: 321.

6. Duangkaew, P, Kaewpa D, and Rongnoparut, P (2011). Use of cytototoxicity assay for evaluation of pyrethroid detoxification of mosquito cytochrome P450. Tropical Biomedicine. Vol. 28: 293-301.

2. International Abstracts:

1. Panida Duangkaew, Kaewpa, and Pornpimol Rongnoparut (2012) Use of cell-based assay in evaluation of insecticide detoxification capability of mosquito cytochrome P450 6P7. 8th SETAC Asia/Pacific Annual Meeting: Learning from History and Applying Advancing Science to Build a Safer and Sustainable Environment, Society of Environmental Toxicology and Chemistry, Kumamoto, Japan, Sep 2012

2. Rattanawadee Kotewong, Panida Duangkaew, Pornpimol Rongnoparut (2012) Expression of membrane-bound *Anopheles minimus* cytochrome P450 6P7 (CYP6P7) in *Escherichia coli*. 13th FAOBMB International Congress of Biochemistry and Molecular Biology, Bangkok, Thailand November 2012

3. Sirikun Pethuan, Panida Duangkaew and Pornpimol Rongnoparut (2010) Inhibition activity of *Rhinacanthus nasutus* and *Stemona spp.* extracts against cytochrome p450 enzymes of *Anopheles minimus* mosquito. 8th International Symposium on Biocontrol and Biotechnology, Pattaya, Thailand. 4-6 October 2010. Awarded Second prize in best academic poster presentation

4. Panida Duangkaew, Soamrutai Boonsuepsakul, Pornpimol Rongnoparut (2010) Use of cytotoxicity assay for evaluation of pyrethroid detoxification activity of mosquito CYP6AA3 enzyme. 8th International Symposium on Biocontrol and Biotechnology, Pattaya, Thailand. 4-6 October 2010. Awarded Honorable mentioned prize for poster presentation

5. Panida Lertkiatmongkol, Ekachai Jenvitheesuk, Pornpimol Rongnoparut (2010) homology modeling of CYP6AA3, the pyrethroid detoxifying enzyme of malaria vector *Anopheles minimus*. 8th International Symposium on Biocontrol and Biotechnology, Pattaya, Thailand. 4-6 October 2010.

3. การนำผลงานไปใช้ประโยชน์

Fluorescent-based and cell-based methods could be applied for rapid screening of inhibitory compounds of cytochrome P450 enzymes that metabolize insecticides. Moreover we have gained knowledge on purified compounds of *R. nasutus* that show synergistic effect on pyrethroid cytotoxicity. Our study thus is in line with the need of new compounds for insecticide resistance management. Upon testing purified compounds with mosquitoes and effect on environments, they can be further developed for practical use in vector control.

APPENDIX

Article

CHARACTERIZATION OF MOSQUITO CYP6P7 AND CYP6AA3: DIFFERENCES IN SUBSTRATE PREFERENCE AND KINETIC PROPERTIES

Panida Duangkaew and Sirikun Pethuan
Department of Biochemistry, Faculty of Science, Mahidol University, Bangkok, Thailand

Dolnapa Kaewpa
Division of Biology, Faculty of Science and Technology, Rajamangala University of Technology Thanyaburi, Pathum Thani, Thailand

Soamrutai Boonsuepsakul
Department of Biochemistry, Faculty of Science, Mahidol University, Bangkok, Thailand

Songklod Sarapusit
Department of Biochemistry, Faculty of Science, Burapha University, Chonburi, Thailand

Pornpimol Rongnoparut
Department of Biochemistry, Faculty of Science, Mahidol University, Bangkok, Thailand

Cytochrome P450 monooxygenases are involved in insecticide resistance in insects. We previously observed an increase in CYP6P7 and CYP6AA3 mRNA expression in Anopheles minimus mosquitoes during the selection for deltamethrin resistance in the laboratory. CYP6AA3 has been shown to metabolize deltamethrin, while no information is known for CYP6P7. In this study, CYP6P7 was heterologously expressed in the Spodoptera frugiperda (Sf9) insect cells via baculovirus-mediated

Grant sponsors: BIOTEC, National Science and Technology Development Agency; Royal Golden Jubilee Program; Thailand Research Fund, and Mahidol University.
Correspondence to: Pornpimol Rongnoparut, Department of Biochemistry, Faculty of Science, Mahidol University, Rama 6 Rd, Phyatai, Bangkok 10400, Thailand. E-mail: scprn@mahidol.ac.th

ARCHIVES OF INSECT BIOCHEMISTRY AND PHYSIOLOGY, Vol. 76, No. 4, 236–248 (2011)
Published online in Wiley Online Library (wileyonlinelibrary.com).
 DOI: 10.1002/arch.20413

expression system. The expressed CYP6P7 protein was used for exploitation of its enzymatic activity against insecticides after reconstitution with the An. minimus NADPH-cytochrome P450 reductase enzyme in vitro. The ability of CYP6P7 to metabolize pyrethroids and insecticides in the organophosphate and carbamate groups was compared with CYP6AA3. The results revealed that both CYP6P7 and CYP6AA3 proteins could metabolize permethrin, cypermethrin, and deltamethrin pyrethroid insecticides, but showed the absence of activity against bioallethrin (pyrethroid), chlorpyrifos (organophosphate), and propoxur (carbamate). CYP6P7 had limited capacity in metabolizing λ-cyhalothrin (pyrethroid), while CYP6AA3 displayed activity toward λ-cyhalothrin. Kinetic properties suggested that CYP6AA3 had higher efficiency in metabolizing type I than type II pyrethroids, while catalytic efficiency of CYP6P7 toward both types was not significantly different. Their kinetic parameters in insecticide metabolism and preliminary inhibition studies by test compounds in the flavonoid, furanocoumarin, and methylenedioxyphenyl groups elucidated that CYP6P7 had different enzyme properties compared with CYP6AA3. © 2011 Wiley Periodicals, Inc.

Keywords: cytochrome P450; pyrethroid; CYP6P7; CYP6AA3; kinetic study

INTRODUCTION

Cytochrome P450 monooxygenases (P450s or CYPs) constitute a superfamily of heme-containing monooxygenases that play roles in the metabolisms of endogenous and exogenous compounds, including insecticides (Feyereisen, 1999). In insects, increased expression level of P450s, leading to enhanced detoxification of insecticides, is suggested to play a role in insecticide resistance (Feyereisen, 1999; Scott, 2008). A link between insecticide resistance, high level of monooxygenase activity, increased P450 expression, and ability of P450s to metabolize insecticides has been noted in various insects. For instance, an increase in CYP6D1 mRNA and protein expression level has been observed in the Learn Pyrethroid Resistant (LPR) strain of *Musca domestica*, and CYP6D1 microsomal enzyme has been shown to metabolize pyrethroids at a higher level in LPR strain than the susceptible strain (Wheelock and Scott, 1992; Tomita et al., 1995; Zhang and Scott, 1996). Overexpression of CYP6BQ9 and CYP6P3 in association with pyrethroid resistance has been reported in deltamethrin-resistant strain of *Tribolium castaneum* and permethrin-resistant field *Anopheles gambiae* mosquitoes, respectively, and heterogously expressed enzymes of *CYP6BQ9* and *CYP6P3* demonstrate activities in pyrethroid metabolism (Müller et al., 2008; Zhu et al., 2010).

Anopheles minimus is one of the primary malaria vectors in Thailand. We previously selected a laboratory strain of *An. minimus* species A for deltamethrin resistance (Chareonviriyaphap et al., 2002). We observed elevated enzyme activities of mixed function oxidases in the resistant mosquitoes, suggesting that P450s could act as a primary route of insecticide detoxification (Chareonviriyaphap et al., 2003). Further studies demonstrated that, among the CYP6 P450 cDNA fragments obtained, *CYP6P7*, *CYP6P8*, and *CYP6AA3* genes were overexpressed in deltamethrin-resistant mosquitoes (Rongnoparut et al., 2003; Rodpradit et al., 2005). The increase in CYP6P7 and CYP6AA3 transcripts was correlated with increased resistance to deltamethrin in

mosquitoes during selection, while there was no such correlation observed for CYP6P8 (Rodpradit et al., 2005). The results suggested that both CYP6P7 and CYP6AA3 might play a role in deltamethrin resistance. However, the fold of increase in CYP6P7 and CYP6AA3 transcripts was different (Rodpradit et al., 2005). Thus, the knowledge of catalytic activities and differences between CYP6P7 and CYP6AA3 in insecticide metabolism may provide a better understanding of insecticide detoxification mechanisms in this mosquito. We previously cloned and expressed the functional CYP6AA3 protein via baculovirus-mediated insect cell expression system and CYP6AA3 showed ability to metabolize deltamethrin in vitro (Kaewpa et al., 2007; Boonsuepsakul et al., 2008). In this study, we expressed CYP6P7 in Sf9 insect cells via baculovirus-mediated expression and investigated CYP6P7 enzymatic activity in insecticide metabolism after reconstituting it with *An. minimus* NADPH-cytochrome P450 reductase (CPR) in a NADPH-regenerating system in vitro. The ability of CYP6P7 in metabolizing pyrethroids and insecticides in the organophosphate and carbamate groups was compared with CYP6AA3. The results revealed that CYP6P7 and CYP6AA3 were capable of metabolizing both types I and II pyrethroids with different substrate preference, but no detectable activity against test organophosphate and carbamate compounds was observed. Kinetic properties and results of preliminary inhibition studies indicated that CYP6P7 was different from CYP6AA3.

MATERIALS AND METHODS

Materials

The chemical compounds, including deltamethrin, permethrin, cypermethrin, λ-cyhalothrin, bioallethrin, chlorpyrifos, propoxur, benzyloxyresorufin, ethoxyresorufin, methoxyresorufin, penthoxyresorufin, 1, 2-didodecanoyl-rac-glycero-3-phosphocholine (DLPC), glucose-6-phosphate, leupeptin, nicotinamide adenosine diphosphate reduced form (NADPH), nicotinamide adenosine diphosphate ($NADP^+$), phenylmethylsulphonyl fluoride (PMSF), dimethyl sulfoxide, α-naphthoflavone, β-naphthoflavone, 5-methoxypsolaren (bergapten), 8-methoxypsoralen (xanthotoxin), piperonyl butoxide (PBO), piperine, and glucose-6-phosphate dehydrogenase (G6PDH) enzyme, were purchased from Sigma-Aldrich (St. Louis, MO). The organic solvents, including acetonitrile (ACN) and ethyl acetate, were of high-performance liquid chromatography (HPLC) grade, obtained from Fisher Scientific (Fair Lawn, NJ). The Sf9 insect cell line and SF-900 II SFM culture media were from Invitrogen (Carlsbad, CA).

Cell Culture and Baculovirus-Mediated Expression of P450s

Expression of CYP6AA3 protein via baculovius-mediated expression in Sf9 cells was prepared following the protocol of Kaewpa et al. (2007). Production of recombinant baculovirus for the expression of CYP6P7 was carried out as previously described (Kaewpa et al., 2007). Briefly, CYP6P7 cDNA isolated from deltamethrin-resistant *An. minimus* (Rodpradit et al., 2005) was subcloned into the transfer vector pBacPAK8 (BD Biosciences, Palo Alto, CA), and co-transfected with linearized BacPAK6 viral DNA into Sf9 cells cultured in SF900 II SFM media at 28°C. For the expression of CYP6P7 protein, Sf9 cells were infected with the CYP6P7 expressed virus (2.5×10^8 plaque-forming units/ml) at multiplicities of infection of 3 (Kaewpa et al., 2007). The infected

cells were harvested at 70–80 hr after infection and resuspended in sodium phosphate buffer pH 7.2 containing 1 mM EDTA, 0.5 mM PMSF, 5 μg/ml leupeptin, 0.1 mM DTT, and 20% glycerol, and were subjected to microsome preparation using differential centrifugation as described (Boonsuepsakul et al., 2008). The CYP6AA3 or CYP6P7 expressed protein in membrane fraction was observed by sodium dodecyl sulfate polyacrylamide gel electrophoresis (SDS-PAGE) and P450 content was measured by reduced-CO difference spectrum analysis according to Omura and Sato (1964).

In Vitro Reconstitution of CYP6P7 and CYP6AA3 Enzymatic Activities Against Insecticides

The in vitro reconstitution assays in the presence of insecticide substrate were performed as previously described with some modifications (Kaewpa et al., 2007). In brief, membrane fraction containing 10 pmol of either CYP6P7 or CYP6AA3 was reconstituted with purified *An. minimus* CPR in the ratio of 3:1 in enzymatic assays (Kaewpa et al., 2007). Insecticides used in the assays included type I pyrethroid (bioallethrin and permethrin), type II pyrethroid (cypermethrin, deltamethrin, and λ-cyhalothrin), carbamate (propoxur), and organophosphate (chlorpyrifos) compounds. The reconstituted P450-reductase system was assayed at 30°C in the presence of DLPC, NADPH-regenerating system (0.6 mM $NADP^+$, 6 mM glucose-6-phosphate, 2 mM $MgCl_2$, 1 U of G6PDH), and 80 μM of insecticide in the total volume of 250 μl. Reaction was initiated by the addition of NADPH-regenerating system. Bioallethrin (100 μM) was used as an internal standard and was added after the reaction was terminated with 30 μl of 2 N HCl at different time points. When testing enzyme activity with bioallethrin as a substrate, deltamethrin was used as an internal standard. The remaining substrate was extracted with 750 μl ethyl acetate, and the extract was dried under a stream of N_2 gas, dissolved with ACN before subjected to HPLC analysis using C18-reverse phase column (Nova-Pak®C18 4 μM 3.9 × 150 mm; Waters, Milford, MA). HPLC gradient was initiated at 50% ACN in water (v/v) for 5 min, a linear gradient from 50 to 100% ACN over 3 min, 100% ACN was held for 8 min, followed by a linear gradient returning to 50% ACN over 3 min, and final equilibration with 50% ACN for 6 min. Unmetabolized insecticide and internal standard peaks were monitored by UV detection at 220 nm. The substrate peak area in each reaction was compared with that of time zero. The enzyme activity was determined as substrate disappearance/min/pmol P450. Each of reconstitution experiments was performed in three independent repetitions and internal standard was used for normalization among reactions. Control reactions were performed including reactions without NADPH, in the presence of PBO (P450 inhibitor), and using parental Sf9 membrane.

In Vitro Reconstitution of CYP6P7 and CYP6AA3 Enzymatic Activities With Fluorescent Substrates

The P450-mediated *O*-dealkylation reaction of each of resorufin derivatives (10 μM final concentration) was performed in 50 mM Tris–HCl buffer pH 7.5, in a total volume of 500 μl. Membrane fractions containing either CYP6P7 or CYP6AA3 (~25 pmol each) were used and enzymatic activities were assayed after reconstituted with purified CPR in the ratio of 3:1. Fluorescent substrates dissolved in dimethyl sulfoxide (1% final concentration) were benzyloxyresorufin, ethoxyresorufin, methoxyresorufin, and penthoxyresorufin. Each reaction was initiated by the addition of NADPH to a final concentration of 1 mM. Resorufin product was measured at

$\lambda_{ex} = 530$ and $\lambda_{em} = 590$ nm using RF-5301 PC spectrofluorophotometer (Shimadzu, Kyoto, Japan). The amount of resorufin product was calculated referring to the resorufin standard curve. Rate of resorufin formation was expressed as pmol resorufin/min/pmol P450.

Steady-State Kinetic Parameter Analysis

To obtain the steady-state kinetic parameters (K_m and V_{max}), reaction rates were measured under linear conditions using different substrate concentrations ranging from 0 to 320 μM for permethrin, 0–640 μM for deltamethrin, λ-cyhalothrin, and cypermethrin, and 0–16 μM for benzyloxyresorufin. The kinetic parameters K_m and V_{max} were determined from the plot of substrate concentrations vs. initial velocity (V_0) by fitting experimental data to the Michaelis–Menten equation, using nonlinear regression analysis of GraphPad Prism 5 (GraphPad Software Inc., San Diego, CA). The catalytic efficiency, defined as V_{max}/K_m, was calculated from the estimated K_m and V_{max} values.

Fluorescence-Based CYP6P7 and CYP6AA3 Inhibition Assay

In this study, we used benzyloxyresorufin as a substrate for preliminary studies of CYP6P7 and CYP6AA3 inhibition assays. Reaction conditions were performed as described for fluorescence reconstitution assays. Inhibitors tested were α-naphthoflavone, β-naphthoflavone, xanthotoxin, bergapten, PBO, and piperine. Assays were carried out by incubating benzyloxyresorufin substrate at the concentration approximately K_m value (0.5 μM for CYP6P7 and 2 μM for CYP6AA3) in the presence of different concentrations of individual test inhibitors dissolved in dimethyl sulfoxide (1% final concentration). Inhibitory effect of each compound at each concentration was calculated as percent relative inhibition compared with the vehicle control reaction.

Time- and NADPH-dependent inhibition activity of test compounds against benzyloxyresorufin-*O*-debenzylation (BROD) activities of CYP6P7 and CYP6AA3 was preliminarily investigated as a primary indication of mechanism-based inhibition. Assays were performed by pre-incubating enzyme with various concentrations of test compounds in the presence or absence of NADPH for 30 min before the addition of benzyloxyresorufin. The IC_{50} values were determined and compared between reactions pre-incubating with and without NADPH. An indication of mechanism-based inhibition is the IC_{50} shift to lower range in the assay pre-incubating with NADPH (Fowler and Zhang, 2008). Type of inhibition and apparent inhibition constant K_i were determined if the test inhibitor gave reversible inhibition pattern. Various concentrations of inhibitors and substrates were used for the generation of Lineweaver–Burk plots using GraphPad Prism 5. Type of inhibition was determined graphically from Lineweaver–Burk plots. The K_i values were obtained via secondary plots of the slopes from Lineweaver–Burk plots.

RESULTS

Characterization of CYP6P7 and CYP6AA3 Activities in Insecticide Metabolism

The *An. minimus* CYP6P7 protein was successfully expressed in Sf9 insect cells via baculovirus-directed expression system. Total P450 content calculated from the characteristic spectrum was approximately 200–300 pmol per milligram membrane protein, and membrane preparation of the functional CYP6P7 was used for the

reconstitution of enzymatic assays as previously described (Boonsuepsakul et al., 2008). In this study, we examined CYP6P7 enzymatic activity against insecticides commonly used in mosquito vector control programs and agricultural practices in Thailand (Chareonviriyaphap et al., 1999; Thapinta and Hudak, 2000; Vector Borne Disease Annual Report, 2002–2003). These included type I and type II pyrethroids, (bioallethrin, permethrin, λ-cyhalothrin, cypermethrin, and deltamethrin), organophosphate (chlorpyrifos), and carbamate (propoxur) insecticides. As shown in Figure 1, CYP6P7 could metabolize both type I and type II pyrethroids, namely permethrin, cypermethrin, and deltamethrin, while there was no detectable enzyme activity against bioallethrin and λ-cyhalothrin using methods described in this study. In parallel, there was an absence of CYP6P7 activity toward chlorpyrifos and propoxur. The absence of CYP6P7 activity in the reactions without NADPH and in the presence of PBO (P450 inhibitor) indicated that the detected enzyme activities in insecticide metabolism were due to the cytochrome P450 CYP6P7 protein (unreported data). When tested these insecticide compounds with CYP6AA3, the results demonstrated that CYP6AA3 could metabolize all test pyrethroids except bioallethrin. Similar to CYP6P7, there was absence of CYP6AA3 activity in chlorpyrifos and propoxur degradation. The cypermethrin consumption rate of CYP6P7 was higher than CYP6AA3, whereas its permethrin consumption rate was lower than CYP6AA3 (Fig. 1).

Kinetic Analysis of CYP6P7 and CYP6AA3 Enzymes

The steady-state kinetics of CYP6P7 in metabolizing pyrethroids were investigated at various substrate concentrations and compared with CYP6AA3. The apparent K_m, V_{max} and catalytic efficiency (V_{max}/K_m) were determined from the best nonlinear fit of data to the Michaelis–Menten equation ($r^2 > 0.9$). As shown in Table 1, the catalytic efficiency (V_{max}/K_m) values of CYP6P7 for permethrin, cypermethrin, and deltamethrin were not significantly different. On the other hand, CYP6AA3 could metabolize type I pyrethroid permethrin with significantly higher efficiency than all type II pyrethroids. The better catalytic efficiency of CYP6AA3 toward permethrin was contributed by both its lower K_m and higher V_{max} values than toward type II pyrethroids.

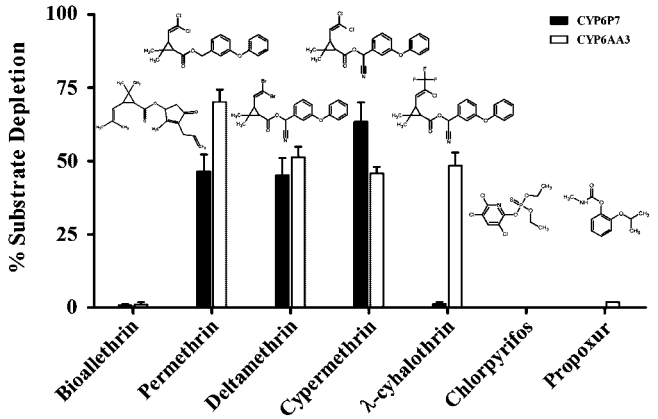

Figure 1. The CYP6P7- and CYP6AA3-mediated insecticide metabolism. The reconstitution assays were performed using 80 μM final concentration of each insecticide substrate. Insecticide metabolisms were measured and expressed as percent substrate depletion over 30 min of incubation. Values are mean ± SD of three replicated experiments.

Table 1. Kinetic Constants for CYP6P7- and CYP6AA3-Mediated Pyrethroid Metabolism

	CYP6P7[a]			*CYP6AA3*[a]		
Compounds	K_m (μM)	V_{max}[b]	V_{max}/K_m	K_m (μM)	V_{max}[b]	V_{max}/K_m
Type I pyrethroids						
Permethrin	69.7±10.5	65.7±1.6	0.96±0.13	41.0±8.5	124.2±1.2	3.03±0.34[c]
Type II pyrethroids						
Cypermethrin	97.3±6.4	83.3±7.6	0.86±0.05	70.0±7.1	40.0±7.1	0.57±0.04
Deltamethrin	73.3±2.9	55.3±5.7	0.75±0.05	80.2±2.0	60.2±3.6	0.75±0.03
λ-Cyhalothrin	N.D.[d]	N.D.[d]	N.D.[d]	78.3±7.0	60.7±1.1	0.78±0.06

[a]Values are mean±SD of three replicated experiments.
[b]V_{max} was measured as pmol substrate disappearance/min/pmol P450.
[c]Significant differences between V_{max}/K_m values of CYP6AA3 in pyrethroid metabolisms, as determined by one-way ANOVA Tukey's multiple comparison test ($P<0.05$). All V_{max}/K_m values of CYP6P7 in metabolizing pyrethroids were not significantly different.
[d]N.D., not determined.

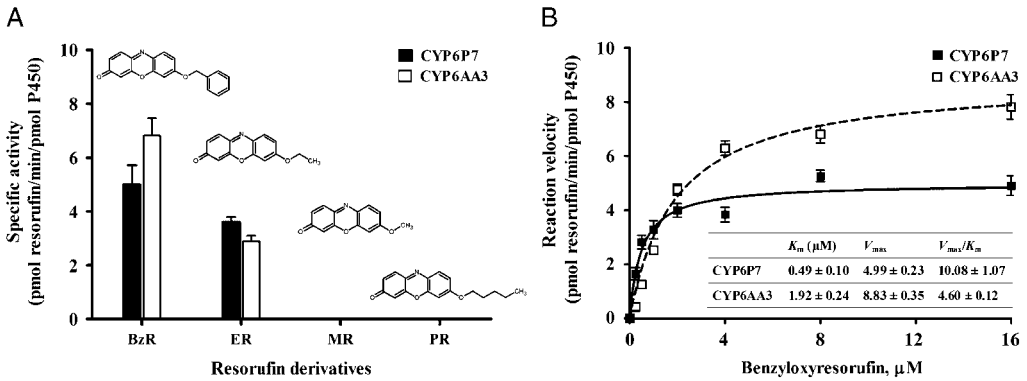

Figure 2. Specific activities of CYP6P7 and CYP6AA3 toward resorufin derivatives (**A**) and Michaelis–Menten plot of CYP6P7- and CYP6AA3-BROD activities (**B**). The resorufin derivatives are benzyloxyresorufin (BzR), ethoxyresorufin (ER), methoxyresorufin (MR), and penthoxyresorufin (PR). Data are mean±SD of triplicates.

Metabolism of the Fluorescent Substrates

To characterize for potential fluorogenic substrate probe and for use in inhibition studies of CYP6P7 and CYP6AA3, four resorufin fluorogenic substrates containing different alkyl groups including benzyloxyresorufin, ethoxyresorufin, methoxyresorufin, and penthoxyresorufin were screened. Both CYP6P7 and CYP6AA3 could metabolize benzyloxyresorufin and ethoxyresorufin, with higher specific activities toward benzyloxyresorufin than ethoxyresorufin, while there was absence of activities against methoxyresorufin and penthoxyresorufin (Fig. 2A). Thus, benzyloxyresorufin was used as a substrate in inhibition studies. From kinetic studies, CYP6P7 could metabolize benzyloxyresorufin with approximately twofold higher efficiency than CYP6AA3, contributed by low binding constant to benzyloxyresorufin (Fig. 2B).

Analysis of CYP6P7 and CYP6AA3 Enzyme Inhibition

To further characterize CYP6P7 and CYP6AA3 enzymes, we used known P450 inhibitors with different structures to compare their inhibition profile against these two

Table 2. IC_{50} Values for Inhibition of CYP6P7- or CYP6AA3-Mediated BROD Activities

	IC_{50} (μM)[a]			
	CYP6P7, pre-incubation		*CYP6AA3, pre-incubation*	
Inhibitor	*(−) NADPH*	*(+) NADPH*	*(−) NADPH*	*(+) NADPH*
Flavonoid				
α-Naphthoflavone	2.90±0.27	3.03±0.45	0.37±0.06	0.38±0.06
β-Naphthoflavone	17.25±3.67	33.35±9.90	19.22±3.13[b]	34.44±5.95[b]
Furanocoumarin				
Bergapten	52.76±6.77[b]	114.00±11.81[b]	93.77±10.87[b]	170.30±16.88[b]
Xanthotoxin	33.77±3.54[b]	78.93±10.04[b]	51.04±2.15	52.17±2.86
MDP compound				
PBO	31.77±3.21[b]	16.22±1.81[b]	9.91±0.81[b]	4.04±0.31[b]
Piperine	52.86±6.92[b]	3.48±0.36[b]	15.26±1.21[b]	4.86±0.79[b]

[a]Values are mean±SD of triplicate experiments.
[b]Significant differences between (−) NADPH and (+) NADPH, $P<0.05$, Student's *t*-test.

P450s. The compounds included flavonoids (α- and β-naphthoflavone), furanocoumarins (bergapten and xanthotoxin), methylenedioxyphenyl, or MDP-containing compounds (PBO and piperine). To initially examine whether test compounds could inhibit both P450s in a mechanism-based inhibition pattern, the experiments were carried out by pre-incubating each test compound with the enzyme mixture in the presence or absence of NADPH for 30 min before the addition of benzyloxyresorufin substrate. Both PBO and piperine showed time and NADPH-dependent inhibition activities against both enzymes, indicating a typical mechanism-based inhibition characteristic (Table 2). CYP6P7 was less efficiently inhibited by PBO than CYP6AA3.

Among all test inhibitors, α-naphthoflavone had the most potent inhibitory activity against both enzymes, and it inhibited CYP6P7 with IC_{50} and K_i values higher than CYP6AA3 (see Table 2, Fig. 3). The IC_{50} values of α-naphthoflavone against both enzymes were similar under pre-incubations with and without NADPH. The CYP6P7 activity was inhibited by bergapten and xanthotoxin more efficiently when pre-incubated without NADPH than in the presence of NADPH. This was observed by the significantly higher IC_{50} value shift on pre-incubations of bergapten and xanthotoxin with NADPH. For CYP6AA3, the significantly higher IC_{50} value shift was observed for β-naphthoflavone and bergapten, but not for xanthotoxin.

Differences in higher IC_{50} value shift of xanthotoxin observed between CYP6P7 and CYP6AA3 prompted us to further investigate type of enzyme inhibition by xanthotoxin compared with bergapten and, in addition, to α-naphthoflavone which is the most potent inhibitor. Study of type of inhibition was performed and Lineweaver–Burk plots are shown in Figure 3. The K_i values shown in Figure 3 were comparable to IC_{50} values in Table 2. The results elucidated that α-naphthoflavone could uncompetitively inhibit both enzymes, while bergapten inactivated both enzymes in a mixed-type inhibition pattern. The difference in type of inhibition was noted for xanthotoxin as it uncompetitively inhibited CYP6AA3 enzyme, while inhibition against CYP6P7 was mixed type.

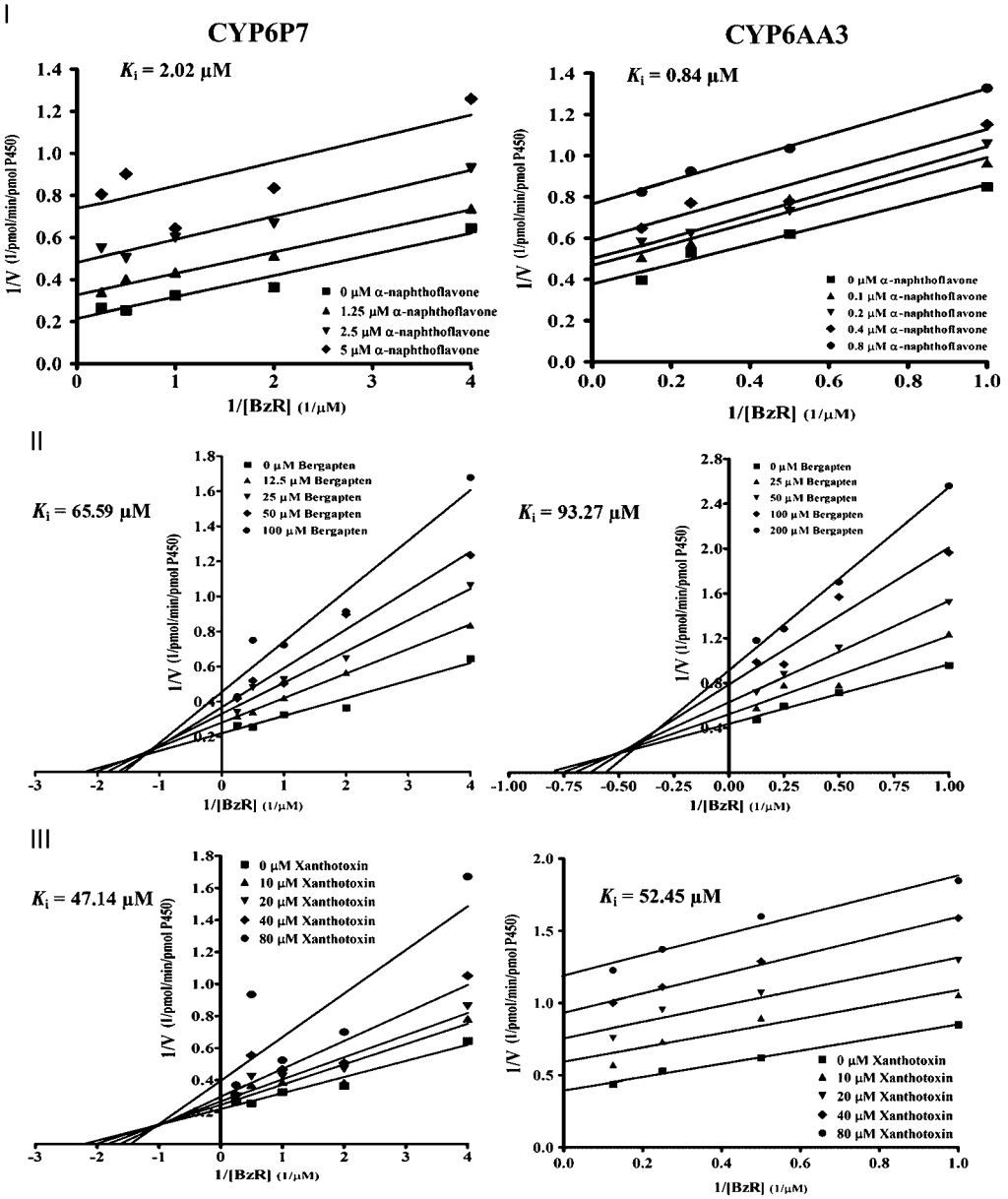

Figure 3. Lineweaver–Burk plots for the inhibition of CYP6P7- or CYP6AA3-BROD activities by α-naphthoflavone (I) bergapten (II), and xanthotoxin (III). Data are means of triplicate experiments.

DISCUSSION

In this study, the role of CYP6P7 and CYP6AA3 in the metabolisms of type I and type II pyrethroids, organophosphate, and carbamate was investigated. The reconstitution enzymatic assays measuring substrate depletion revealed that both CYP6P7 and CYP6AA3 could metabolize pyrethroids but were incapable of degrading test organophosphate and carbamate compounds, suggesting that both enzymes could

play a role in detoxification of pyrethroids in mosquitoes in vivo. The ability of both enzymes in metabolizing permethrin, cypermethrin, and deltamethrin may partly rely on the presence of phenoxybenzyl group in the alcohol moiety of substrate (see Fig. 1). This is accentuated by that CYP6P7 and CYP6AA3 lacked enzymatic activities toward bioallethrin and more structurally distant chlorpyrifos and propoxur insecticides, determined by methods used in this study. A clear difference existed between CYP6P7 and CYP6AA3 activities as demonstrated by the absence of CYP6P7 activity in degradation of λ-cyhalothrin, while CYP6AA3 could metabolize λ-cyhalothrin with similar kinetic values as for deltamethrin. The presence of CF_3- at the dihalovinyl groups in the acid moiety of λ-cyhalothrin (see Fig. 1) could be responsible for the absence of CYP6P7 enzyme activity.

CYP6P7 could metabolize pyrethroids with values of catalytic efficiency not significantly different between the two pyrethroid types. In contrast, CYP6AA3 was more active toward type I than type II pyrethroids, similar to human CYP2C19 and rat CYP2C6, in having higher rate of eliminating permethrin than λ-cyhalothrin and cypermethrin (Scollon et al., 2009). Moreover, CYP6P7 and CYP6AA3 metabolized deltamethrin with similar efficiency (an equal value of 0.75), but were 5- to 10-fold less efficient than human CYP2C8 and CYP2C19 as well as rat CYP2C6 and CYP2C11 (values range from 4.2 to 6.9, Godin et al., 2007).

Both CYP6P7 and CYP6AA3 enzymes possess K_m values either higher or in the same range as other insect P450s, but they have better capacity in metabolizing pyrethroids than other insect P450s, attributed by their higher rate of pyrethroid degradation. For instance, *A. gambiae* CYP6P3 has higher affinity for deltamethrin ($K_m = 5.9\,\mu M$) but its low V_{max} value ($1.8\,min^{-1}$; Müller et al., 2008) makes CYP6P3 approximately two to threefolds less efficient than *An. minimus* enzymes. In *Helicoverpa zea*, CYP6B8, co-expressed with house fly CPR in baculovirus expression system, has K_m values in the same range as CYP6P7 and CYP6AA3, but its efficiency in degrading cypermethrin is approximately three to sixfold lower than those reported herein (Li et al., 2004). Higher P450 turnover rate could be due to efficient catalytic site of P450s or due to high electron transfer rate through CPR redox partner. For example, CYP6AB3v2 can metabolize imperatorin substrate at a rate of about threefold faster than the CYP6AB3v1 variant form, due to higher NADPH consumption rate (Mao et al., 2007).

The ability of CYP6P7 and CYP6AA3 in metabolizing pyrethroids lends support to their role in deltamethrin detoxification in *An. minimus* (Rodpradit et al., 2005). Consistently, CYP6P8 protein, expressed via baculovirus-mediated expression system, did not show detectable activity against pyrethroids with the methods used (unreported data). Thus, sequence similarity may not contribute to functions of P450 enzymes, since CYP6P7 has higher amino acid identity to CYP6P8 (61% identity) than to CYP6AA3 (40% identity) but the metabolic capacity toward insecticides of CYP6P7 is more related to CYP6AA3 than CYP6P8. An example is shown in *H. zea* that CYP6B8 and CYP321A1 proteins share only 32% primary sequence identity, but both can metabolize cypermethrin (Li et al., 2004; Sasabe et al., 2004; Rupasinghe et al., 2007). It could imply that three-dimensional structures of active sites of insect P450s may play a role in their substrate selectivity rather than sequence similarity among enzymes.

The fluorescence alkyloxyresorufins have been reported as substrates for several P450s (Scott et al., 2000; Mclaughlin et al., 2008). In this study, *An. minimus* CYP6P7 and CYP6AA3 could metabolize benzyloxyresorufin that contains planar aromatic benzene ring substituted group more efficiently than ethoxyresorufin that contains

substituted hydrocarbon chain. CYP6P7 has higher affinity to benzyloxyresorufin than CYP6AA3, emphasizing differences in metabolic capability between these two enzymes. Using benzyloxyresorufin as substrate, we characterized the inhibition of CYP6P7- and CYP6AA3-BROD activities using known P450 inhibitors of different structures. The MDP-containing compounds (PBO and piperine) have been shown inhibiting human, rat, and insect P450s via mechanism-based inhibition (Scott et al., 2000; Bhardwaj et al., 2002; Correia and Ortiz de Montellano, 2005; Subehan et al., 2006). In this study, PBO and piperine also displayed mechanism-based inhibition on CYP6P7 and CYP6AA3. However, CYP6P7 was three to fourfold less susceptible to mechanism-based inhibition by PBO than CYP6AA3. Similarly, α-naphthoflavone was eight times less potent against CYP6P7 than CYP6AA3. In other insect P450s, α-naphthoflavone exhibited strong inhibitory effect against *An. gambiae* CYP6Z2-BROD activity with the IC_{50} value of 0.007 μM (Mclaughlin et al., 2008) and against housefly CYP6D1- methoxyresorufin-*O*-demethylation activities (MROD) activity with the IC_{50} value of 0.28 μM (Scott et al., 2000), a value approximately similar to CYP6AA3. In β-naphthoflavone, the position of the naphthyl group could account for approximately five to sevenfold lower inhibitory effect against CYP6P7 and CYP6AA3 than α-naphthoflavone.

It appears that both bergapten and xanthotoxin exhibited low inhibitory effect against both P450s. Moreover, pre-incubation with bergapten and xanthotoxin in the presence of NADPH decreased their inhibition effect on CYP6P7 activity, but only bergapten decreased the inhibition effect on CYP6AA3. Similar reduction of inhibition was observed for phenacetin and diclofenac, for example, against CYP1A2 and CYP2C9 activities, respectively (Yamamoto et al., 2002). Since phenacetin and diclofenac are also substrates of CYP1A2 and CYP2C9, respectively, thus it explains the reduced inhibitory effect of these compounds against P450 activities (Yamamoto et al., 2002). Further study of CYP6P7 and CYP6AA3 activities with bergapten in the absence of benzyloxyresorufin substrate to determine whether it could behave as substrate could help explaining the results of this study.

We further analyzed the type of inhibition and compared between CYP6P7 and CYP6AA3. It appears that xanthotoxin uncompetitively inhibited CYP6AA3, implicating that xanthotoxin could reversibly bind the CYP6AA3–benzyloxyresorufin complex. In contrast, xanthotoxin inhibited CYP6P7 in a mixed-type inhibition pattern, suggesting that it could competitively interact with free CYP6P7 at or near benzyloxyresorufin binding site and noncompetitively bind to the allosteric site (Segal, 1975; Correia and Ortiz de Montellano, 2005). Such inhibition results emphasize differences of CYP6P7 and CYP6AA3 properties.

The results obtained in this study address that CYP6P7 and CYP6AA3 may partly share structural properties that influence overlapping but different substrate specificity and catalytic efficiency. Moreover inhibition studies revealed that both CYP6P7 and CYP6AA3 were differently inhibited by test inhibitors. Taken together, it could imply that different properties of CYP6P7 and CYP6AA3 may be advantageous to *An. minimus* by their working together in detoxifying insecticides. Nevertheless, the results of this study do not exclude the possibility that other P450s in this mosquito could play role in insecticide detoxification. However, how CYP6P7 and CYP6AA3 have a redundancy of metabolizing overlapping set of pyrethroids and how they contribute to actual detoxification in *An. minimus* in vivo are not known. Finally, the results obtained from this study could contribute to better control of this mosquito vector.

ACKNOWLEDGMENTS

This work was supported by BIOTEC, National Science and Technology Development Agency (NSTDA); Royal Golden Jubilee Program (RGJ); and partly supported by Thailand Research Fund (TRF) and Mahidol University.

LITERATURE CITED

Bhardwaj RK, Glaeser H, Becquemont L, Klotz U, Gupta SK, Fromm MF. 2002. Piperine, a major constituent of black pepper, inhibits human P-glycoprotein and CYP3A4. J Pharmacol Exp Ther 302:645–650.

Boonsuepsakul S, Luepromchai E, Rongnoparut P. 2008. Characterization of *Anopheles minimus* CYP6AA3 expressed in recombinant baculovirus system. Arch Insect Biochem Physiol 69:13–21.

Chareonviriyaphap T, Aum-aung B, Ratanatham S. 1999. Current insecticide resistance patterns in mosquito vectors in Thailand. Southeast Asian J Trop Med Public Health 30:184–194.

Chareonviriyaphap T, Rongnoparut P, Juntarumporn P. 2002. Selection for pyrethroid resistance in a colony of *Anopheles minimus* species A, a malaria vector in Thailand. J Vector Ecol 27:222–229.

Chareonviriyaphap T, Rongnoparut P, Chantarumporn P, Bangs MJ. 2003. Biochemical detection of pyrethroid resistance mechanisms in *Anopheles minimus* in Thailand. J Vector Ecol 28:108–116.

Correia MA, Ortiz de Montellano PR. 2005. Inhibition of cytochrome P450 enzymes. In: Ortiz de Montellano PR, editor. Cytochrome P450: structure, mechanism, and biochemistry, 3rd ed. New York: Kluwer Academic/Plenum Publishers. p 247–322.

Feyereisen R. 1999. Insect P450 enzymes. Annu Rev Entomol 44:507–533.

Fowler S, Zhang H. 2008. *In vitro* evaluation of reversible and irreversible cytochrome P450 inhibition: current status on methodologies and their utility for predicting drug–drug interactions. AAPS J 10:410–424.

Godin SJ, Crow JA, Scollon EJ, Hughes MF, DeVito MJ, Ross MK. 2007. Identification of rat and human cytochrome P450 isoforms and a rat serum esterase that metabolize the pyrethroid insecticides deltamethrin and esfenvalerate. Drug Metab Dispos 35:1664–1671.

Kaewpa D, Boonsuepsakul S, Rongnoparut P. 2007. Functional expression of mosquito NADPH-cytochrome P450 reductase in *Escherichia coli*. J Econ Entomol 100:946–953.

Li X, Baudry J, Berenbaum MR, Schuler MA. 2004. Structural and functional divergence of insect CYP6B proteins: from specialist to generalist cytochrome P450. Proc Natl Acad Sci USA 101:2939–2944.

Mao W, Rupasinghe SG, Zangerl AR, Berenbaum MR, Schuler MA. 2007. Allelic variation in the *Depressaria pastinacella* CYP6AB3 protein enhances metabolism of plant allelochemicals by altering a proximal surface residue and potential interactions with cytochrome P450 reductase. J Biol Chem 282:10544–10552.

Mclaughlin LA, Niazi U, Bibby J, David JP, Vontas J, Hemingway J, Ranson H, Sutcliffe MJ, Paine MJI. 2008. Characterization of inhibitors and substrates of *Anopheles gambiae* CYP6Z2. Insect Mol Biol 17:125–135.

Müller P, Warr E, Stevenson BJ, Pignatelli PM, Morgan JC, Steven A, Yawson AE, Mitchell SN, Ranson H, Hemingway J, Paine MJI, Donnelly MJ. 2008. Field-caught permethrin-resistant *Anopheles gambiae* overexpress CYP6P3, a P450 that metabolises pyrethroids. PLoS Genet 4:e1000286.

Omura T, Sato R. 1964. The carbon monoxide-biding pigment of liver microsome. I. Evidence for its hemoprotein nature. J Biol Chem 239:2370–2378.

Rodpradit P, Boonsuepsakul S, Chareonviriyaphap T, Bangs MJ, Rongnoparut P. 2005. Cytochrome P450 genes: molecular cloning and overexpression in a pyrethroid-resistant strain of *Anopheles minimus* mosquito. J Am Mosq Control Assoc 21:71–79.

Rongnoparut P, Boonsuepsakul S, Chareonviriyaphap T, Thanomsing N. 2003. Cloning of cytochrome P450, CYP6P5, and CYP6AA2 from *Anopheles minimus* resistant to deltamethrin. J Vector Ecol 28:150–158.

Rupasinghe SG, Wen Z, Chiu TL, Schuler MA. 2007. *Helicoverpa zea* CYP6B8 and CYP321A1: different molecular solutions to the problem of metabolizing plant toxins and insecticides. Protein Eng Des Sel 20:615–624.

Sasabe M, Wen Z, Berenbaum MR, Schuler MA. 2004. Molecular analysis of CYP321A1, a novel cytochrome P450 involved in metabolism of plant allelochemicals (furanocoumarins) and insecticides (cypermethrin) in *Helicoverpa zea*. Gene 338:163–175.

Scollon EJ, Starr JM, Godin SJ, DeVito MJ, Hughes MF. 2009. *In vitro* metabolism of pyrethroid pesticides by rat and human hepatic microsomes and cytochrome P450 isoforms. Drug Metab Dispos 37:221–228.

Scott JG. 2008. Insect cytochrome P450s: thinking beyond detoxification. In: Liu N, editor. Recent advances in insect physiology, toxicology and molecular biology. Kerala, India: Research Signpost. p 117–124.

Scott JG, Foroozesh M, Hopkins NE, Alefantis TG, Alworth WL. 2000. Inhibition of cytochrome P450 6D1 by alkynylarenes, methylenedioxyarenes, and other substituted aromatics. Pestic Biochem Physiol 67:63–71.

Segal IH. 1975. Enzyme kinetics: behavior and analysis of rapid equilibrium and steady-state enzyme systems. New York: Wiley. 975p.

Subehan, Usia T, Kadota S, Tezuka Y. 2006. Mechanism-based inhibition of human liver microsomal cytochrome P450 2D6 (CYP2D6) by alkamides of *Piper nigrum*. Planta Med 72:527–532.

Thapinta A, Hudak PF. 2000. Pesticide use and residual occurrence in Thailand. Environ Monit Assess 60:103–114.

Tomita T, Liu N, Smith FF, Sridhar P, Scott JG. 1995. Molecular mechanisms involved in increased expression of a cytochrome P450 responsible for pyrethroid resistance in the housefly, *Musca domestica*. Insect Mol Biol 4:135–140.

Vector Borne Disease Annual Report. 2002–2003. Bureau of Vector Borne Disease, Department of Communicable Disease Control, Ministry of Public Health, Thailand.

Wheelock GD, Scott JG. 1992. The role of cytochrome $P450_{lpr}$ in deltamethrin metabolism by pyrethroid-resistant and susceptible strains of house flies. Pestic Biochem Physiol 43:67–77.

Yamamoto T, Suzuki A, Kohno Y. 2002. Application of microtiter plate assay to evaluate inhibitory effects of various compounds on nine cytochrome P450 isoforms and to estimate their inhibition patterns. Drug Metab Pharmacokin 17:437–448.

Zhang M, Scott JG. 1996. Cytochrome b_5 is essential for cytochrome P450 6D1-mediated cypermethrin resistance in LPR house flies. Pestic Biochem Physiol 55:150–156.

Zhu F, Parthasarathy R, Bai H, Woithe K, Kaussmann M, Nauen R, Harrison DA, Palli SR. 2010. A brain-specific cytochrome P450 responsible for the majority of deltamethrin resistance in the QTC279 strain of *Tribolium castaneum*. Proc Natl Acad Sci USA 107:8557–8562.

Tropical Biomedicine 28(2): 293–301 (2011)

Protective efficacy of *Anopheles minimus* CYP6P7 and CYP6AA3 against cytotoxicity of pyrethroid insecticides in *Spodoptera frugiperda* (Sf9) insect cells

Duangkaew, P.[1], Kaewpa, D.[2] and Rongnoparut, P.[1*]
[1] Department of Biochemistry, Faculty of Science, Mahidol University, Bangkok, Thailand 10400
[2] Division of Biology, Faculty of Science and Technology, Rajamangala University of Technology Thanyaburi, Pathum Thani, Thailand 12110
[*] Correspondence author email: scprn@mahidol.ac.th
Received 15 November 2010; received in revised form 6 January 2011; accepted 23 January 2011

Abstract. Cytochrome P450 monooxygenases (P450s) are enzymes known to metabolize a wide variety of compounds including insecticides. Their overexpression leading to enhanced insecticide detoxification could result in insecticide resistance in insects. The increased mRNA expression of two P450 genes, *CYP6P7* and *CYP6AA3*, has been previously observed in laboratory-selected deltamethrin-resistant *Anopheles minimus*, a major malaria vector in Southeast Asia, suggesting their role in detoxification of pyrethroids. In this study CYP6P7 and CYP6AA3 were expressed in insect *Spodoptera frugiperda* (Sf9) cells via baculovirus-directed expression system. Insecticide detoxification capabilities of Sf9 cells with and without expression of CYP6P7 or CYP6AA3 were evaluated using 3-(4,5-dimethyl-thiazol-2-yl)-2,5-diphenyltetrazolium bromide (MTT) assays. The results revealed that CYP6P7- or CYP6AA3-expressing cells showed significantly higher cytoprotective capability than parental Sf9 cells against cytotoxicity of pyrethroids including permethrin, cypermethrin and deltamethrin. Such cytoprotective effect was not observed for bioallethrin (pyrethroid), chlorpyrifos (organophosphate) and propoxur (carbamate). Moreover, expression of CYP6AA3, but not CYP6P7, could protect cells against λ-cyhalothrin cytotoxicity. In MTT assays upon co-incubation with piperonyl butoxide (P450 inhibitor), cytoprotective ability of CYP6P7 and CYP6AA3 against deltamethrin was diminished, implying that pyrethroid detoxification was due to activities of P450 enzymes. Insecticide detoxification capabilities of CYP6P7 and CYP6AA3 observed from MTT assays were correlated to their pyrethroid metabolizing activities observed from *in vitro* reconstitution enzymatic assays. Thus MTT assays using cells expressing P450 enzymes of interest could be primarily used to determine detoxification activities of enzymes against cytotoxic insecticides.

INTRODUCTION

Control of mosquito vectors relying on applications with chemical insecticides is an important strategy in preventing transmission of vector-borne diseases, including malaria. Pyrethroid insecticides are currently used worldwide in agriculture and for vector control, however long-term extensive use of insecticides has been a major cause of development of insecticide resistance among mosquito populations (Coleman & Hemingway, 2007). Consequently, resistance can lead to reduced efficacy of vector control programme. Pyrethroid resistance in mosquito vectors of malaria has been reported in several countries in Africa and Southeast Asia, including Thailand (Charoenviriyaphap *et al.*, 1999; Bortel *et al.*, 2008; Munhenga *et al.*, 2008; Cuamba *et al.*, 2010; Matowo *et al.*, 2010).

Cytochrome P450 monooxygenases (P450s) comprise a superfamily of enzymes that catalyze metabolisms of endogenous and xenobiotic compounds, including

insecticides (Feyereisen, 1999). Examinations of various insects have suggested involvement of P450s in resistance to different insecticides, by virtue of enhanced expression of P450s and thus increased detoxification of insecticides. (Feyereisen, 1999). Overexpression of P450s has been observed in several pyrethroid resistant insects such as increased expression of *CYP6D1* has been found in pyrethroid resistant *Musca domestica* (Tomita *et al.*, 1995), *CYP6P3* and *CYP6M2* in multiple pyrethroid resistant *Anopheles gambiae* (Djouaka *et al.*, 2008).

Anopheles minimus is one of malaria vectors in Southeast Asia, including Thailand, Loas, Cambodia, and Vietnam. We previously determined that P450 enzymes might act as a primary route of deltamethrin detoxification during laboratory selection for deltamethrin resistance in *An. minimus* (Chareonviriyaphap *et al.*, 2003). In parallel during selection, increased mRNA expression of *CYP6P7* and *CYP6AA3* was observed (Rongnoparut *et al.*, 2003; Rodpradit *et al.*, 2005). Thus CYP6P7 and CYP6AA3 could be implicated to play a role in detoxification of deltamethrin in this mosquito.

Pyrethroids are known to commonly target on sodium channels of nervous system. Other toxic effects of pyrethroids toward cells include causing DNA damage, inhibition of mitochondrial complex I, and induction of reactive oxygen species (ROS) accumulation (Gassner *et al.*, 1997; Villarini *et al.*, 1998; Naravaneni *et al.*, 2005; Patel *et al.*, 2007). Cytotoxic effects of organophosphate and carbamate insecticides have also been reported such as oxidative stress, alteration of mitochondria function (Swann *et al.*, 1996; Schmuck & Mihail, 2004; Maran *et al.*, 2010). Thus treatment of cells with cytotoxic insecticides in cytotoxicity assays can cause cell mortality unless cells possess ability to detoxify insecticides. This is supported by that *Spodoptera frugiperda* (Sf9) insect cells expressing CYP6AA3 have significantly higher cell viability upon treatment with deltamethrin than cells without CYP6AA3 expression in MTT cytotoxicity assay, suggesting that CYP6AA3 could detoxify deltamethrin in Sf9 cells (Boonsuepsakul *et al.*, 2008).

In this study, we further employed MTT cytotoxicity assays to investigate detoxification capability of Sf9 cells expressing CYP6P7 or CYP6AA3 against pyrethroid, organophosphate and carbamate insecticides that are commonly used in Thailand. Enzymatic assays of CYP6P7 and CYP6AA3 against insecticides were performed and compared to results obtained from MTT assays.

MATERIALS AND METHODS

Chemicals

The chemical compounds including deltamethrin, permethrin, cypermethrin, λ-cyhalothrin, bioallethrin, chlorpyrifos, propoxur, leupeptin, phenylmethylsulphonyl fluoride (PMSF), dimethyl sulfoxide (DMSO), and piperonyl butoxide (PBO) were purchased from Sigma-Aldrich (St. Louis, MO). 3-(4,5-dimethylthiazol-2-yl)-2,5-diphenyltetrazolium bromide (MTT) were purchased from USB (Cleveland, OH).

Cell culture and baculovirus-mediated insect cell expression of P450 proteins

The Sf9 insect cell line and SF-900 II SFM culture media were purchased from Invitrogen (Carlsbad, CA), and Sf9 cells were cultured in SF900 II serum-free media at 28°C. The recombinant baculovirus, either containing CYP6AA3 or CYP6P7, was produced following manufacturer's instruction as previously described (Kaewpa *et al.*, 2007). Briefly, CYP6P7 or CYP6AA3 cDNA isolated from deltamethrin resistant *An. minimus* (Rongnoparut *et al.*, 2003; Rodpradit *et al.*, 2005) was subcloned into the transfer vector pBacPAK8 (BD Biosciences, Palo Alto, CA), co-transfected with a linearized BacPAK6 viral DNA into Sf9 cells. The resulting recombinant virus, upon purification, was used in the expression of enzymes. For cytotoxicity assays, Sf9 cells were infected with CYP6P7 or CYP6AA3 recombinant virus at multiplicity of infection (moi) equal to 1. After 72 hours post-infection,

cells expressing CYP6P7 or CYP6AA3 were harvested and seeded onto 24-well plate for cytotoxicity assays. These conditions followed the methods described by Kaewpa *et al.* (2007) and Boonsuepsakul *et al.* (2008). Expression of P450 proteins was detected by sodium dodecyl sulfate-polyacrylamide gel electrophoresis (SDS-PAGE).

Expression of P450s for *in vitro* enzymatic activity assay was performed as described by Boonsuepsakul *et al.* (2008). In brief, Sf9 cells were infected with either CYP6P7 or CYP6AA3-expressed virus at moi equal to 3. The infected cells were harvested at 70-80 hours post-infection and resuspended in sodium phosphate buffer pH 7.2 containing 1 mM EDTA, 0.5 mM PMSF, 5 µg/ml leupeptin, 0.1 mM DTT, and 20% glycerol. The harvested cells were lysed and subjected to differential centrifugation, resulting in microsomal pellet which was solubilized in sodium phosphate buffer pH 7.2 containing 150 mM KCl and 1% (v/v) Triton X-100. The microsomes of Sf9 cells infected with either CYP6P7 or CYP6AA3 recombinant virus were used in enzymatic reconstitution assays as described in Kaewpa *et al.* (2007). The expressed proteins in microsomal fractions were observed by SDS-PAGE and total P450 content was measured by reduced-CO difference spectrum analysis according to Omura & Sato (1964).

Cell treatment and MTT cytotoxicity assays

Cytotoxicity effect of insecticides evaluated by MTT assays was performed as previously described (Boonsuepsakul *et al.*, 2008). Insecticides used in this study included bioallethrin, cypermethrin, chlorpyrifos, deltamethrin, permethrin, propoxur and λ-cyhalothrin. We previously used cells infected with baculovirus containing BacPak6 viral DNA as control in parallel with uninfected parental Sf9 cells, and both control cells showed same response to deltamethrin (Boonsuepsakul *et al.*, 2008). In this study we thus used only uninfected Sf9 cells as control in MTT assays, and cells treated with DMSO solvent alone was a negative control. CYP6P7- or CYP6AA3-expressing cells and control Sf9 cells were seeded at 2×10^5 cells per well in 24-well culture plates. Cells were allowed to attach to wells for 3 hours, insecticides ranging from 0.1 to 500 µM final concentrations were subsequently added into each well and cells were left exposing to each insecticide for 72 hr. When insecticides were used at higher concentration than 500 µM, they were precipitated in culture media, particularly for pyrethroids. Thus concentrations of pyrethroids over 500 µM were not evaluated in MTT assays. Following insecticide treatment, culture media were removed and each well was washed twice with Luckhoff's buffer (132 mM NaCl, 3.5 mM KCl, 1 mM $CaCl_2$, 0.5 mM $MgCl_2$, and 20 mM HEPES). Cell viability was determined using MTT assay. This was accomplished by addition of 200 µl MTT solution (5 mg/ml in Luckhoff's buffer) and further subjected to 4-hour incubation at 28°C. Subsequently, MTT solution was removed and DMSO was added to dissolve the purple formazan precipitate formed by activity of mitochondrial enzymes in live cells (Mosmann, 1983). The absorbance of formazan product was measured at 540 nm using Multiskan EX microtiter plate reader (Thermo Labsystems, Finland). Cell viability upon incubation with each insecticide was expressed as percentage of viable cells relative to cells treated with DMSO solvent alone which was assigned as 100% viability. The value of 50% lethal concentration (LC_{50}) was evaluated from the plot of percentage of cell viability against different concentrations of each insecticide. Higher LC_{50} value represents higher ability to survive toxicity of insecticides.

In enzyme inhibition study, cells were co-incubated with 100 µM deltamethrin and PBO (known P450 inhibitor) at concentrations of 0.1, 1 and 10 µM (in each case the final concentration of DMSO in media was 1%). This range of PBO concentrations was less than LD_{50} value (25 µM) of PBO against Sf9 cells pre-determined by MTT assays (data not shown). Inhibition of P450s by PBO was measured as cell survival against deltamethrin cytotoxicity in the presence of PBO, after normalization with that of cells treated with PBO only. Each MTT assay measuring cytotoxic effect of insecticides and

measuring inhibitory effect by PBO was done in triplicate.

In vitro insecticide metabolism by CYP6P7 and CYP6AA3

The *in vitro* reconstitution assays in the presence of insecticide substrate were performed as previously described (Kaewpa *et al.*, 2007). Briefly reconstitution reactions were carried out at 30°C in 0.1 M sodium phosphate buffer pH 7.2 in the presence of 10 pmol of either CYP6P7 or CYP6AA3 and was reconstituted with purified *An. minimus* NADPH-dependent cytochrome P450 reductase (P450 redox partner) in the ratio of 3:1, 80 µM of test insecticide, and NADPH-regenerating system. Internal standard (bioallethrin) and remaining of insecticide at each reaction time were analyzed by HPLC analysis and peaks were monitored by UV detection at 220 nm. The substrate peak area at each time point was calculated as percentage of remaining residual substrate compared to that of time zero which was assigned to be 100%. When bioallethrin was a substrate, deltamethrin was used as internal standard. To determine metabolisms mediated by CYP6P7 and CYP6AA3, amount of each insecticide consumed at each incubation time was calculated as percentage of depletion of each insecticide compared to the initial amount at time zero. Each of reconstitution experiments was performed in triplicate and internal standard was used for normalization. Control reactions were performed by incubating reactions without NADPH-regenerating system, and reaction using microsome of uninfected Sf9 cells.

Statistical analysis

Data were statistically analyzed by GraphPad Prism version 5 (GraphPad Software Inc., San Diego, CA) using ANOVA with Tukey's Multiple comparison test. Results with $p < 0.05$ were considered to be significantly different.

RESULTS

In this study, cytotoxicity of insecticides was examined with Sf9 insect cells, with and without expression of CYP6P7 or CYP6AA3, using MTT cytotoxicity assays. CYP6P7 and CYP6AA3 were expressed via baculovirus-directed expression system. The results revealed higher cell viability against cytotoxic effects of permethrin, cypermethrin and deltamethrin in CYP6P7- or CYP6AA3-expressing cells than parental Sf9 cells for all given insecticide concentrations (Figure 1B-D). This is demonstrated by 5- to 13-fold higher LC_{50} values observed in CYP6P7- and CYP6AA3-expressing cells than control Sf9 parental cells. It could be noted that response to λ-cyhalothrin cytotoxicity was different between cells expressing CYP6P7 and CYP6AA3, as demonstrated by 3.7-fold higher LC_{50} value observed in CYP6AA3-expressing cells than in CYP6P7-expressing cells and parental Sf9 cells (Figure 1E). Upon treatment with bioallethrin, chlorpyrifos, and propoxur, percentage of cell viability of CYP6P7- and CYP6AA3-expressing cells and LC_{50} values were similar to control Sf9 cells (Figures 1A, F, and G).

In order to determine whether increased cell survival against pyrethroid cytotoxicity found in cells expressing CYP6P7 or CYP6AA3 was due to activity of P450s, we assayed deltamethrin cytotoxicity in the presence of different concentrations of PBO, P450 inhibitor. Decrease of cell viability against deltamethrin cytotoxicity was observed when cells expressing CYP6P7 and CYP6AA3 were treated with increasing concentrations of PBO (Figure 2). Since PBO also possessed cytotoxic effect against Sf9 cells (see Materials and Methods section), thus percent cell viability of P450-expressing cells shown in Figure 2 was obtained after normalization with that of cells treated with PBO only. Percentage of cell survival against deltamethrin of CYP6P7- or CYP6AA3-expressing cells in the presence of 10 µM PBO was significantly decreased, compared to those without PBO ($p<0.05$). In Sf9 control cells, after normalization, percentage of cells surviving deltamethrin cytotoxicity remained similar throughout treatment with different PBO concentrations (Figure 2).

Enzymatic activities of CYP6P7 and CYP6AA3 against pyrethroid, organo-phosphate, and carbamate insecticides were

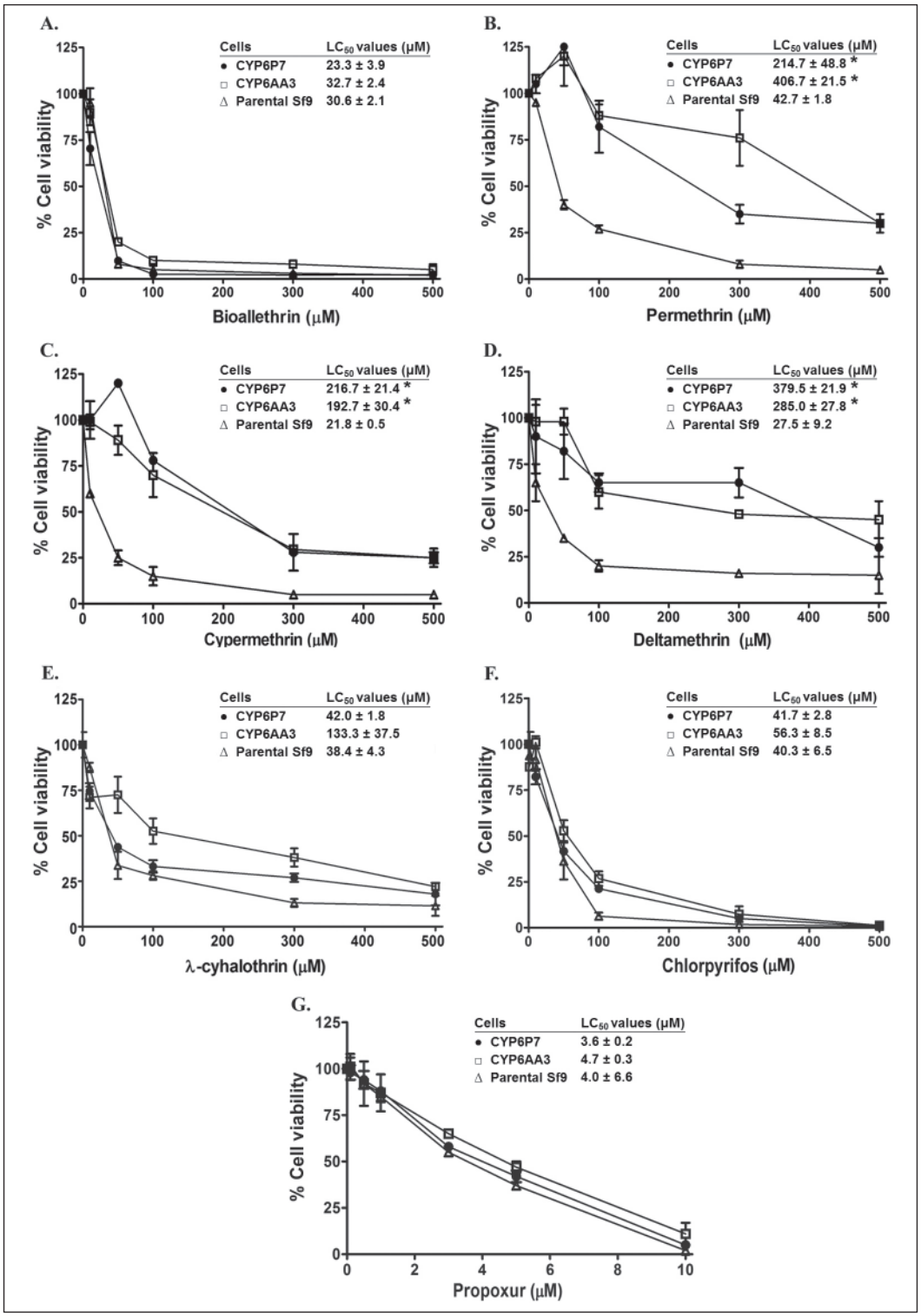

Figure 1. Viability of CYP6P7-expressing Sf9 cells (●), CYP6AA3-expressing Sf9 cells (□) and parental Sf9 cells (△) upon incubation with various insecticides. Percentage of cell viability was measured using MTT cytotoxicity assays as described in Materials and Methods. Data are means ± S.D. of three replicated experiments. Asterisk (*) represents the value significantly different from control cells ($p < 0.05$, one-way ANOVA, Tukey's Multiple Comparison Test)

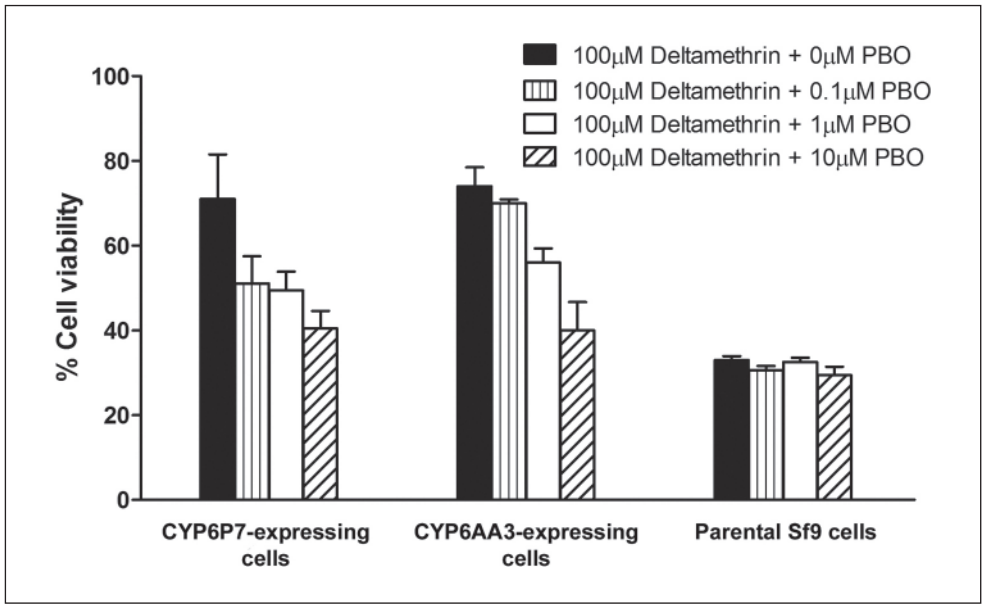

Figure 2. Effect of deltamethrin on viability of cells expressing CYP6P7, CYP6AA3, and parental Sf9 cells in the presence of PBO. Cells were co-incubated with deltamethrin and PBO, and percentage of cell viability after normalization with that treated with PBO only was obtained as described in Materials and Methods. Data are means ± S.D. of three replicated experiments

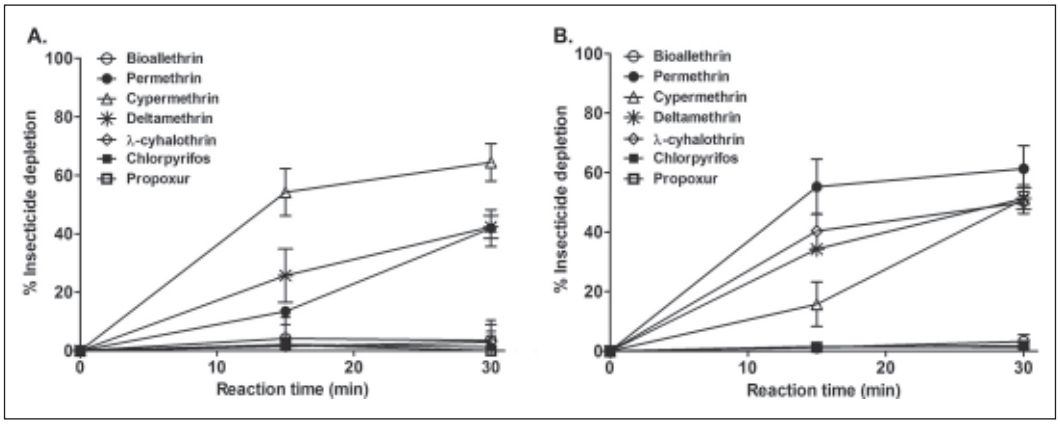

Figure 3. Plot of the time course of insecticide depletion mediated by CYP6P7 (**A**) and CYP6AA3 (**B**) enzymes using in vitro reconstitution assays, performed as described in Kaewpa *et al.* (2007). Degradation of insecticide mediated by CYP6P7 and CYP6AA3 was calculated as percentage of insecticide consumed in the reactions at each incubation time compared to time zero, after normalization with internal standard. Data are means ± S.D. of triplicate experiments

investigated using CYP6P7- or CYP6AA3 reconstituted with their redox partner enzyme, the NADPH-dependent cytochrome P450 reductase. As shown in Figure 3 CYP6P7 and CYP6AA3 showed enzymatic activities toward permethrin, cypermethrin and deltamethrin, but no detectable activities were observed with bioallethrin, chlorpyrifos, and propoxur. Moreover, in contrast to CYP6AA3, CYP6P7 had undetectable enzyme activity in metabolizing λ-cyhalothrin. These results were thus in agreement with the ability of CYP6P7 and CYP6AA3 in protecting cells against cytotoxic effects of test insecticides.

DISCUSSION

The results of this study showed that expression of CYP6P7 and CYP6AA3 could help protecting insect Sf9 cells from cytotoxicity of several pyrethroids. Presence of PBO diminished CYP6P7- and CYP6AA3-mediated cytoprotection of Sf9 cells against deltamethrin cytotoxicity, suggesting that cytoprotection against pyrethroids was due to CYP6P7 and CYP6AA3 enzymes. Moreover, results from MTT cytotoxicity assays corresponded to those of *in vitro* reconstitution enzymatic assays. In this study we detected cytotoxic effect of PBO against Sf9 cells, PBO toxicity has also been reported, as it causes tumors and adverse effects in laboratory rodents (Takahashi *et al*., 1997; Okamiya *et al*., 1998).

As shown in this study, Sf9 parental cells were susceptible to cytotoxicity of test insecticides with LC_{50} values less than 50 µM. Sensitivity of insect Sf9 cells to cytotoxic effects of compounds such as fungal metabolites (Fornelli *et al*., 2004), pyridalyl insecticide (Saito *et al*., 2005) have been reported. Thus susceptibility of Sf9 parental cells to insecticide cytotoxicity observed in the present study is advantageous to determining capability of P450 enzymes in detoxifying insecticides. Capability of P450 in detoxifying cytotoxic xenochemicals were previously reported using insect cells expressing P450 enzyme via baculovirus-directed expression (Grant *et al*., 1996). Moreover Sf21 cells expressing human CYP1A1 were used to investigate toxicity of naphthalene (Greene *et al*., 2000).

The results of this study revealed that CYP6P7 and CYP6AA3 could function in metabolizing of permethrin, cypermethrin, and deltamethrin, however role in metabolisms of bioallethrin, chlorpyrifos and propoxur was not observed. Thus abilities of CYP6P7 and CYP6AA3 in detoxifying pyrethroids support their role in conferring deltamethrin resistance in *An. minimus* mosquito (Rodpradit *et al*., 2005). A difference was noted in that while CYP6AA3 showed metabolic activity and cytoprotective activity against λ-cyhalothrin, these capabilities were not observed for CYP6P7. The results thus indicated differences in properties of these two enzymes.

A characteristic of P450s that has been noted is their variation in substrate specificity such as a single P450 could metabolize more than one substrate (Scott, 1999). *In vitro* metabolisms of insecticides by insect P450s have been reported such as ability of CYP6P3 of *An. gambiae* in metabolizing more than one pyrethroid substrates including deltamethrin and permethrin (Mûller *et al*., 2008), and CYP6D1 of *M. domestica* in metabolisms of deltamethrin and cypermethrin (Wheelock & Scott, 1992; Zhang & Scott, 1996). In this study, results of both in situ detoxification assays and *in vitro* enzymatic assays demonstrated variation of CYP6P7 and CYP6AA3 activities toward different pyrethroids and with different specificities, suggesting their abilities to metabolize and detoxify several pyrethroid insecticides in *An. minimus* mosquito. Moreover, ability of CYP6P7 and CYP6AA3 to detoxify pyrethroids observed in this study, although without co-expression of *An. minimus* cytochrome P450 reductase, indicated that the NADPH-dependent cytochrome P450 reductase enzyme of Sf9 cells could help supporting activity of these mosquito P450s.

In conclusion, the results obtained in this study elucidate the ability of CYP6P7 and CYP6AA3 in detoxification of several pyrethroids and emphasize the possible role of CYP6P7 and CYP6AA3 enzymes in conferring pyrethroid resistance in *An. minimus* mosquito. A correlation of results from MTT cytotoxicity assays and *in vitro* enzymatic activity assays emphasizes usefulness of employing P450-expressing Sf9 cells to pre-screen detoxification capability of P450s against cytotoxic insecticides using MTT cytotoxicity assays.

Acknowledgements. We thank Sirikun Pethuan and Dr. Soamrutai Boonsuepsakul for technical support, and Dr. Songklod Sarapusit for criticisms. This work is funded by Royal Golden Jubilee Program (RGJ); BIOTEC, National Science and Technology Development Agency (NSTDA); and partly

supported by Thailand Research Fund (TRF) and Mahidol University.

REFERENCES

Boonsuepsakul, S., Luepromchai, E. & Rongnoparut, P. (2008). Characterization of *Anopheles minimus* CYP6AA3 expressed in recombinant baculovirus system. *Archives of Insect Biochemistry and Physiology* **69**: 13-21.

Bortel, W.V., Trung, H.D., Thuan, L.K., Sochantha, T., Socheat, D., Sumrandee, C., Baimai, V., Keokenchanh, K., Samlane, P., Roelants, P., Denis, L., Verhaeghen, K., Obsomer, V. & Coosemans, M. (2008). The insecticide resistance status of malaria vectors in the Mekong region. *Malaria Journal* **7**: 102.

Chareonviriyaphap, T., Aum-aung, B. & Ratanatham, S. (1999). Current insecticide resistance patterns in mosquito vectors in Thailand. *Southeast Asian Journal of Tropical Medicine and Public Health* **30**: 184-194.

Chareonviriyaphap, T., Rongnoparut, P., Chantarumporn, P. & Bangs, M.J. (2003). Biochemical detection of pyrethroid resistance mechanisms in *Anopheles minimus* in Thailand. *Journal of Vector Ecology* **28**: 108-116.

Coleman, M. & Hemingway, J. (2007). Insecticide resistance monitoring and evaluation in disease transmitting mosquitoes. *Journal of Pesticide Science* **32**: 69-76.

Cuamba, N., Morgan, J.C., Irving, H., Steven, A. & Wondji, C.S. (2010). High level of pyrethroid resistance in an *Anopheles funestus* population of the Chokwe district in Mozambique. *PLoS ONE* **5**: e11010.

Djouaka, R.F., Bakare, A.A., Coulibaly, O.N., Akogbeto, M.C., Ranson, H., Hemingway, J. & Strode, C. (2008). Expression of the cytochrome P450s, *CYP6P3* and *CYP6M2* are significantly elevated in multiple pyrethroid resistant populations of *Anopheles gambiae* s.s. from Southern Benin and Nigeria. *BMC genomics* **9**: 538.

Feyereisen, R. (1999). Insect P450 enzymes. *Annual Review of Entomology* **44**: 507-533.

Fornelli, F., Minervini, F. & Logrieco, A. (2004). Cytotoxicity of fungal metabolites to lepidopteran (*Spodoptera frugiperda*) cell line (Sf-9). *Journal of Invertebrate Pathology* **85:** 74-79.

Gassner, B., Wãthrich, A., Scholtysik, G. & Solioz, M. (1997). The pyrethroids permethrin and cyhalothrin are potent inhibitors of the mitochondrial complex I. *The Journal of Pharmacology and Experimental Therapeutics* **281**: 855-860.

Grant, D.F., Greene, J.F., Pinot, F., Borhan, B., Moghaddam, M.F., Hummock, B.D., McCutchen, B., Ohkawa, H., Luo, G. & Guenthner, T.M. (1996). Development of an *in situ* toxicity assay system using recombinant baculoviruses. *Biochemical Pharmacology* **51**: 503-515.

Greene, J.F., Zheng, J., Grant, D.F. & Hammock, B.D. (2000). Cytotoxicity of 1,2-epoxynaphthalene is correlated with protein binding and *in situ* glutathione depletion in cytochrome P4501A1 expressing Sf-21 cells. *Toxicological Sciences* **53**: 352-360.

Kaewpa, D., Boonsuepsakul, S. & Rongnoparut, P. (2007). Functional expression of mosquito NADPH-cytochrome P450 reductase in *Escherichia coli*. *Journal of Economic Entomology* **100**: 946-953.

Maran, E., Fernández-FranŸon, M., Font, G. & Ruiz, M.J. (2010). Effects of aldicarb and propoxur on cytotoxicity and lipid peroxidation in CHO-K1 cells. *Food and Chemical Toxicology* **48**: 1592-1596.

Matowo, J., Kulkarni, M.A., Mosha, F.W., Oxborough, R.M., Kitau, J.A., Tenu, F. & Rowland, M. (2010). Biochemical basis of permethrin resistance in *Anopheles arabiensis* from Lower Moshi, north-eastern Tanzania. *Malaria Journal* **9**: 193.

Mosmann, T. (1983). Rapid colorimetric assay for cellular growth and survival: application to proliferation and cytotoxicity assays. *Journal of lmmunological Methods* **65**: 55-63.

Müller, P., Warr, E., Stevenson, B.J., Pignatelli, P.M., Morgan, J.C., Steven, A., Yawson, A.E., Mitchell, S.N., Ranson, H., Hemingway, J., Paine, M.J.I. & Donnelly, M.J. (2008). Field-caught permethrin-resistant *Anopheles gambiae* over-express CYP6P3, a P450 that metabolises pyrethroids. *PLoS Genetics* **4**: e1000286.

Munhenga, G., Masendu, H.T., Brooke, B.D., Hunt, R.H. & Koekemoer, L.K. (2008). Pyrethroid resistance in the major malaria vector *Anopheles arabiensis* from Gwave, a malaria-endemic area in Zimbabwe. *Malaria Journal* **7**: 247.

Naravaneni, R. & Jamil, K. (2005). Evaluation of cytogenetic effects of lambda-cyhalothrin on human lymphocytes. *Journal of Biochemical and Molecular Toxicology* **19**: 304-310.

Okamiya, H., Mitsumori, K., Onodera, H., Ito, S., Imazawa, T., Yasuhara, K. & Takahashi, M. (1998). Mechanistic study on liver tumor promoting effects of piperonyl butoxide in rats. *Archives of Toxicology* **72**: 744-750.

Omura, T. & Sato, R. (1964). The carbon monoxide-biding pigment of liver microsome I. Evidence for its hemoprotein nature. *Journal of Biological Chemistry* **239**: 2370-2378.

Patel, S., Bajpayee, M., Pandey, A.K., Parmar, D. & Dhawan, A. (2007). *In vitro* induction of cytotoxicity and DNA strand breaks in CHO cells exposed to cypermethrin, pendimethalin and dichlorvos. *Toxicology In Vitro* **21**: 1409-1418.

Rodpradit, P., Boonsuepsakul, S., Chareonviriyaphap, T., Bangs, M.J. & Rongnoparut, P. (2005). Cytochrome P450 genes: molecular cloning and overexpression in a pyrethroid-resistant strain of *Anopheles minimus* mosquito. *Journal of the American Mosquito Control Association* **21**: 71-79.

Rongnoparut, P., Boonsuepsakul, S., Chareonviriyaphap, T. & Thanomsing, N. (2003). Cloning of cytochrome P450, *CYP6P5*, and *CYP6AA2* from *Anopheles minimus* resistant to deltamethrin. *Journal of Vector Ecology* **28**: 150-158.

Saito, S., Sakamoto, N. & Umeda, K. (2005). Effects of pyridalyl, a novel insecticidal agent, on cultured Sf9 cells. *Journal of Pesticide Science* **30**: 17-21.

Schmuck, G. & Mihail, F. (2004). Effects of the carbamates fenoxycarb, propamocarb and propoxur on energy supply, glucose utilization and SH-groups in neurons. *Archives of Toxicology* **78**: 330-337.

Scott, J.G. (1999). Cytochromes P450 and insecticide resistance. *Insect Biochemistry and Molecular Biology* **29**: 757-777.

Swann, J.M., Schultz, T.W. & Kennedy, J.R. (1996). The effects of the organophosphorous insecticides Dursban™ and Lorsban™ on the ciliated epithelium of the frog palate *in vitro*. *Archives of Environmental Contamination and Toxicology* **30**: 188-194.

Takahashi, O., Oishi, S., Fujitani, T., Tanaka, T. & Yoneyama, M. (1997). Chronic toxicity studies of piperonyl butoxide in CD-1 mice: Induction of hepatocellular carcinoma. *Toxicology* **124**: 95-103.

Tomita, T., Liu, N., Smith, F.F., Sridhar, P. & Scott, J.G. (1995). Molecular mechanisms involved in increased expression of a cytochrome P450 responsible for pyrethroid resistance in the housefly, *Musca domestica*. *Insect Molecular Biology* **4**: 135-140.

Villarini, M., Moretti, M., Pasquini, R., Scassellati-Sforzolini, G., Fatigoni, C., Marcarelli, M., Monarca, S. & Rodríguez, A.V. (1998). In vitro genotoxic effects of the insecticide deltamethrin in human peripheral blood leukocytes: DNA damage ('comet' assay) in relation to the induction of sister-chromatid exchanges and micronuclei. *Toxicology* **130**: 129-139.

Wheelock, G.D. & Scott, J.G. (1992). The role of cytochrome $P450_{lpr}$ in deltamethrin metabolism by pyrethroid-resistant and susceptible strains of house flies. *Pesticide Biochemistry and Physiology* **43**: 67-77.

Zhang, M. & Scott, J.G. (1996). Cytochrome b_5 is essential for cytochrome P450 6D1-mediated cypermethrin resistance in LPR house flies. *Pesticide Biochemistry and Physiology* **55**: 150-156.

Int. J. Mol. Sci. **2013**, *14*, 1788-1801; doi:10.3390/ijms14011788

OPEN ACCESS
International Journal of
Molecular Sciences
ISSN 1422-0067
www.mdpi.com/journal/ijms

Article

Modeling of *Anopheles minimus* Mosquito NADPH-Cytochrome P450 Oxidoreductase (CYPOR) and Mutagenesis Analysis

Songklod Sarapusit [1,*], Panida Lertkiatmongkol [2], Panida Duangkaew [3] and Pornpimol Rongnoparut [2]

[1] Department of Biochemistry, Faculty of Science, Burapha University, Chonburi 20131, Thailand
[2] Department of Biochemistry, Faculty of Science, Mahidol University, Bangkok 10400, Thailand; E-Mails: prunuspersica@gmail.com (P.L.); pornpimol.ron@mahidol.ac.th (P.R.)
[3] Faculty of Animal Sciences and Agricultural Technology, Silpakorn University, Petchaburi IT Campus, Petchaburi 76120, Thailand; E-Mail: panida.d@su.ac.th

***** Author to whom correspondence should be addressed; E-Mail: songklod@buu.ac.th; Tel.: +66-038-103-058; Fax: +66-038-393-495.

Received: 25 September 2012; in revised form: 19 November 2012 / Accepted: 5 January 2013 / Published: 16 January 2013

Abstract: Malaria is one of the most dangerous mosquito-borne diseases in many tropical countries, including Thailand. Studies in a deltamethrin resistant strain of *Anopheles minimus* mosquito, suggest cytochrome P450 enzymes contribute to the detoxification of pyrethroid insecticides. Purified *A. minimus* CYPOR enzyme (AnCYPOR), which is the redox partner of cytochrome P450s, loses flavin-adenosine di-nucleotide (FAD) and FLAVIN mono-nucleotide (FMN) cofactors that affect its enzyme activity. Replacement of leucine residues at positions 86 and 219 with phenylalanines in FMN binding domain increases FMN binding, enzyme stability, and cytochrome *c* reduction activity. Membrane-Bound L86F/L219F-AnCYPOR increases *A. minimus* P450-mediated pyrethroid metabolism *in vitro*. In this study, we constructed a comparative model structure of AnCYPOR using a rat CYPOR structure as a template. Overall model structure is similar to rat CYPOR, with some prominent differences. Based on primary sequence and structural analysis of rat and *A. minimus* CYPOR, C427R, W678A, and W678H mutations were generated together with L86F/L219F resulting in three soluble Δ55 triple mutants. The C427R triple AnCYPOR mutant retained a higher amount of FAD binding and increased cytochrome *c* reduction activity compared to wild-type and L86F/L219F-Δ55AnCYPOR double mutant. However W678A and W678H mutations did not increase FAD and NAD(P)H bindings. The L86F/L219F double and C427R triple

membrane-bound AnCYPOR mutants supported benzyloxyresorufin *O*-deakylation (BROD) mediated by mosquito CYP6AA3 with a two- to three-fold increase in efficiency over wild-type AnCYPOR. The use of rat CYPOR in place of AnCYPOR most efficiently supported CYP6AA3-mediated BROD compared to all AnCYPORs.

Keywords: *Anopheles minimus* mosquito; cytochrome P450 oxidoreductase (CYPOR); structure; FAD and NAD(P)H bindings

1. Introduction

The reemergence of malaria, a disease transmitted to humans by mosquitoes, is associated with vector resistance in many tropical countries due to the persistent use of pyrethroid insecticides [1,2]. The insecticide resistance has been reported in *Anopheles minimus* mosquito, one of the malaria primary vectors in Thailand [3]. A common mechanism for insecticide resistance involves an elevation in insecticide detoxification. Cytochrome P450 monooxygenases (P450) are important enzymes in pyrethroid metabolism and have been implicated in insecticide resistance in many insects [4]. In *A. minimus*, an elevated level of CYP6AA3 and CYP6P7 transcripts has been detected during selection for deltamethrin resistance [5,6]. Heterologously expressed CYP6AA3 and CYP6P7 enzymes in an insect-baculovirus system have shown capability to specifically metabolize type I and type II pyrethroids *in vitro* [7–9].

Catalysis by P450 enzymes requires an electron supplement from NADPH-cytochrome P450 oxidoreductase enzyme (CYPOR), a membrane-bound enzyme that transfers electrons, from NADPH to P450s via FAD and FMN cofactors [10–12]. RNA interference indicated the influential role of mosquito CYPOR enzyme in permethrin resistance in *A. gambiae*, a major malaria vector in Africa [13]. Thus, studies of CYPOR properties in *A. minimus*, may provide important information for the malarial vector control program in Thailand.

The membrane-bound *A. minimus* CYPOR (flAnCYPOR) cDNA has been isolated and expressed in *Escherichia coli* [7]. The purified flAnCYPOR enzyme can support baculovirus-expressed CYP6AA3 and CYP6P7 to metabolize pyrethroid insecticides and benzyloxyresorufin fluorescent substrate *in vitro*, but the purified enzyme is prone to lose FAD and FMN cofactors compared to rat CYPOR [7–9,14,15]. In addition, higher trypsin sensitivity of AnCYPOR indicates a more open conformation or high flexibility of the soluble Δ55AnCYPOR enzyme compared to rat CYPOR structure. Unlike rat and house fly CYPORs, the open/highly flexible structure of AnCYPOR could explain that AnCYPOR loosely binds flavin cofactors and can be reconstituted with exogenous FMN and FAD *in vitro* [14–17]. Substitutions of leucine 86 and leucine 219 with phenylalanine in the FMN-binding domain generate a L86F/L219F double mutant of both soluble (Δ55) and membrane-bound (fl) forms that improve FMN retention, but remain loosely bound to FAD cofactor. Binding of FAD is not improved when phenylalanine at 456 is replaced with the conserved alanine residue in the FAD-binding domain of the enzyme [14,15]. The L86F/L219F mutation increases enzyme stability and turnover number without drastically changing kinetic mechanism and substrate-binding constants, NADPH K_m, and cytochrome *c* K_m [14,15]. Consequently, a higher catalytic efficiency of L86F/L219F-flAnCYPOR increases

CYP6AA3-mediated deltamethrin degradation activity *in vitro* [15]. Addition of exogenous FAD contributes to a greater increase in CYP6AA3-mediated activity supported by the wild-type and L86F/L219F mutant flAnCYPOR enzymes. In this context, why the *A. minimus* CYPOR is enormously different from rat CYPOR in stability, activity in its native form and in the ease in which flavin cofactors are lost remains unanswered.

Recently, investigation of *A. gambiae* CYPOR, AgCYPOR, which shares 93% of its amino acid sequence with *A. minimus* CYPOR, has indicated a loss of both FMN and FAD cofactors in the purified AgCYPOR enzyme. Moreover, AgCYPOR binds NAD(P)H differently from human CYPOR [18], suggesting substantially different enzymatic properties in mosquito CYPORs. Functional analyses of mosquito and mammalian CYPOR in combination with a structural comparison may help to explain different properties. In this study, comparative modeling of AnCYPOR was performed and the predicted models were compared to known crystal structure of rat CYPOR [10]. Based on sequence analysis and model comparison, two residues that might affect FAD binding and enzyme catalysis, C427 and W678, were selected to generate triple mutants, in addition to L86F and L219F. Biochemical properties of L86F/L219F/C427R, L86F/L219F/W678A, and L86F/L219F/W678H soluble Δ55-triple mutants and catalysis by L86F/L219F double and C427R triple membrane-bound mutants in support of BROD mediated by CYP6AA3 were investigated. Moreover, as a primary step to understand different properties of AnCYPOR and rat CYPOR in electron transfer to P450 partner enzyme, we employed rat CYPOR in place of mosquito CYPOR as a redox partner enzyme of mosquito P450 in the reconstitution enzymatic assay. Our results have contributed to an understanding of the typical nature of mosquito CYPOR compared to rat CYPOR, and its efficacy in electron transfer in mosquito P450-mediated metabolisms.

2. Results and Discussion

2.1. Overall Structure of AnCYPOR

A predicted AnCYPOR homology model generated using rat CYPOR as a template (pdb code: 1JA1, [19]) was chosen based on a consensus judgment of discrete optimized protein energy (DOPE) and residue specific all-atom probability discriminatory function (RAPDF) scores. Figure 1 shows an oval, bowl-like 3D structure of the AnCYPOR homolog in the presence of $NADP^+$, FAD, and FMN. The overall AnCYPOR structure contains three structural domains including FMN-binding, FAD/$NADP^+$-binding, and connecting domains. The FMN, FAD and NADP(H) are positions in the middle of the structure as found in rat CYPOR [10,19]. The model has an overall ProSA-z score of −11.01. Ramachandran plot analysis revealed 88.7% and 0.6% of residues in most favorable and disallowed regions, respectively (Figure S1). Three residues (V256, N503, and E506) residing in disallowed region locate in the connecting domain which functions to bring the two flavins together and modulate electron transfer between them [10,19,20]. The crystal structure of rat CYPOR lacks 63 *N*-terminal amino acids and starts with Val64, so the corresponding first residue in AnCYPOR is Thr64. Although structure of the membrane-binding region of AnCYPOR could not be determined in the model, sequence alignment indicated a clear difference in membrane-binding sequence from rat CYPOR (Figure S2).

Figure 1. Homology model of wild-type *Anopheles minimus* CYPOR (AnCYPOR). Wild-Type AnCYPOR model demonstrates conserved regions of the flavin mono-nucleotide (FMN)-binding domain, the connecting domain, and the flavin-adenosine di-nucleotide (FAD)/NAD(P)H-binding domain that are colored blue, green, and red, respectively. The mutated positions are labeled and shown in spheres. Arrows indicate deviations among the structures of template rat CYPOR (PDB:1JA1) (green), wild-type AnCYPOR (blue), and double mutant AnCYPOR (yellow) in the FMN-binding domain, the connecting domain, and the FAD/NAD(P)H-binding domain. The cofactor FMN, FAD, and NADPH are represented by magenta, purple, and grey sticks, respectively.

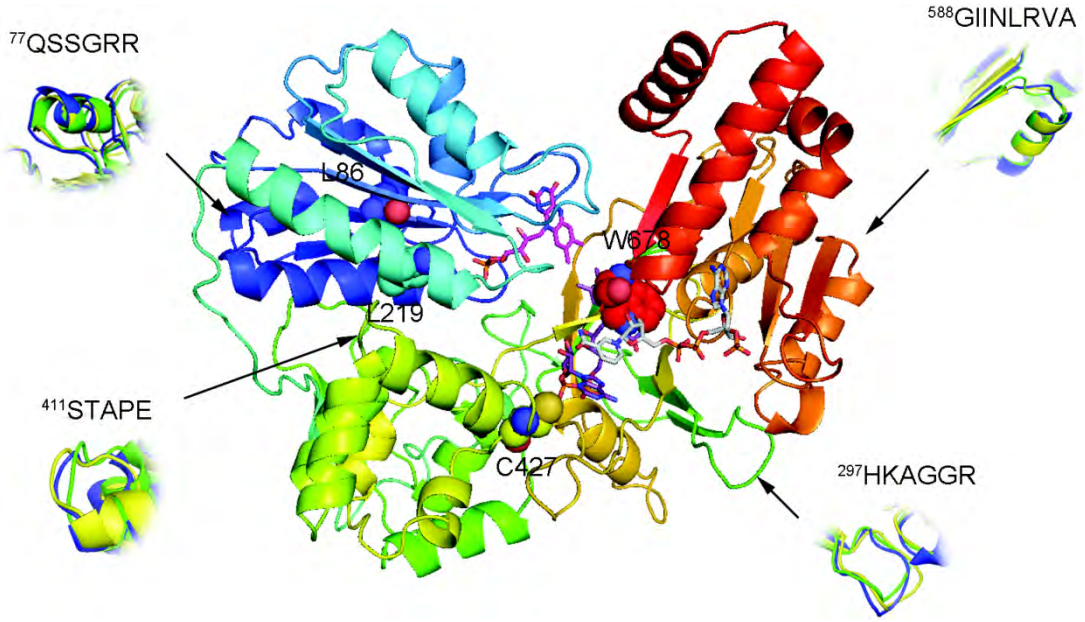

Figure 2. Binding interaction with FAD in AnCYPOR. Replacement of cysteine (**A**) with arginine (**B**) could result in more molecular interactions between the enzyme and FAD in mutant than in wild-type AnCYPOR in correspond to interactions towards FAD previously described in rat CYPOR [10]. Wild-Type and C427R triple mutant AnCYPOR are shown in blue and magenta cartoons, respectively. FAD is represented by grey stick. Nitrogen, oxygen, phosphorus, and sulfur are colored blue, red, orange, and yellow, respectively.

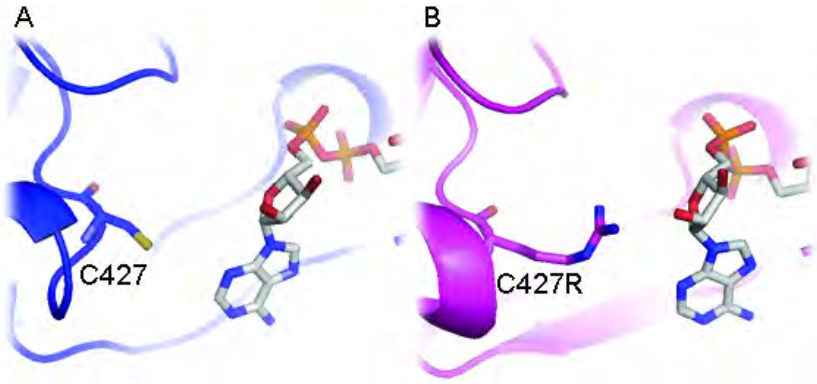

Superimposition of the wildtype- and L86F/L219F-AnCYPOR with rat CYPOR showed topology differences in all domains (Figure 1). Deviations are found in one location in FMN-binding domain

(^{77}QSSGRR, the connecting loop between helix A and β-sheet 1), one in FAD-binding region (^{297}HKAGGR at the tip of β-sheet 8), one loop in NAD(P)H binding region (^{588}GIINLRVA), and ^{411}STAPE at the tip of helix K in connecting domain. These differences may reflect enzyme properties and conformational change during AnCYPOR catalysis compared to rat CYPOR.

2.2. Predicted FAD-Binding Region

Although replacement of two leucine residues successfully increases FMN binding, possibly through altered topology of the loop at ^{77}QSSGRR that superimposes well with rat structure than wild-type AnCYPOR, the L86F/L219F-Δ55AnCYPOR remains loosely bound to FAD cofactor. Therefore, a topology change in ^{297}HKAGGR of L86F/L219F from wild-type AnCYPOR to that of rat CYPOR may not affect FAD binding (Figure 1). Relative to that of rat CYPOR structure, the re-side and the si-face of FAD ring are similarly stacked by the indole ring of W678 and the si-face by Y459 in AnCYPOR. The interaction of FAD isoalloxazine ring with side chains of S460, T475, A476 and V474 of AnCYPOR is also similar to rat CYPOR [10]. The rest of the FAD molecule lies at the interface between the FAD-binding domain, but polypeptide chains surrounding FAD show variable degrees of homology with rat CYPOR (Figure 1 and supplemental Figure 2). In addition, residues participating in stabilization of FAD binding in AnCYPOR are notably different from rat CYPOR. Residues observed in rat CYPOR are R424, R454, T491, Y478 and V489 [10], while in AnCYPOR they are R457, T494, Y481 and V492. The rat R424, which is important for interaction with FAD, is missing from AnCYPOR. Instead, a Cys residue was observed at position 427 (Figure S2). The short chain sulfhydryl-group of C427 might drastically abolish interaction with FAD, leading to a loose binding of FAD to the enzyme (Figure 2). Recently, disruption of local H bonding with FAD pyrophosphate moiety leading to weaker FAD binding, unstable protein, and loss of catalytic activity has been reported in V492E and R457H two naturally occurring missense mutations of human CYPOR [21]. Thus we replaced Cys with Arg together with L86F/L219F and generated a soluble triple mutant (L86F/L219F/C427R-Δ55AnCYPOR). The triple mutant could increase FAD binding about 1.5 folds of double mutant L86F/L219F-Δ55AnCYPOR, and about 1.3 folds compared to the wild-type-Δ55AnCYPOR (Table 1). The NADPH-dependent cytochrome *c* reduction activity in C427R triple mutant without supplementation of FAD was about two and four folds higher than L86F/L219F double mutant and wild-type-Δ55AnCYPORs, respectively (Figure 3). Supplementation with FAD reduced the difference in the cytochrome *c* reduction activity between the C427R triple mutant and the double mutant. The activity of this triple mutant enzyme is about 0.5 fold of rat CYPOR activity (51.5 μmol/min/mg) [17]. The results suggest a role of C427 in FAD binding and as a consequence increased AnCYPOR catalysis. Supplementation of FAD could further elevate the activity of C427R triple soluble mutant, indicating another factor might also influence FAD binding. The absence of cytochrome *c* reduction activity in the reaction omitted AnCYPOR enzyme excludes the possibility of an external electron transfer pathway to cytochrome *c* by exogenous flavins (unreported data). This increase in enzymatic activity of mutant AnCYPORs upon FAD supplement during enzyme catalysis had been reported in Y459A and V492E human mutant CYPOR enzymes that are loosely bound to FAD [22,23]. In addition, the C427R triple mutant had similar K_m values for NADPH and cytochrome c substrates to those of L86F/L219F double mutant, but its catalytic electron

transfer rate (V_{max}) was approximately two folds higher (data not shown). Nonetheless K_m values of L86F/L219F double and C427R triple mutants were not substantially different from wild-type-Δ55AnCYPOR indicating that the mutations did not significantly alter structure or substrate binding mode of enzyme (Table 2). The K_m values for cytochrome *c* and NADPH of wild-type-Δ55AnCYPOR in this study is noticeably lower than that previously reported [14] due to enzymatic assays performed in this study were in low ionic strength (0.1 M Tris pH 7.5) condition, while in previous report the assays were at high ionic strength (0.3 M Potassium phosphate pH 7.7). Effect of ionic strength on substrate binding of CYPOR has also been reported [11].

Table 1. Flavin content analysis of Δ55AnCYPOR.

Enzyme	FMN [a]	FAD [a]
Wild-type-Δ55AnCYPOR	0.52 ± 0.01	0.64 ± 0.03
L86F/L219F-Δ55AnCYPOR	0.97 ± 0.02	0.56 ± 0.01
L86F/L219F/C427R-Δ55AnCYPOR	0.98 ± 0.01	0.82 ± 0.02
L86F/L219F/W678A-Δ55AnCYPOR	0.96 ± 0.04	0.55 ± 0.02
L86F/L219F/W678H-Δ55AnCYPOR	0.97 ± 0.02	0.57 ± 0.04
Δ63AgCYPOR [b]	0.72 ± 0.01	0.80 ± 0.01
Human CYPOR [b]	0.88 ± 0.01	0.92 ± 0.02

[a] Flavin content is expressed as mean ± SD for mol of flavins per mol of protein in triplicate experiments. Standard flavin was measured and used for a plot of standard curve; [b] Lian *et al.*, 2011 [18].

Figure 3. Specific activity of Δ55AnCYPOR enzymes with cytochrome *c* substrate. Specific activity is expressed as μmol of substrate reduced/min/mg of protein. Data are the average of duplicate measurements. Protein concentration was determined using Bio-Rad protein assay reagent and bovine serum albumin (BSA) as standard. When exogenous cofactors were tested, 2 μM of each of exogenous flavin cofactors were added and pre-incubated with enzyme in each assay reaction.

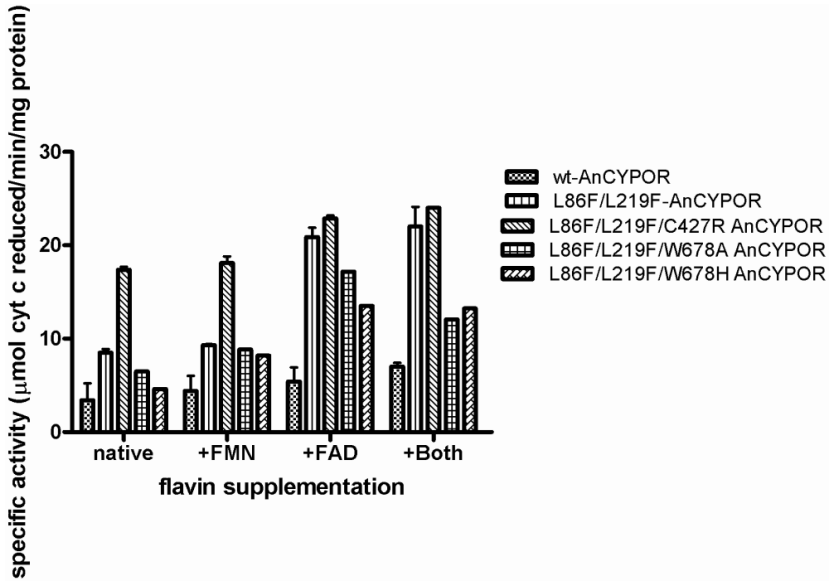

Table 2. Kinetic constants for cytochrome *c* reduction under substrate saturation condition by Δ55AnCYPOR enzymes.

Enzyme	Kinetic constant (μM) [a]		
	Cytochrome *c* K_m	NADPH K_m	NADH K_m
Δ55AnCYPOR			
-wt	27.39 ± 1.41	9.61 ± 0.30	8.40 ± 0.10
-L86F/L219F	16.41 ± 2.22	6.49 ± 1.19	11.64 ± 1.44
-L86F/L219F/C427R	17.92 ± 1.79	7.02 ± 1.75	6.67 ± 2.23
-L86F/L219F/W678A	16.24 ± 1.56	3.34 ± 0.83	7.08 ± 2.06
-L86F/L219F/W678H	18.43 ± 2.12	1.91 ± 0.44	7.72 ± 1.33

[a] Values were obtained from substrate saturation steady-state kinetic studies in the presence of extra flavins as described in Materials and Methods and are means ± SD from triplicate experiments.

2.3. FAD/NADPH Binding Residues in AnCYPOR

Unlike FMN- and FAD-binding regions, there is no substantial alteration among residues in their roles in NADPH binding (R301, S597, R598, K603, Y605, T607, N636 and M637) and catalysis (S459, C631 and D676) in AnCYPOR model structure. However, one minor difference in rotameric conformation from rat CYPOR structure was found in NAD(P)H binding domain at the end of β-sheet 21 (^{678}WS), located at the nicotinamide-binding site and covering the isoalloxazine ring of FAD cofactor. This conserved tryptophan (Trp) residue has been proposed to flip and facilitate nicotinamide binding and thus hydride transfer [10,19]. To investigate the contribution of such difference in rotameric conformation in nicotinamide binding and catalysis of AnCYPOR, we replaced W678 with alanine and histidine as both replacements play critical role in catalytic activity and nicotinamide binding of human and rat CYPORs [24,25].

In contrast to C427R construct, the Ala and His replacements at W678, (L86F/L219F/W678A-Δ55AnCYPOR and L86F/L219F/W678H-Δ55AnCYPOR) neither increased FAD binding nor cytochrome *c* reduction activity (Table 1 and Figure 3). However, cytochrome *c* reduction activity was decreased compared to L86F/L219F double mutant and C427R triple mutant. Mutations with aliphatic (W678A) and planar (W678H) residue substitutions decreased catalytic activity to 77% and 55% of that of L86F/L219F double mutant, respectively. The decrease in cytochrome *c* activity has been reported in the W676A and W676H human CYPOR mutants that retain 5 and 22% of cytochrome *c* activity, respectively [24,25]. Moreover, non-linear regression steady-state kinetic analysis using cytochrome *c* as an electron acceptor in this study revealed that removal of bulky Trp residue in W678A and W678H increased NADPH binding affinity by two- to three-fold compared to wild-type and L86F/L219F mutant AnCYPOR enzymes, but not that to NADH (Table 2). This differs from human CYPOR mutants in which both W676A and W676H mutants lower both NADPH K_m, and NADH K_m [24,25]. Specific charge interactions of amino acid residues with 2′-phosphate of NADPH are responsible for discrimination against binding of NADH [24]. Thus, it is conceivable that W678 is only crucial for catalysis and NADPH binding in AnCYPOR, and not nicotinamde selectivity of NAD(P)H and NADH substrates. Whether deviation we observed at ^{588}GIINLRVA (Figure 1) might involve in 2'-phosphate binding of NADPH is not known. This deviation might explain low binding affinity of *A. minimus* CYPOR to 2',5'-ADP column compared to human and rat CYPOR [18,26].

Values of 2'AMP K_i for AnCYPOR are four-fold higher than those for rat CYPOR, suggesting significant differences in NAD(P)H binding property between rat CYPOR and AnCYPOR [14,15]. Low binding affinity to 2',5'ADP column has also been observed for the mosquito AgCYPOR [18]. A two-fold higher IC_{50} in suppression of AgCYPOR by 2'AMP has also been reported compared to human CYPOR [18]. It is thus speculated that W678 could affect electron transfer rate and electron transfer activity, while dramatic change in polypeptide chain that specifically interact with NAD(P)H such as that of ^{588}GIINLRVA might result in low nucleotide (2',5'-ADP, 2'-AMP and NAD(P)H) binding affinity. However, the amino acids in the ^{588}GIINLRVA polypeptide chain are distant from those of rat CYPOR.

Further mutational investigation of this polypeptide on nicotinamide selectivity may provide important information that could help to understand the catalytic basis of AnCYPOR.

2.4. Electron Transfer Step Is a Rate-Limiting Step in Mosquito P450 Metabolism

As P450 catalysis requires electron supplement from CYPOR, therefore, such a mutation that affects cytochrome *c* reduction activity could affect the P450-mediated oxygenase reaction *in vitro* [27]. This is supported by an increased efficiency of L86F/L219F-flAnCYPOR and L86F/L219F/C427R-flAnCYPOR mutants in supporting BROD mediated by mosquito CYP6AA3 enzyme by 2.4 and 3 times, respectively compared to wild-type (Table 3). Moreover rat CYPOR which has higher cytochrome *c* reduction activity than wild-type AnCYPOR and all AnCYPOR mutants could increase mosquito P450 activity more than wild-type flAnCYPOR by 5.5 times. These increases in velocity by L86F/L219F, C427R mutants, and rat CYPOR had no effect on substrate binding value (K_m). The results suggest that *in vitro* mosquito P450 activity is an electron transfer rate dependent reaction. In human CYPOR, the loss of FAD and FMN from its binding site caused by mutation is the major cause of diminished P450 activity. For example, the R457H and V492E mutations at the FAD-binding site in human CYPOR result in an impaired function of CYP17A1 (17a-hydroxylase/17, 20-lyase), CYP19A1 (aromatase) and CYP1A2 *in vitro* [23,28–30]. Recently, a study on heme oxygenase I (HO-I) activity also indicated a decrease in CYPOR activity affected HO-I catalytic rate, and rate of bilirubin formation by HO-I enzyme is CYPOR-activity dependent [31]. Detailed saturated kinetic studies reveal that a decrease in HO-I activity is caused by a decrease in catalytic rate (V_{max}), not substrate binding (K_m) of HO-I [31]. Thus, we hypothesize the high catalytic activity of the mosquito CYP6AA3-mediated enzymatic activity found in the present study originates from a high electron transfer rate of rat CYPOR, C427R and L86F/L219F-flAnCYPOR activity compared to that of wildtype-flAnCYPOR enzyme. This, to our knowledge, is the first mosquito P450-mammalian CYPOR reconstitution that is more efficient than the native mosquito P450-CYPOR complex.

Table 3. The *in vitro* reconstitution assays of CYP6AA3 mosquito P450 with three different CYPOR enzymes.

CYPOR constructs	Cytochrome *c* reduction activity (U/mg protein) [a]	CYP3AA3-mediated BROD activity (pmole resorufin produced/min/pmol P450) [a]	
		K_m (μM)	V_{max} (min^{-1})
wt-AnCYPOR	0.35 ± 0.02	1.90 ± 0.61	3.10 ± 0.38
L86F/L219F-AnCYPOR	0.87 ± 0.04	1.89 ± 0.53	7.36 ± 0.78
L86F/L219F/C427R-AnCYPOR	1.62 ± 0.09	1.73 ± 0.17	10.20 ± 0.37
Rat CYPOR	18.55 ± 0.42	1.69 ± 0.24	17.40 ± 0.90

[a] Data are average of duplicate measurements.

3. Experimental Section

3.1. Materials

Flavin mono-nucleotide (FMN), flavin-adenosine di-nucleotide (FAD), cytochrome *c*, nicotinamide adenosine diphosphate ($NADP^+$), nicotinamide adenosine diphosphate reduced form (NADPH) and phenylmethylsulphonyl fluoride (PMSF) were purchased from Sigma-Aldrich (St. Louis, MO, USA). Isopropyl-β-D-thiogalactopyranoside (IPTG) was obtained from USB (Cleveland, OH, USA), Ni^{2+}-NTA affinity column from Qiagen (Valencia, CA, USA), and Bio-Rad protein assay kit from Bio-Rad (Hercules, CA, USA). Quickchange site-directed Polymerase Chain Reaction (PCR) mutagenesis kit was purchased from Stratagene (LaJolla, CA, USA) and was used according to the manufacturer's instructions.

3.2. Structure Prediction of Wild-Type and Mutant CYPOR

The amino acid sequence of wild-type *A. minimus* CYPOR was obtained from GenBank (ABL75156.1) and was used to search for template using PSI-BLAST against protein structures deposited in Brookhaven Protein Data Bank [32] for comparative modeling. Rat CYPOR-triple mutant (PDB:1JA1, [19]), exhibiting high resolved power of 1.80 Å and sharing 55% sequence identity to *A. minimus* CYPOR, was selected as the template. The first 63 residues were omitted from modeling since the *N*-terminus is associated with membrane anchor and membrane portion is absent in the template structure. Sequence alignment derived from ClustalW program of various CYPOR enzymes with some manual adjustment is shown in supplemental Figure 2. Alignments of AnCYPOR wild-type and mutants against the template were subsequently subjected to homology modeling using MODELLER9v6 [33]. A set of 1000 models for wild-type and mutant AnCYPORs was independently constructed. The cofactor FAD, FMN, and NADPH were positioned in target models as in the 1JA1 template. The most promising models of wild-type and mutant CYPORs were discriminated from incorrectly-folded structures using DOPE [34] and RAPDF [35] scoring functions. Candidate models were further energy minimized using AMBER ff03 all atom force field implemented in Amber10 [36] to remove bad van der Waals contacts. Model refinement was performed using steepest descent (SD) for 3000 iterations and followed by conjugated gradient (CG) minimizations until the energy gradient was less than 0.05 kcal/mol. The final energy minimized models were evaluated for conformation

qualities using ProSAII [37,38] and Procheck [39]. Models were visualized and displayed using PyMOL (Schrödinger LLC, NY, USA).

3.3. Site-Directed Mutagenesis of AnCYPORs

Three amino acids were separately introduced into pET28a-L86F/L219FΔ55AnCYPOR plasmid DNA by Quickchange PCR mutagenesis kit as described in manufacturer's instructions to generate triple mutants of the following substitutions: C427R, W678H and W678A. The sequences of primers used in this experiment are listed in Table 4. The same primer set was employed to generate C427R membrane-bound triple mutant using pTrc-L86F/L219F-flAnCYPOR plasmid DNA as template. All of the mutations were verified by DNA sequencing and the resultant plasmids were transformed into BL21 (DE3) *E. coli* cells.

Table 4. Primer used for mutagenesis study.

Constructs	Primer	Sequence
C427R	sense	5'-GGTACAAGACAGCCGCCGGAACGTAGTGCA-3'
	anti-sense	5'-TGCACTACGTTCCGGCGGCTGTCTTGTACC-3'
W678H	sense	5'-ACGTTACTCGGCGGACGTGCACAGCTAATCGACGGGCACA-3'
	anti-sense	5'-TGTGCCCGTCGATTAGCTGTGCACGTCCGCCGAGTAACGT-3'
W678A	sense	5'-ACGTTACTCGGCGGACGTGGCAAGCTAATCGACGGGCACA-3'
	anti-sense	5'-TGTGCCCGTCGATTAGCTTGCCACGTCCGCCGAGTAACGT-3'

Mutated codons are underlined.

3.4. Expression and Purification of AnCYPOR and Rat CYPOR Enzymes

Protein expression and purification of AnCYPORs were performed as previously described [14,15], while that of rat CYPOR followed Shen *et al*. (1989; [17]) with a slight modification. The *E. coli* C43 (DE3) carrying pIN-rat CYPOR plasmid was grown at 37 °C in TB broth containing 100 μg/mL ampicillin until OD_{600} was about 0.8 and protein expression induced by addition of 0.5 mM IPTG. Cells were allowed to grow for an additional 48 h and harvested by centrifugation at 5000× *g* for 15 min and resuspended in binding buffer (50 mM Tris pH 7.7, 0.1 M NaCl, 10% glycerol, and 20 mM imidazole) containing 0.2% Triton X-100. Cells were lysed by sonication and the supernatant was applied to a Ni^{2+}-NTA affinity column previously equilibrated with the binding buffer. The column was extensively washed with binding buffer followed by the same buffer containing 30 mM imidazole. The protein was eluted by increasing imidazole concentration to 100 mM. Purity of protein was assessed by SDS-PAGE. Pure fractions were pooled, concentrated and stored at −80 °C until use. Protein concentration was determined by the Bio-Rad protein assay using bovine serum albumin (BSA) as standard.

3.5. Expression and Purification of CYP6AA3 from Insect-Baculovirus System

Recombinant baculovirus containing CYP6AA3 cDNA was used for protein expression in *Spodoptera frugiperda* (Sf9) insect cells as previously described [7]. Briefly, Sf9 cells were infected with the CYP6AA3 expressed virus (2.5×10^8 plaque-forming units/mL) at the multiplicities of infection of 3. Infected cells were harvested at 70–80 h post infection and resuspended in sodium phosphate buffer pH 7.2 containing 1 mM EDTA, 0.5 mM PMSF, 5 μg/mL leupeptin, 0.1 mM DTT,

and 20% glycerol, and subjected to microsome preparation using differential centrifugation. CYP6AA3 protein expression was observed by SDS-PAGE analysis. Total P450 content was measured from CO-different spectrum analysis [40].

3.6. Measurement of Flavin Contents and Activity Assay

Commercial FMN and FAD were further purified by high performance liquid chromatography (HPLC) and used for generation of a standard curve and for cofactor supplementation experiments. Concentrations of standard FAD and FMN solutions were determined spectrophotometrically at 450 nm using extinction coefficients of 11.3 and 12.2 mM^{-1} cm^{-1}, respectively. FAD and FMN contents of each sample were measured using a fluorometric method as described previously [41]. The Bio-Rad protein assay was utilized to determine concentration of protein using rat CYPOR as standard. The rat CYPOR protein concentration was determined using spectrophotometric method [42]. The CYPOR-mediated cytochrome *c* reduction was carried out in 0.1 M Tris-HCl buffer, pH 7.5 as previously described [7] with minor modifications. After 1 min pre-incubation of enzyme in buffer with 40 μM cytochrome *c* at 25 °C, the reaction was initiated by addition of 50 μM NADPH. NADPH-dependent cytochrome *c* reduction was followed by a change in absorbance at 550 nm. Velocities are expressed as μmol/min/mg protein. One unit of enzyme was defined as the amount of enzyme catalyzing the reduction of 3 μmol of cytochrome *c* per minute under described conditions [43]. Substrate saturation steady-state kinetic studies of cytochrome *c* reduction were performed in 0.1 M Tris-Cl buffer, pH 7.5 at 25 °C in a final volume of 0.75 mL. Substrate saturation experiments were performed by varying NADPH concentration (2, 5, 7.5, 15, 25, 50 and 100 μM) and NADH concentration (0.3, 0.5, 1, 2, 5 and 10 mM). The reaction was started by addition of enzyme and the initial velocity data were analyzed by non-linear regression using the Grafit 6.0 software package.

3.7. CYP6AA3-Mediated BROD Assay

CYP6AA3-Mediated benzyloxyresorufin *O*-dealkylation reaction (BROD) was performed in 50 mM Tris-HCl buffer pH 7.5, in a total volume of 500 μL. Microsomes containing CYP6AA3 (~25 pmole) were used and enzymatic assays were reconstituted with either the purified AnCYPOR or rat CYPOR in the ratio of 3:1 and carried out with BR substrate (0.5, 1, 2, 4, 8 μM) as described [7]. Enzyme activity was measured with a RF-5301 PC spectrofluorophotometer (Shimadzu, Kyoto, Japan) at λ_{ex} = 530 and λ_{em} = 590 nm. The amount of resorufin product was calculated referring to the resorufin standard curve as described in Duangkaew *et al.*, 2011 [9]. Apparent K_m and V_{max} values were estimated by non-linear regression analysis using GraphPad Prism 5 software package.

4. Conclusions

In summary, comparative modeling of AnCYPOR structure demonstrated differences in topology arrangement of AnCYPOR enzyme compared to rat CYPOR structure. AnCYPOR overall structure is comparable to rat CYPOR, however, numerous differences in amino acid residues and topology were found. Detail analysis revealed major differences in FMN- and FAD/NAD(P)H binding domains that might lead to differences in enzymatic properties and catalysis of mosquito CYPOR from mammalian

CYPORs. Mutagenesis studies further indicated that C427 is critical for FAD binding in AnCYPOR. In addition, NAD(P)H binding and catalysis of this mosquito CYPOR is remarkably different from mammalian CYPORs. It is apparent that a low stoichiometry of FAD may not matter much in this enzyme, at least *in vitro*, as FAD can be easily reconstituted into the FAD binding site of AnCYPOR.

Acknowledgments

All computations were performed on Linux high performance clusters by courtesy of Sissades Tongsima, Biostatistics and Informatics laboratory, Genome Institute, NSTDA Thailand. This work is financially supported by Faculty of Science, Burapha University (S.S.) and Thailand Research Fund and Mahidol University (P.R.). We thank Frederick W. H. Beamish for criticism and reading the manuscript.

References

1. Scott, J.F. Cytochromes P450 and insecticide resistance. *Insect Biochem. Mol. Biol.* **1999**, *29*, 757–777.
2. Rivero, A.; Vézilier, J.; Weill, M.; Read, A.F.; Gandon, S. Insecticide control of vector-borne diseases: When is insecticide resistance a problem? *PLoS Pathog*. **2010**, *6*, e1001000.
3. Chareonviriyaphap, T.; Aum-Aung, B.; Ratanatham, S. Current insecticide resistance pattern in mosquito vectors in Thailand. *Southeast Asian J. Trop. Med. Public Health* **1999**, *30*, 184–194.
4. Feyereisen, R. Insect P450 enzyme. *Annu. Rev. Entomol.* **1999**, *44*, 507–533.
5. Rongnoparut, P.; Boonsuepsakul, S.; Chareonviriyaphap, T.; Thanomsing, N. Molecular cloning and expression of cytochrome P450, CYP6P5 and CYP6AA2, from *Anopheles minimus* strain resistant to deltamethrin. *J. Vector Ecol.* **2003**, *2*, 150–158.
6. Rodpradit, P.; Boonsuepsakul, S.; Chareonviriyaphap, T.; Bangs, M.J.; Rongnoparut, P. Cytochrome P450 genes: Molecular cloning and over expression in a pyrethroid-resistant strain of *Anopheles minimus* mosquito. *J. Am. Mosq. Control Assoc.* **2005**, *21*, 71–79.
7. Kaewpa, D.; Boonsuepsakul, S.; Rongnoparut, P. Functional expression of mosquito NADPH-cytochrome P450 reductase in *Escherichia coli*. *J. Econ. Entomol.* **2007**, *100*, 946–953.
8. Boonsuepsakul, S.; Luepromchai, E.; Rongnoparut, P. Characterization of *Anopheles minimus* CYP6AA3 expressed in a recombinant baculovirus system. *Arch. Insect Biochem. Physiol.* **2008**, *69*, 13–21.
9. Duangkaew, P.; Pet-Huan, S.; Kaewpa, D.; Boonsuepsakul, S.; Sarapusit, S.; Rongnoparut, P. Characterization of mosquito CYP6P7 and CYP6AA3: Differences in substrate preference and kinetic properties. *Arch. Insect Biochem. Physiol*. **2011**, *76*, 1–13.
10. Wang, M.; Roberts, D.L.; Paschke, R.; Shea, T.M.; Masters, B.S.S.; Kim, J.J.P. Three-Dimensional structure of NADPH-cytochrome P450 reductase: Prototype for FMN- and FAD-containing enzymes. *Proc. Natl. Acad. Sci. USA* **1997**, *94*, 8411–8416.
11. Murataliev, M.B.; Feyereisen, R.; Walker, F.A. Electron transfer by diflavin reductase. *Biochim. Biophys. Acta* **2004**, 1698, 1–26.
12. Paine, M.J.I.; Scrutton, N.S.; Munro, A.W.; Gutierrez, A.; Roberts, G.C.K.; Wolf, C.R. Electron transfer partner of cytochrome P450. In *Cytochrome P450*: *Structure, Mechanism and Biochemistry*, 3rd ed.; Ortiz de Montellano, P.R., Ed.; Kluwer Academic/Plenum Publishers: New York, NY, USA, 2005; pp. 115–148.

13. Lycett, G.L.; McLaughlin, L.A.; Ranson, H.; Hemingway, J.; Kafatos, F.C.; Loukeris, T.G.; Paine, M.J.I. *Anopheles gambiae* P450 reductase is highly expressed in oeocytes and *in vivo* knockdown increases permethrin susceptibility. *Insect Mol. Biol.* **2006**, *15*, 321–327.
14. Sarapusit, S.; Xia, C.W.; Misra, I.; Rongnoparut, P.; Kim, J.J.P. NADPH-cytochrome P450-oxidoreductase from the mosquito *Anopheles minimus*: Kinetic studies and the influence of leu86 and leu219 on cofactor binding and protein stability. *Arch. Biochem. Biophys.* **2008**, *477*, 53–59.
15. Sarapusit, S.; Pet-huan, S.; Rongnoparut, P. Mosquito NADPH-cytochrome P450-oxidoreductase mutation: Kinetic and role in CYP6AA3-mediated deltamethrin metabolism. *Arch. Insect Biochem. Physiol*. **2010**, *73*, 232–244.
16. Mayer, R.T.; Durrant, J.L. Preparation of homogenous NADPH-cytochrome (P450) reductase from house flies using affinity chromatography techniques. *J. Biol. Chem.* **1979**, *254*, 756–761.
17. Shen, A.L.; Porter, T.D.; Wilson, T.E.; Kasper, C.B. Structural analysis of the FMN binding domain of NADPH-cytochrome P450 oxidoreductase by site-directed mutagenesis. *J. Biol. Chem.* **1989**, *254*, 7584–7589.
18. Lian, L.-Y.; Widdowson, P.; McLaughlin, L.A.; Paine, M.J.I. Biochemical comparison of *Anopheles gambiae* and human NADPH P450 reductases reveals different 2′-5′-ADP and FMN binding traits. *PLoS One* **2011**, *6*, e20574.
19. Hubbard, P.A.; Shen, A.L.; Paschke, R.; Kasper, C.B.; Kim, J.J.P. NADPH-cytochrome P450 oxidoreductase: Structural basis for hydride and electron transfer. *J. Biol. Chem*. **2001**, *276*, 29163–29170.
20. Hamdane, D.; Xia, C.; Im, S.C.; Zhang, H.; Kim, J.J.P.; Waskell, L. Structure and function of an NADPH-cytochrome P450 oxidoreductase in an open conformation capable of reducing cytochrome P450. *J. Biol. Chem.* **2009**, *284*, 11374–11384.
21. Xia, C.; Panda, S.P.; Marohnic, C.C.; Martasek, P.; Masters, B.S.; Kim, J.J.P. Structural basis for human NADPH-cytochrome P450 oxidoreductase deficiency. *Proc. Natl. Acad. Sci. USA* **2011**, *108*, 13486–13489.
22. Marohnic, C.; Panda, S.; Martisek, P.; Masters, B.S.S. Diminished FAD binding in the Y459H and V492E Antley-Bixler syndrome mutants of human cytochrome P450 reductase. *J. Biol. Chem*. **2006**, *281*, 35975–35982.
23. Kranendonk, M.; Marochic, C.; Panda, S.P.; Duarte, M.P.; Oliveira, J.S.; Masters, B.S.S. Impairment of CYP1A2-mediated xenobiotic metabolism by Antley-Bixler syndrome variants of cytochrome P450 oxidoreductase. *Arch. Biochem. Biophys.* **2008**, *475*, 93–99.
24. Dőhr, O.; Paine, M.J.; Friedberg, T.; Robert, G.C.; Wolf, R. Engineering of a functional human NADH-dependent cytochrome P450 system. *Proc. Natl. Acad. Sci. USA* **2001**, *98*, 81–86.
25. Elmore, C.L.; Porter, T.D. Modification of the nucleotide cofactor binding site of cytochrome P450 reductase to enhance turnover with NADH *in vivo*. *J. Biol. Chem*. **2002**, *277*, 48960–48964.
26. Sarapusit, S. The study on the NADPH-Cytochrome P450 oxidoreductase from *Anopheles minimus* mosquito. Ph.D. Thesis, Mahidol Univerisity, Thailand, 2009.
27. Gomes, A.M.; Winter, S.; Klein, K.; Turpeinen, M.; Schaeffeler, E.; Schwab, M.; Zanger, U.M. Pharmacogenomics of human liver cytochrome P450 oxidoreductase: Multifactorial analysis and impact on microsomal drug oxidation. *Pharmacogenomics J*. **2009**, *10*, 579–599.

28. Flűck, C.E.; Tajima, T.; Pandey, A.V.; Arlt, W.; Okuhara, K.; Verge, C.F.; Jabs, E.W.; Mendonca, B.B.; Fujieda, K.; Miller, W.L. Mutant P450 oxidoreductase causes disordered steroidogenesis with and without Antley-Bixler syndrome. *Nat. Genet*. **2004**, *36*, 228–230.
29. Pandey, A.V.; Kempna, P.; Hofer, G.; Mullis, P.E.; Flűck, C.E. Modulation of human CYP19A1 activity by mutant NADPH P450 oxidoreducatse. *Mol. Endocrinol*. **2007**, *21*, 2579–2595.
30. Palma, B.B.; Sousa, E.M.S.; Vosmeer, C.R.; Lastdrager, J.; Rueff, J.; Vermeulen, N.P.; Kranendonk, M. Functional characterization of eight human cytochrome P450 1A2 gene variants by recombinant protein expression. *Pharmacogenomics J*. **2010**, *10*, 478–488.
31. Pandey, A.V.; Flűck, C.E.; Mullis, P.E. Altered heme catabolism by heme oxygenase-1 caused by mutations in human NADPH cytochrome P450 reductase. *Biochem. Biophys. Res. Commun*. **2010**, *400*, 374–378.
32. Berman, H.M.; Westbrook, J.; Feng, Z.; Gilliland, G.; Bhat, T.N.; Weissig, H.; Shindyalov, I.N.; Bourne, P.E. The Protein Data Bank. *Nucleic Acids Res.* **2000**, *28*, 235–242.
33. Sali, A.; Blundell, T.L. Comparative protein modelling by satisfaction of spatial restraints. *J. Mol. Biol*. **1993**, 234, 779–815.
34. Shen, M.Y.; Sali, A. Statistical potential for assessment and prediction of protein structures. *Protein Sci.* **2006**, 15, 2507–2524.
35. Samudrala, R.; Moult, J. An all-atom distance-dependent conditional probability discriminatory function for protein structure prediction. *J. Mol. Biol.* **1998**, *275*, 895–916.
36. Case, D.A.; Darden, T.A.; Cheatham, T.E.; Simmerling, C.L.; Wang, J.; Duke, R.E.; Luo, R.; Crowley, M.; Walker, R.C.; Zhang, W.; *et al*. *AMBER 10*; University of California: San Francisco, CA, USA, 2008.
37. Sippl, M.J. Recognition of errors in three-dimensional structures of proteins. *Proteins* **1993**, *17*, 355–362.
38. Wiederstein, M.; Sippl, M.J. ProSA-Web: Interactive web service for the recognition of errors in three-dimensional structures of proteins. *Nucleic Acids Res.* **2007**, *35*, W407–W410.
39. Laskowski, R.A.; MacArthur, M.W.; Moss, D.S.; Thornton, J.M. PROCHECK: A program to check the stereochemical quality of protein structures. *J. Appl. Cryst.* **1993**, *26*, 283–291.
40. Omura, T.; Sato, R. The carbon monoxide-binding pigment of liver microsome. I. Evidence for its hemoprotein nature. *J. Biol. Chem*. **1964**, *239*, 48–54.
41. Aliverti, A.; Curti, B.; Varoni, M.A. Identifying and quantitating FAD and FMN in simple and in iron-sulfur-containing flavoproteins. In *Flavoprotein Protocols*, 2nd ed.; Chapman, S.K., Reid, G.A., Eds.; Humana Press: Totowa, NJ, USA, 1999; pp. 9–23.
42. Voznesensky, A.I.; Schenkman, J.B.; Pernecky, S.J.; Coon, M.J. The NH_2-teminal region of rabbit CYP2E1 is not essential for interaction with NADPH-cytochrome P450 reductase. *Biochem. Biophys. Res. Commun*. **1994**, *203*, 156–161.
43. Lamb, D.C.; Warrilow, A.G.S.; Venkateswarlu, K.; Kelly, D.E.; Kelly, S.L. Activity and kinetic mechanism of native and soluble NADPH-cytochrome P450 reductase. *Biochem. Biophys. Res. Commun.* **2001**, *286*, 48–54.

Supplementary Information

Figure S1. Ramachandran plot of a predicted AnCYPOR structure. The number of residues in the plot starts from Thr64 of the AnCYPOR amino acid sequence.

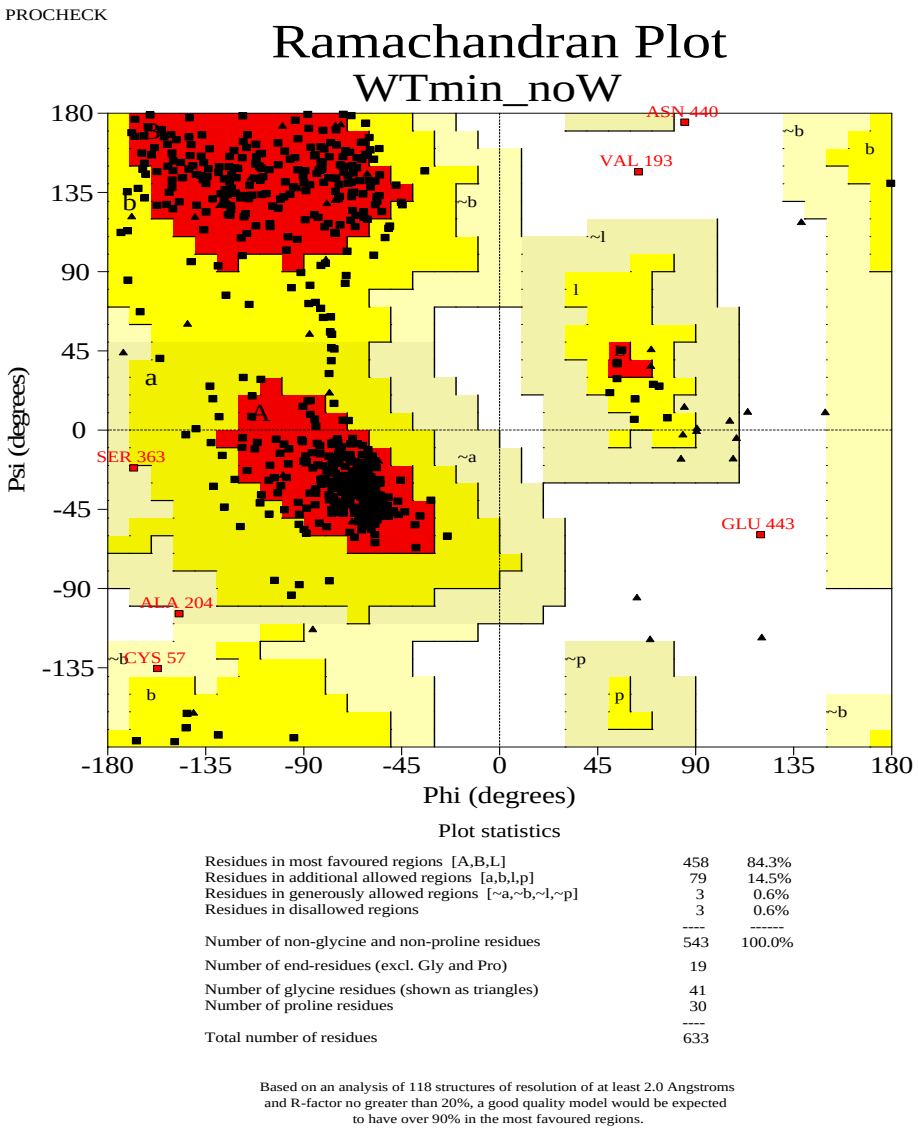

Figure S2. Sequence alignment of NADPH-cytochrome P450 oxidoreductases from various organisms. Amino acid sequences from CYPOR homologs of human (NCBI NP_000932.3), rat (NP_113764.1), fruit fly (*D. melanogaster*, NP_477158.1), and *An. gambiae* (AAO24765.1) were aligned with *An. minimus* CYPOR (ABL75156.1) and displayed by ClustalW. The residue numbers of the sequences are shown. Identical amino acids are represented as dashes. The regions previously reported as the binding sites of the coenzymes are boxed.

```
An. minimus              MDAQAETEMPTGSVS   DEPFLGPLDIILLVCLLAGTAWYLLKGKKKENQASQFKS 54
An. gambiae              ----T---V-A----   ----------V---S------W---------S------- 54
D. melanogaster          -ASEQTIDGAAAIP-GGG------L--VA—AV—IG--A-F-F-RSR---EEP  TR- 55
H. sapiens            MIN-GDSHVDTSS-V-EAVAEEVSLFSMT-M—FSLIVGLLTYWF--FR----EVP      55
R. norvegicus            -GDSH-DTSA-MPEAVAEEVSLFSTT-MV-FSLIVGVLTYWFIFRK---EIP      52
```

Figure S2. *Cont.*

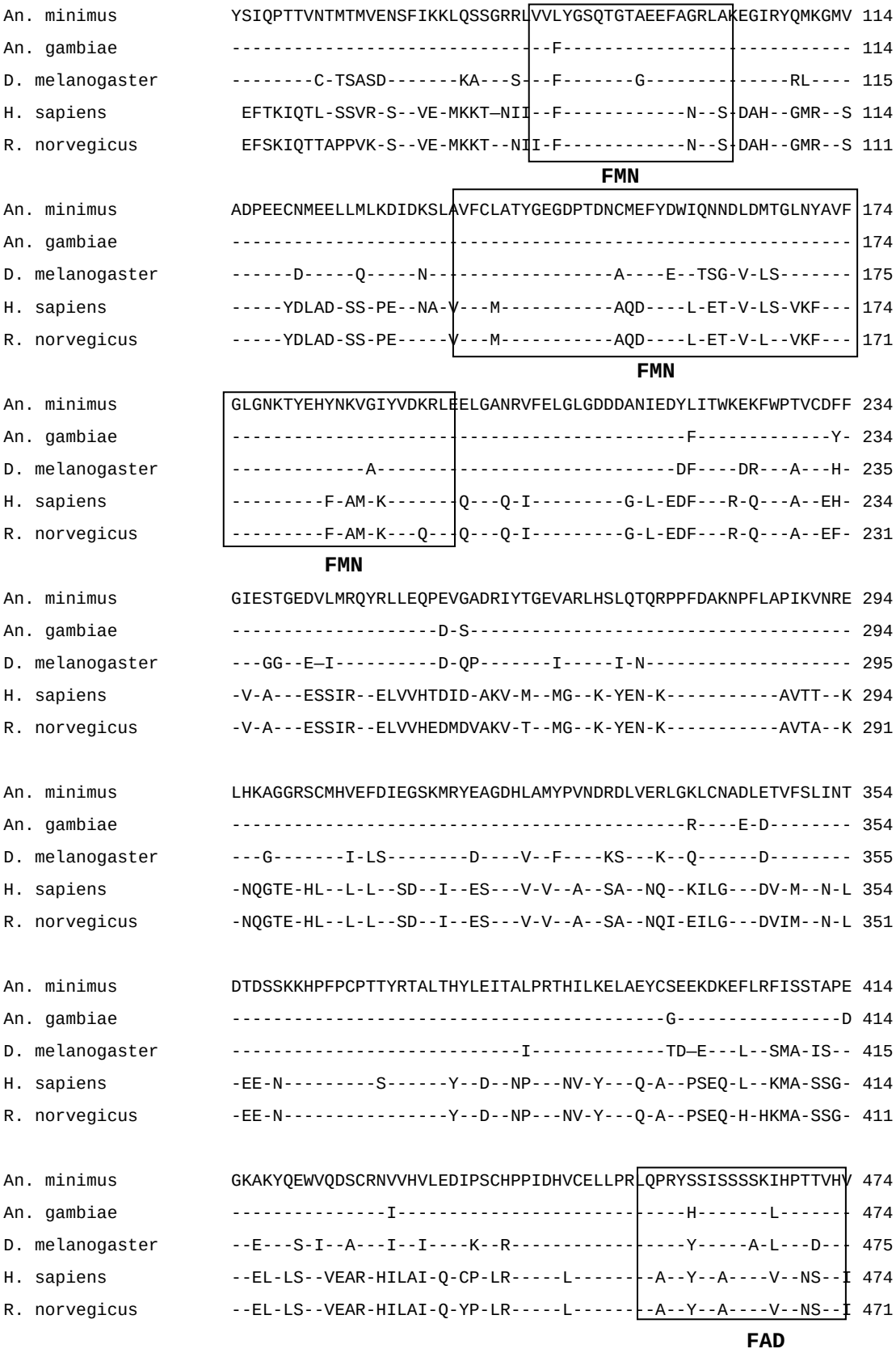

Figure S2. *Cont.*

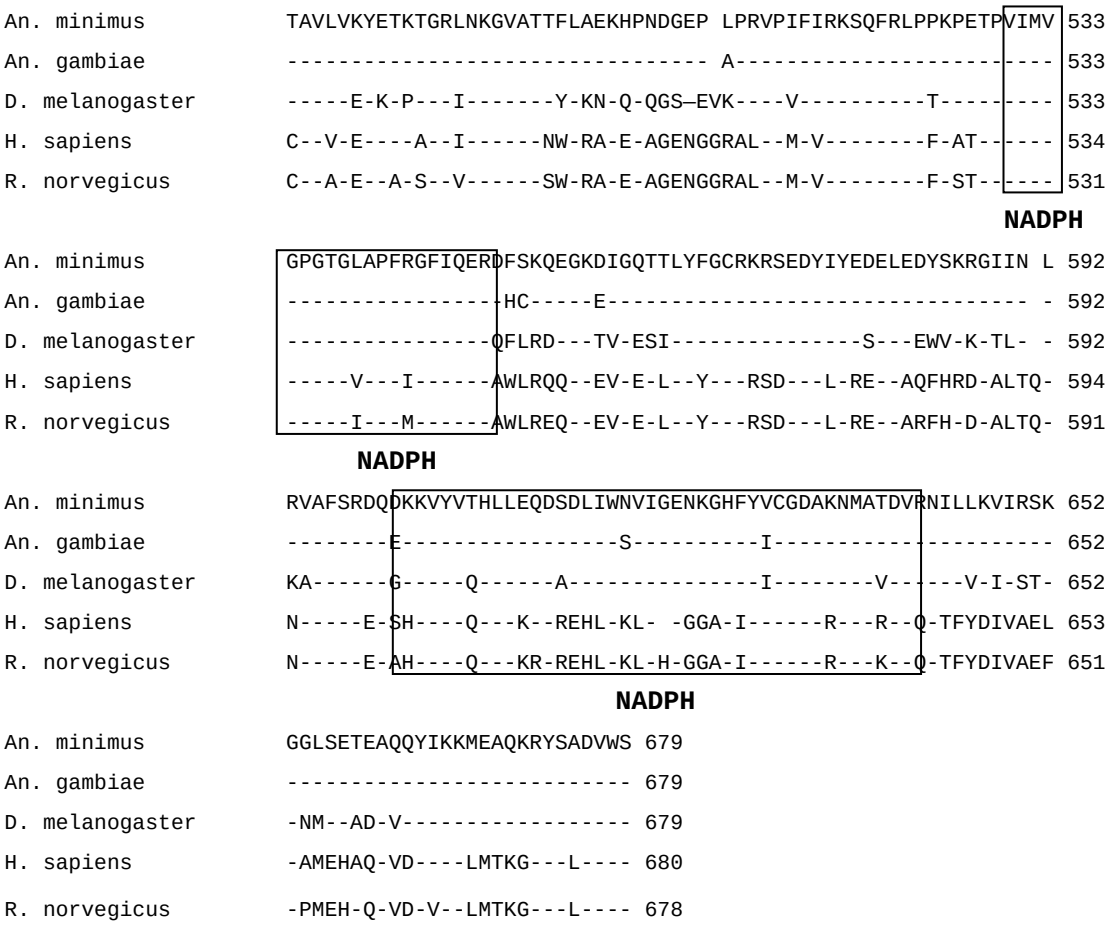

BMC Research Notes

SHORT REPORT Open Access

Homology modeling of mosquito cytochrome P450 enzymes involved in pyrethroid metabolism: insights into differences in substrate selectivity

Panida Lertkiatmongkol[1], Ekachai Jenwitheesuk[2] and Pornpimol Rongnoparut[1*]

Abstract

Background: Cytochrome P450 enzymes (P450s) have been implicated in insecticide resistance. *Anopheles minumus* mosquito P450 isoforms CYP6AA3 and CYP6P7 are capable of metabolizing pyrethroid insecticides, however CYP6P8 lacks activity against this class of compounds.

Findings: Homology models of the three *An. minimus* P450 enzymes were constructed using the multiple template alignment method. The predicted enzyme model structures were compared and used for molecular docking with insecticides and compared with results of *in vitro* enzymatic assays. The three model structures comprise common P450 folds but differences in geometry of their active-site cavities and substrate access channels are prominent. The CYP6AA3 model has a large active site allowing it to accommodate multiple conformations of pyrethroids. The predicted CYP6P7 active site is more constrained and less accessible to binding of pyrethroids. Moreover the predicted hydrophobic interface in the active-site cavities of CYP6AA3 and CYP6P7 may contribute to their substrate selectivity. The absence of CYP6P8 activity toward pyrethroids appears to be due to its small substrate access channel and the presence of R114 and R216 that may prevent access of pyrethroids to the enzyme heme center.

Conclusions: Differences in active site topologies among CYPAA3, CYP6P7, and CYP6P8 enzymes may impact substrate binding and selectivity. Information obtained using homology models has the potential to enhance the understanding of pyrethroid metabolism and detoxification mediated by P450 enzymes.

Findings

Insecticide resistance is a growing problem in the control of mosquito species that serve as vectors in the spread of malaria. One of the major classes of insecticide detoxification enzymes is the heme-containing cytochrome P450 monooxygenases (P450s). These enzymes are responsible for the metabolism of endogenous and exogenous compounds and the expression of several P450s is increased in insecticide resistant insects [1]. P450 enzymes are thought to promote resistance due to their ability to metabolize insecticidal compounds [2-5] however, the link between increased expression of P450s and insecticide resistance has not been clearly established. Structural information on insect P450s together with investigation of their function in insecticide metabolism may help to increase the understanding of their roles in insecticide detoxification and resistance. To date, crystal structures of insect P450s have not been resolved and structural studies relying on *in silico* homology modeling approaches have been used to gain insight into the molecular basis of insecticide binding [2,6,7].

We previously observed elevated expression of P450 isoforms *CYP6AA3*, *CYP6P7*, and *CYP6P8* in a laboratory-selected deltamethrin-resistant *An. minimus* mosquito, a major malaria vector in Thailand, relative to the parent susceptible strain [8]. The increase in CYP6AA3 and CYP6P7 transcripts correlated with increased

* Correspondence: scprn@mahidol.ac.th
[1]Department of Biochemistry, Faculty of Science, Mahidol University, Phayatai, Bangkok 10400, Thailand
Full list of author information is available at the end of the article

deltamethrin resistance, however CYP6P8 did not enhance resistance to deltamethrin. Our results are consistent with the known overlapping metabolic profiles of CYP6AA3 and CYP6P7 against type I and II pyrethroids [5]. The homology between CYP6P7 to CYP6P8 (61% amino acid identity) does not support a role for CYP6P8 in pyrethroid metabolism [5]. In this study, homology modeling of *An. minimus* CYP6AA3, CYP6P7, and CYP6P8 enzymes was conducted and molecular docking was performed with various insecticide compounds. Our analysis was able to predict the molecular basis of P450 activity against pyrethroid compounds and has the potential to assist in the investigation of new compounds that can bypass resistance due to P450 enzymes.

Methods

Amino acid sequences of CYP6AA3 (GenBank: AAN05727.1), CYP6P7 (GenBank: AAR88141.1), and CYP6P8 (GenBank: AAR88142.1) were aligned against protein structures deposited in Brookhaven Protein Data Bank (PDB) [9] using PSI-BLAST. Crystal structures of ligand-free CYP3A4 (PDB: 1TQN) [10], CYP2C8 (PDB: 1PQ2) [11], and CYP2C9 (PDB: 1OG2) [12] were used as templates since their sequences were most similar to the target P450s (14-33% primary sequence identity). The templates structures do not contain residues in N-terminal membrane-binding domain and thus the first 25 residues at the N-termini of the three target P450s were not included in model construction (see Additional files 1 and 2 for sequence alignment and percent sequence identity).

Comparative modeling of CYP6AA3, CYP6P7, and CYP6P8 was performed using a restrained-based approach implemented in MODELLER9v6 [13]. Multiple amino acid sequence alignment of CYP3A4, CYP2C8, and CYP2C9 template structures was performed using the SALIGN module in MODELLER9v6, and subsequently aligned individually with target enzymes. A set of 1000 models for each target enzyme was constructed. The coordinates of heme in the models were obtained from CYP3A4 (1TQN) and positioned in targets as in the 1TQN template. The resulting three-dimensional models of CYP6AA3, CYP6P7, and CYP6P8 were sorted according to scores calculated from discrete optimized protein energy (DOPE) scoring function [14]. The knowledge-based conditional probabilities for the residue specific all-atom probability discriminatory function (RAPDF) in RAMP suite was used to discriminate native structures from incorrectly-folded structures [15]. Refinement of models was performed using Amber10 package [16] to reduce steric clashes among residues. The AMBER ff03 all atom force field was applied. The proteins were solvated in TIP3P water molecules with 12 Å cutoff. Solvent was relaxed while backbone atoms were kept restrained for 100 steps of steepest decent followed by 200 steps of conjugated gradient. Subsequently, all atoms were allowed to move freely without any restraint until energy gradient was < 0.05 kcal/mol. The refined models were determined for distribution of phi and psi angles using ProSAII [17,18] and Procheck [19].

Three-dimensional structures of pyrethroids (permethrin, bioallethrin, cypermethrin, deltamethrin, and λ-cyhalothrin), alongside organophosphate (chlorpyrifos), and carbamate (propoxur) shown in Additional file 3 were obtained from ChemIDplus database http://chem.sis.nlm.nih.gov/chemidplus/ and used in docking of three target models. Partial charges of ligands and proteins were generated using Gasteiger method with the aid of AutoDockTools [20]. Restrained electrostatic potential atomic charge method described by Oda et al. [21] was used to assign high-spin state of five-coordinated ferrous heme complex to simulate substrate binding state. In addition, oxyferryl state was assigned to heme group of target models following Seifert et al. [22] to compare modes of substrate binding at different heme states. A cubic grid having 60 × 60 × 60 grid points per side and spacing of 0.375 Å was set corresponding to substrate recognition sites (SRSs) of each mosquito P450 model following those of CYP2 family proposed by Gotoh [23]. The second grid was positioned onto substrate access channels extending into binding pocket of individual model. Affinity maps of grids were calculated using AutoGrid program. AutoDock 4.0 program [24] was employed to dock ligands into active-site cavity of target models using Lamarckian genetic algorithm, consisting of 200 runs and 270000 generations, with the maximum number of energy evaluation set to 2.5×10^6. Resulting docked conformations within 2.0 Å root mean square deviation (RMSD) tolerance were clustered and analyzed using AutoDockTools. Conformations with the lowest interaction energy and closest interaction to heme iron were selected. Residues showing interaction with docked ligands with less than 1.0 scaling factor of van der Waal radii were determined. Active sites and substrate access channels of enzyme models were calculated using the VOIDOO program [25] with conventional probe radius of 1.4 Å. Molecular visualization was performed on PyMOL 0.93 (Schrödinger, LLC).

Results and Discussion

Homology models of CYP6AA3, CYP6P7 and CYP6P8 were constructed based on crystal structures of CYP3A4, CYP2C8, and CYP2C9 human P450s that are involved in pyrethroid metabolism [26] using the multiple sequence alignment strategy. Candidate predicted models of three mosquito P450s were selected based on

the consensus judgment of DOPE and RAPDF scores that discriminate native structures from those misfolded. CYP6AA3, CYP6P7, and CYP6P8 models have overall ProSA z-scores of -8.24, -7.39, and -8.09, respectively. Ramachandran plot analyses of CYP6AA3, CYP6P7 and CYP6P8 models reveal 1.6%, 1.2% and 0.5% of the residues, respectively, located in disallowed regions. ProSA z-scores and Ramachandran plot analyses indicate that the three models are all of reasonable quality.

Overall conserved P450 folds are found in the three P450 models (Figure 1), such as helices D, E, I, J, K and L, and cysteine-pocket attaching heme. Structural differences between human and mosquito P450s are attributed to SRSs (Figure 2) spanning access channels and active sites of enzymes. Among the mosquito models, differences in substrate access channels and geometry of predicted active sites are apparent. Searching for possible substrate access channels revealed a surface channel opening in CYP6AA3, designated pw2c following a previous report [27], located between B$^{/}$/C loop, C-terminus of G-helix and N-terminus of I-helix. The putative CYP6P7 pw2b access channel is comprised of residues from B/B$^{/}$loop and β1 sheet, while pw2e is observed in BC loop/B$^{/}$helix and N-terminus of I-helix of CYP6P8 model. Differences in the geometry of the predicted active sites is remarkable with CYP6AA3 having an oval shape and a large volume, 245.69 Å^3 in size (Figure 3A), while CYP6P7 has a restrained narrow opening to the heme prosthetic group and is smaller (volume of 135.11 Å^3, Figure 3B). The CYP6P8 active site has the smallest volume, 68.13 Å^3, attributed to protrusion of guanidino group of R216, and R114 is perpendicular to the channel opening (Figure 3C).

We have reported that CYP6AA3 and CYP6P7 can metabolize pyrethroids (permethrin, cypermethrin, and deltamethrin), but lacked activity against bioallethrin (pyrethroid), chlorpyrifos (organophosphate), and propoxur (carbamate) [5]. Notably CYP6AA3 contains λ-cyhalothrin (pyrethroid) degradation activity while CYP6P7 cannot metabolize this compound [5]. To compare the model structures of CYP6AA3, CYP6P7, and CYP6P8 with regard to their metabolic activities, pyrethroids were docked onto these models. In CYP6AA3, the large substrate channel allows passage of multiple conformations of pyrethroids to fit in active-site cavity, while CYP6P7 provides more restricted access of pyrethroids allowing one or two conformations to fit within the cavity (Table 1). Figure 4 shows an example of the predicted binding of deltamethrin, with multiple conformations, to the CYP6AA3 active site (Figure 4A-D) and a single deltamethrin conformation bound to CYP6P7 (Figure 4E). As such, it can be anticipated that

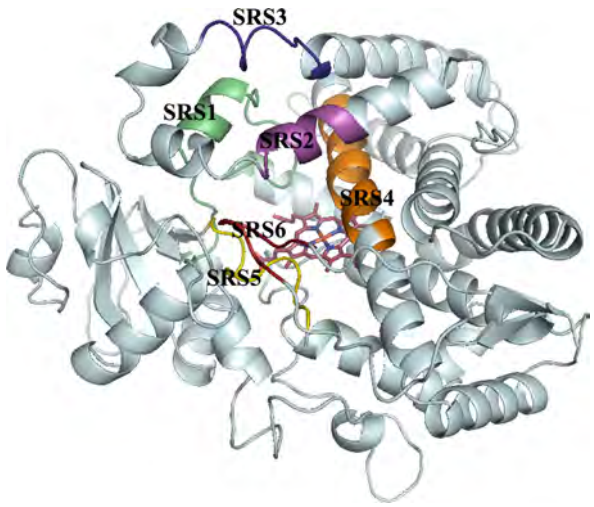

Figure 2 Predicted substrate recognition sites (SRSs). SRSs are colored and designated 1-6 on homology model of CYP6AA3.

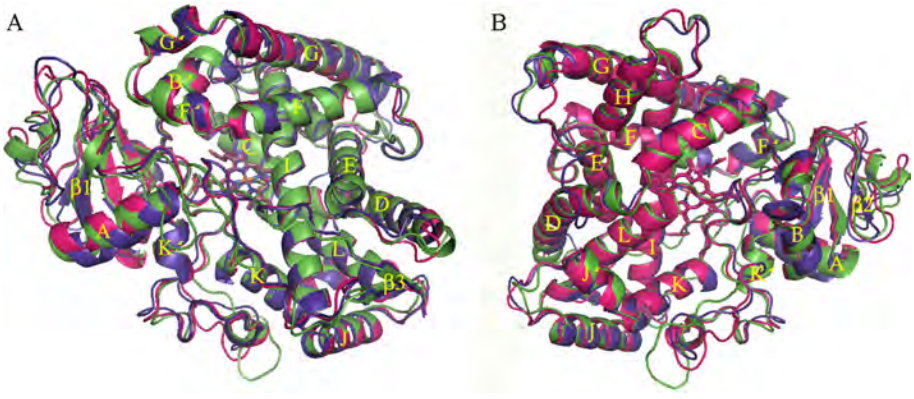

Figure 1 Overall fold and overlay of homology models of CYP6AA3 (green), CYP6P7 (purple), and CYP6P8 (magenta). Model structures are shown in top (A) and back (B) views. Secondary structures of helices A-L and sheets β1-4 are labeled. The heme group in the middle of the structure is represented by stick.

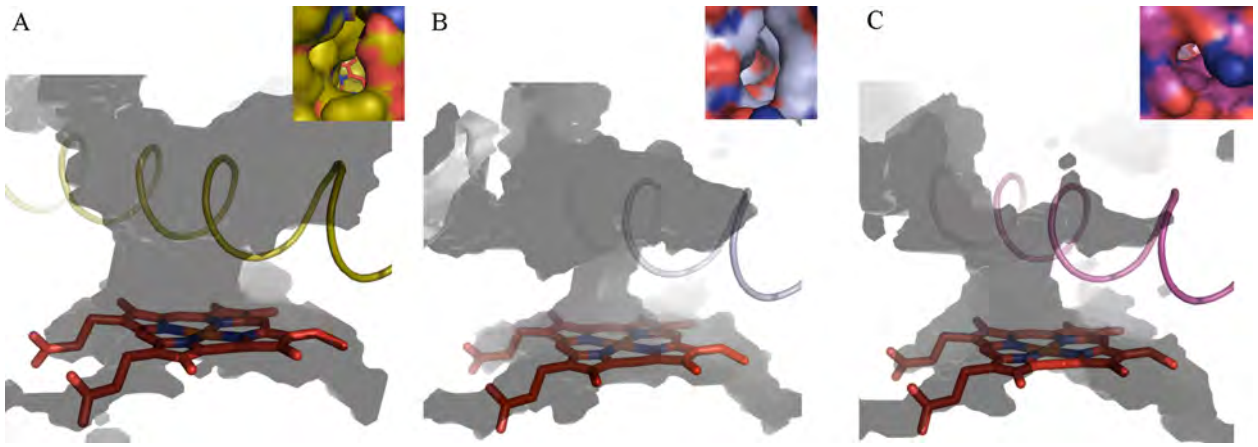

Figure 3 Predicted active sites extending to enzyme surface of CYP6AA3 (A), CYP6P7 (B), and CYP6P8 (C). Active sites were calculated using VOIDOO. I-helices of CYP6AA3 (gold), CYP6P7 (silver), and CYP6P8 (magenta) are depicted in cartoon, spanning across heme. Caption in each figure corresponds to molecular surface view of each access channel. CYP6AA3 and CYP6P7 both display an oval shape of access opening, while CYP6P8 has a relatively small circular pore. The R114 guanidino group is shown projected horizontally to the opening of the CYP6P8 channel. Carbon atoms in caption are colored separately on each structure, oxygen and nitrogen atoms are shown in red and blue, respectively. The heme group in the middle of the structure is represented by red stick.

CYP6AA3-mediated pyrethroid degradation has the potential to generate multiple metabolites according to the position of pyrethroids (geminal dimethyl group, 5- and 4′-phenoxybenzyl carbons, and alpha carbon at cyano group) attacked by the enzyme. This prediction is in agreement with our results showing multiple products from CYP6AA3-mediated deltamethrin degradation [28]. Multiple products have also been detected from pyrethroid metabolism mediated by insect and rodent P450s [4,29-31]. To test whether the binding of insecticides would be altered in different heme states of P450s, the oxyferryl state was simulated in CYP6AA3 and CYP6P7 and docked with deltamethrin. Our results indicate that the docked pyrethroid conformations on the iron-oxo enzyme complex (Additional file 4) are similar to those obtained from high-spin ferrous state (Figure 4), emphasizing the significance of enzyme active-site geometry to influence substrate selectivity and the conformation of substrate binding regardless of the heme state in the enzymes.

Compared to CYP6AA3, CYP6P7 possesses a narrow channel opening to heme iron, resulting in structural constraint toward pyrethroids and limited access to λ-cyhalothrin. The phenoxybenzyl moiety of pyrethroids is predicted to be a favorable attack site for CYP6P7 (Table 1). Moreover the bulky trifluoromethyl group (Additional file 3) causes the 4′-phenoxybenzyl carbon of λ-cyhalothrin moving away from the CYP6P7 heme (4.17 Å) compared to that of cypermethrin (3.31 Å, Table 1), and thus the trifluoromethyl group may be responsible for absence of detectable CYP6P7 activity against λ-cyhalothrin [5]. Analogous findings have been shown for a CYP6B8v1 predicted model that contains a narrow active-site cavity, leading to its ability to metabolize only small flexible molecules but not large rigid molecules [7].

Residues in the CYP6AA3 cavity that interact with pyrethroids in our docking experiments (Table 1) are generally non-polar, implying that binding may occur via hydrophobic interactions with non-polar pyrethroids that have octanol-water partition coefficient (log *P*) values ranging from 6.2-6.8. Since bioallethrin, chlorpyrifos, and propoxur (values of 4.78, 4.96, and 1.52 respectively) are more polar, they would be expected to have less favorable interactions with the active sites of CYP6AA3 and CYP6P7 resulting in a longer distance between these molecules and the heme iron (unpublished data). As a result both CYP6AA3 and CYP6P7 are predicted to be incapable of metabolizing bioallethrin, chlorpyrifos, and propoxur, consistent with our previous results [5]. Binding of thiodicarb (carbamate, log *P* of 1.62), temephos, and fenitrothion (organophosphates, log *P* of 5.96 and 3.3, respectively) to both of these enzymes is also predicted to be unfavorable (unpublished data).

In the CYP6P8 model, the small access channel together with R114 and R216 are predicted to obstruct pyrethroid entry into the active-site cavity (Figure 5), resulting in the absence of CYP6P8 activity toward pyrethroid [5]. Equivalent R114 and R216 residues are not found in CYP6AA3 and CYP6P7 active sites and no such hindrance of pyrethroid access is predicted. The presence of the positively charged guanidino group of R114, speculated to form hydrogen bond with the oxygen on ester of pyrethroid, and R216 lying in narrow path (6.75 Å-width

Table 1 Docking results of CYP6AA3 and CYP6P7 homology models

Enzymes and insecticides[a]	Binding sites[b]	Estimate free energy (kcal/mol)	Distance from heme iron (Å)[c]	Predicted contact residues[d]
CYP6AA3				
Permethrin	Gem	-7.31	3.26	(P217)[2], R220, (F309, A310, T314)[4], T317, (P375, V376)[5], (M491)[6]
	C5-PB	-8.18	3.03	(H120)[1], (V306, F309, A310, E313, T314)[4], (P375)[5], (L492)[6]
	C4′-PB	-7.86	3.97	(E112, P116, H120, F122)[1], (F305, F309, A310, T314)[4], (V376, I380)[5]
Cypermethrin	Gem	-9.10	3.01	(E112, P116, H120)[1], (R220)[2], (F309, A310, T314)[4], (I380, R381)[5]
	C5-PB	-9.6	3.14	(F122)[1], (A310, T314)[4], (P375, V376, P377, R381)[5], (M491, L492)[6]
	C4′-PB	-9.64	4.38	(E112, H120, F122)[1], (V306, F309, A310, T314)[4], (V376, I380, R381, V382)[5]
	CN	-9.41	4.09	(H120, F122)[1], (V306, F309, A310, T314)[4], (P375, V376)[5], (L492)[6]
Deltamethrin	Gem	-8.50	3.45	(E112, H120, F122)[1], (A310, E313, T314)[4], (P375, V376, I380, R381)[5], (M491)[6]
	C5-PB	-8.66	3.31	(H120, F122)[1], (F309, A310, T314)[4], (V376, Q378, I380, R381)[5]
	C4′-PB	-8.52	3.49	(F122)[1], (A310, T314)[4], (P375, V376, I380, R381, V382)[5], (M491, L492)[6]
	CN	-8.74	4.35	(H120, F122)[1], (F309, A310, T314)[4], (P375, V376, P377, Q378, I380, R381)[5]
λ-cyhalothrin	Gem	-7.90	3.31	(H120, F122)[1], (P217, N221)[2], (F309, A310, T314)[4], (P375, V376)[5], (M491, L492)[6]
	C5-PB	-6.94	3.82	(H120, F122)[1], (T314)[4], (V376, R381)[5]
	C4′-PB	-7.65	3.02	(Y109, E112)[1], (R220)[2], (F309, A310, T314)[4], (P375, V376, I380, R381)[5]
	CN	-7.89	3.51	(H120, F122)[1], (V306, F309, A310, E313, T314)[4], T317, (P375, V376, I380)[5], (L492)[6]
CYP6P7				
Permethrin	C5-PB	-6.45	3.35	(L313, A314, E317, T318)[4], (L380, E381, S382, I383, R385)[5], (F494, I495)[6]
Cypermethrin	Gem	-8.92	3.52	(F110, F123)[1], (T220)[2], (L313, A314, T318)[4], (E381, R385)[5], (F494)[6]
	C4′-PB	-9.50	3.31	(L313, A314, E317, T318)[4], (L380, E381, S382, I383, R385)[5], (F494, I495)[6]
Deltamethrin	C4′-PB	-8.17	3.53	(F123)[1], (T220)[2], (A314, T318)[4], (L380, E381, R385)[5], (F494, I495, L496)[6]
λ-cyhalothrin	C4′-PB	-8.52	4.17	(E317, T318)[4], T321, (L380, E381, S382, R385)[5], (I495, L496)[6]

[a]Chemical structures of insecticides are shown in Additional file 3.

[b]Predicted metabolic sites are indicated as following: Gem, geminal-dimethyl group in acid moiety; C5-PB, carbon 5 of phenoxybenzyl group in alcohol moiety; C4′-PB, carbon 4′of phenoxybenzyl group in alcohol moiety; and CN, cyano group. [c]Distances between the heme iron and putative metabolic sites are measured. [d]Residues are grouped based on substrate recognition sites (SRSs) in parentheses. Superscript represents order of SRS.

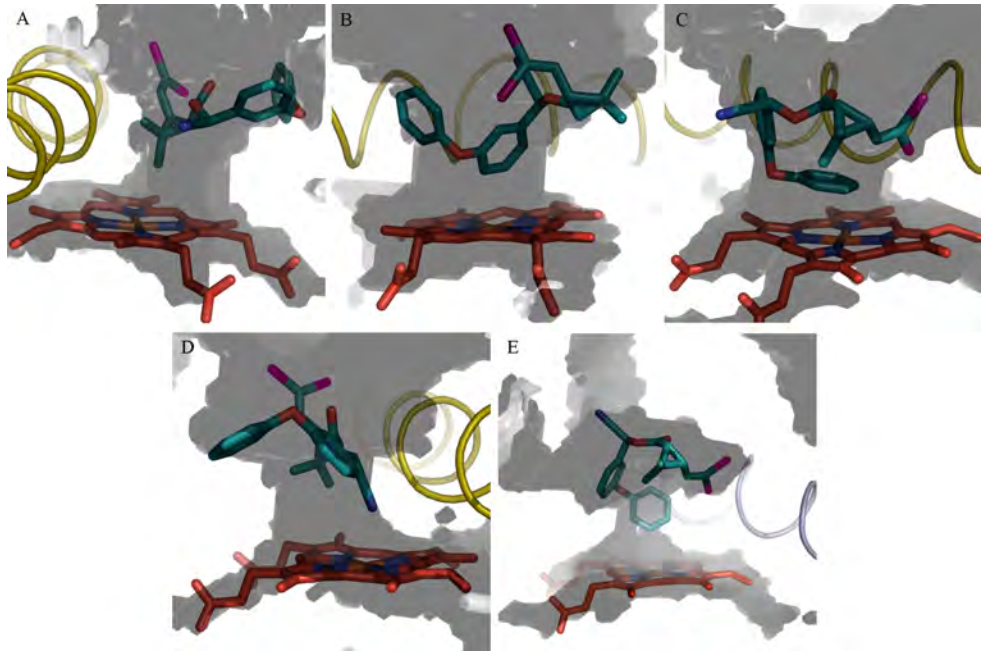

Figure 4 Deltamethrin binding modes in active sites of CYP6AA3 (A-D) and CYP6P7 (E). CYP6AA3 exhibited 4 binding modes of deltamethrin positioning close to heme iron: geminal-dimethyl group (A), 5-phenoxybenzyl carbon (B), 4′-phenoxybenzyl carbon (C), and cyano group (D). Single binding mode of deltamethrin in CYP6P7 was obtained with 4′-phenoxybenzyl carbon as a predicted hydroxylation site (E). Same color is applied for heme and all elements as in Figure 3.

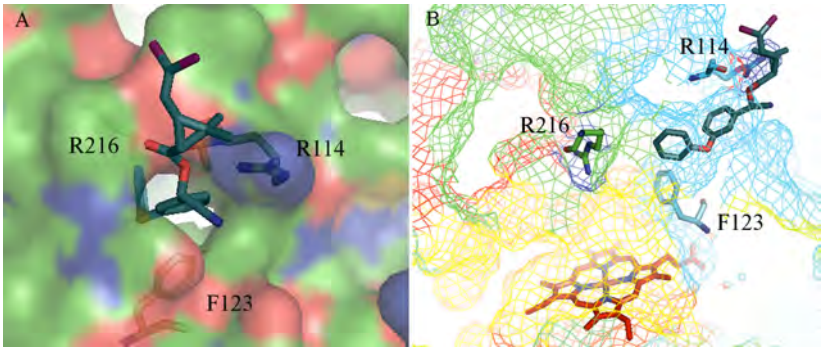

Figure 5 Obstruction of deltamethrin entry into CYP6P8 active site. (A) Predicted hydrogen bond formation between oxygen on ester of deltamethrin and guanidino group of R114. (B) Presence of R216 located across F123 in narrow active site channel. CYP6P8 is in rainbow mesh, ranging from blue (N-terminal) to red (C-terminal). Deltamethrin is represented by teal stick.

across F123) are predicted to impede pyrethroids from passing through the CYP6P8 channel opening (Figure 5B). A similar situation has been observed in protein kinase C, where mutation of amino acids to arginine residues in the C1 domain binding cleft can significantly reduce interaction and membrane translocation of phorbol 12,13-dibutyrate [32]. It is possible that the topology and residues within the CYP6P8 active site might not favorably allow entry of arene compounds such as pyrethroids to the heme center, but may allow entry of small hydrocarbon compounds. Further investigation of CYP6P8-mediated metabolism may reveal its preferred substrates.

Conclusion

The model structures of CYP6AA3, CYP6P7, and CYP6P8 generated in this study have allowed us to better understand the different substrate preferences between these P450 enzymes and the predictions based on our docking studies are consistent with experimental results of pyrethroid metabolism mediated by these three enzymes. Variations in the predicted substrate channels and geometry of active sites appear to be responsible for their differences in binding to pyrethroids. Our findings indicate that differences in metabolic activities among P450 enzymes in insects can be attributed to structural differences that allows for selectivity in their activities against insecticides. These models have the potential to be used in the investigation of candidate P450 inhibitors or in the analysis of the binding and metabolism of insecticide compounds that have potential for use in the control of the mosquito vector.

Additional material

Additional file 1: Figure S1. Multiple sequence alignment of templates and target P450s. Template sequences of CYP3A4 (1TQN chain A), CYP2C9 (1OG2 chain A) and CYP2C8 (1PQN chain A) are aligned against target sequences CYP6AA3, CYP6P7 and CYP6P8. The first 25 residues on N-termini of target sequences are underlined and bolded. Residues mostly identical among templates and targets are marked yellow. Identical residues among all sequences are indicated by asterisks and yellow mark. Residues of target identical to CYP3A4 template are marked grey, whereas target residues identical to CYP2Cs are marked green. Predicted contact residues between targets and ligands are marked blue. Protruding arginine at the entry of substrate access channel in CYP6P8 model is highlighted red and arginine and phenylalanine in the channel are in violet. CYP6AA3 primary sequence comprises 505 residues, CYP6P7 509 residues and CYP6P8 506 residues.

Additional file 2: Table. Percent amino acid sequence similarity between crystallographic templates and target sequences.

Additional file 3: Figure S2. Insecticides used in docking study. Pyrethroids shown are cypermethrin (A), permethrin (B), deltamethrin (C) and λ-cyhalothrin (D). Non-substrate insecticides docked in this study are: propoxur, a type of carbamate insecticide (E); chlorpyrifos, a type of organophosphate insecticide (F); and bioallethrin pyrethroid insecticide (G). Geminal-dimethyl group, 5- and 4′-phenoxybenzyl carbons are indicated by arrows on cypermethrin.

Additional file 4: Figure S3. Docked deltamethrin conformations in oxyferryl state of CYP6AA3 (A-D) and CYP6P7 (E). Predicted metabolic sites are at geminal dimethyl group (A), 5-phenoxybenzyl carbon (B), 4′-phenoxybenzyl carbon (C), cyano group (D), and 4′-phenoxybenzyl carbon in CYP6P7 (E). Helices I of CYP6AA3 and CYP6P7 are shown in gold and silver cartoons, respectively. Oxyferryl heme is represented by grey stick, while deltamethrin is illustrated in green stick. Iron, oxygen, and nitrogen are colored orange, red, and blue, respectively.

Acknowledgements

This work was supported by Thailand Research Fund (TRF) and Mahidol University (Grant number BRG5380002). We thank Dr. Laran T. Jensen for critical reading of this manuscript. All computations were performed on Linux high performance clusters by courtesy of Dr. Sissades Tongsima and technical support by Dr. Anunchai Assawamakin, Biostatistics and Informatics laboratory, Genome Institute, NSTDA Thailand.

Author details

[1]Department of Biochemistry, Faculty of Science, Mahidol University, Phayatai, Bangkok 10400, Thailand. [2]Genome Institute, National Science and Technology Development Agency, Thailand Science Park, Pathumthani 12120, Thailand.

Authors' contributions

PL participated in design of the study, model building and data analysis, and drafting of the manuscript. EJ participated in design and data analysis of the

study. PR participated in design and data analysis of the study, drafting and revising of the manuscript. All authors read and approved the final manuscript.

Competing interests
The authors declare that they have no competing interests.

Received: 13 April 2011 Accepted: 6 September 2011
Published: 6 September 2011

References

1. Feyereisen R: **Insect P450 enzymes.** *Annu Rev Entomol* 1999, **44**:507-533.
2. Karunker I, Morou E, Nikou D, Nauen R, Sertchook R, Stevenson BJ, Paine MJ, Morin S, Vontas J: **Structural model and functional characterization of the *Bemisia tabaci* CYP6CM1vQ, a cytochrome P450 associated with high levels of imidacloprid resistance.** *Insect Biochem Mol Biol* 2009, **39**:697-706.
3. Muller P, Warr E, Stevenson BJ, Pignatelli PM, Morgan JC, Steven A, Yawson AE, Mitchell SN, Ranson H, Hemingway J, Paine MJ, Donnelly MJ: **Field-caught permethrin-resistant *Anopheles gambiae* overexpress CYP6P3, a P450 that metabolises pyrethroids.** *PLoS Genet* 2008, **4**: e1000286.
4. Wheelock G, Scott J: **The role of cytochrome P450lpr in deltamethrin metabolism by pyrethroid-resistant and susceptible strains of house flies.** *Pestic Biochem Physiol* 1992, **43**:67-77.
5. Duangkaew P, Pethuan S, Kaewpa D, Boonsuepsakul S, Sarapusit S, Rongnoparut P: **Characterization of mosquito CYP6P7 and CYP6AA3: differences in substrate preference and kinetic properties.** *Arch Insect Biochem Physiol* 2011, **76**:236-248.
6. Jones RT, Bakker SE, Stone D, Shuttleworth SN, Boundy S, McCart C, Daborn PJ, ffrench-Constant RH, van den Elsen JM: **Homology modelling of *Drosophila* cytochrome P450 enzymes associated with insecticide resistance.** *Pest Manag Sci* 2010, **66**:1106-1115.
7. Rupasinghe SG, Wen Z, Chiu TL, Schuler MA: ***Helicoverpa zea* CYP6B8 and CYP321A1: different molecular solutions to the problem of metabolizing plant toxins and insecticides.** *Protein Eng Des Sel* 2007, **20**:615-624.
8. Rodpradit P, Boonsuepsakul S, Chareonviriyaphap T, Bangs MJ, Rongnoparut P: **Cytochrome P450 genes: molecular cloning and overexpression in a pyrethroid-resistant strain of *Anopheles minimus* mosquito.** *J Am Mosq Control Assoc* 2005, **21**:71-79.
9. Berman HM, Westbrook J, Feng Z, Gilliland G, Bhat TN, Weissig H, Shindyalov IN, Bourne PE: **The Protein Data Bank.** *Nucleic Acids Res* 2000, **28**:235-242.
10. Yano JK, Wester MR, Schoch GA, Griffin KJ, Stout CD, Johnson EF: **The structure of human microsomal cytochrome P450 3A4 determined by X-ray crystallography to 2.05-A resolution.** *J Biol Chem* 2004, **279**:38091-38094.
11. Schoch GA, Yano JK, Wester MR, Griffin KJ, Stout CD, Johnson EF: **Structure of human microsomal cytochrome P450 2C8. Evidence for a peripheral fatty acid binding site.** *J Biol Chem* 2004, **279**:9497-9503.
12. Williams PA, Cosme J, Ward A, Angove HC, Matak Vinkovic D, Jhoti H: **Crystal structure of human cytochrome P450 2C9 with bound warfarin.** *Nature* 2003, **424**:464-468.
13. Sali A, Blundell TL: **Comparative protein modelling by satisfaction of spatial restraints.** *J Mol Biol* 1993, **234**:779-815.
14. Shen MY, Sali A: **Statistical potential for assessment and prediction of protein structures.** *Protein Sci* 2006, **15**:2507-2524.
15. Samudrala R, Moult J: **An all-atom distance-dependent conditional probability discriminatory function for protein structure prediction.** *J Mol Biol* 1998, **275**:895-916.
16. Case DA, Darden TA, Cheatham TE, Simmerling CL, Wang J, Duke RE, Luo R, Crowley M, Walker RC, Zhang W, Merz KM, Wang B, Hayik S, Roitberg A, Seabra G, Kolossváry I, Wong KF, Paesani F, Vanicek J, Wu X, Brozell SR, Steinbrecher T, Gohlke H, Yang L, Tan C, Mongan J, Hornak V, Cui G, Mathews DH, Seetin MG, Sagui C, Babin V, Kollman PA: **AMBER 10.** University of California, San Francisco; 2008.
17. Sippl MJ: **Recognition of errors in three-dimensional structures of proteins.** *Proteins* 1993, **17**:355-362.
18. Wiederstein M, Sippl MJ: **ProSA-web: interactive web service for the recognition of errors in three-dimensional structures of proteins.** *Nucleic Acids Res* 2007, **35**:W407-410.
19. Laskowski RA, MacArthur MW, Moss DS, Thornton JM: **PROCHECK: a program to check the stereochemical quality of protein structures.** *J Appl Cryst* 1993, **26**:283-291.
20. Morris M, Goodsell S, Halliday S, Huey R, Hart E, Belew K, Olson J: **Automated docking using a Lamarckian genetic algorithm and an empirical binding free energy function.** *J Comput Chem* 1998, **19**:1639-1662.
21. Oda A, Yamaotsu N, Hirono S: **New AMBER force field parameters of heme iron for cytochrome P450s determined by quantum chemical calculations of simplified models.** *J Comput Chem* 2005, **26**:818-826.
22. Seifert A, Tatzel S, Schmid RD, Pleiss J: **Multiple molecular dynamics simulations of human p450 monooxygenase CYP2C9: the molecular basis of substrate binding and regioselectivity toward warfarin.** *Proteins* 2006, **64**:147-155.
23. Gotoh O: **Substrate recognition sites in cytochrome P450 family 2 (CYP2) proteins inferred from comparative analyses of amino acid and coding nucleotide sequences.** *J Biol Chem* 1992, **267**:83-90.
24. Huey R, Morris GM, Olson AJ, Goodsell DS: **A semiempirical free energy force field with charge-based desolvation.** *J Comput Chem* 2007, **28**:1145-1152.
25. Kleywegt GJ, Jones TA: **Detection, delineation, measurement and display of cavities in macromolecular structures.** *Acta Crystallogr D Biol Crystallogr* 1994, **50**:178-185.
26. Scollon EJ, Starr JM, Godin SJ, DeVito MJ, Hughes MF: ***In vitro* metabolism of pyrethroid pesticides by rat and human hepatic microsomes and cytochrome P450 isoforms.** *Drug Metab Dispos* 2009, **37**:221-228.
27. Wade RC, Winn PJ, Schlichting I, Sudarko O: **A survey of active site access channels in cytochromes P450.** *J Inorg Biochem* 2004, **98**:1175-1182.
28. Boonsuepsakul S, Luepromchai E, Rongnoparut P: **Characterization of *Anopheles minimus* CYP6AA3 expressed in a recombinant baculovirus system.** *Arch Insect Biochem Physiol* 2008, **69**:13-21.
29. Casida JE: **Michael Elliott's billion dollar crystals and other discoveries in insecticide chemistry.** *Pest Manag Sci* 2010, **66**:1163-1170.
30. Shono T, Ohsawa K, Casida JE: **Metabolism of *trans*- and *cis*-permethrin, *trans*- and *cis*-cypermethrin, and decamethrin by microsomal enzymes.** *J Agric Food Chem* 1979, **27**:316-325.
31. Shono T, Unai T, Casida J: **Metabolism of permethrin isomers in American cockroach adults, house fly adults, and cabbage looper larvae.** *Pestic Biochem Physiol* 1978, **9**:96-106.
32. Pu Y, Peach ML, Garfield SH, Wincovitch S, Marquez VE, Blumberg PM: **Effects on ligand interaction and membrane translocation of the positively charged arginine residues situated along the c1 domain binding cleft in the atypical protein kinase C isoforms.** *J Biol Chem* 2006, **281**:33773-33788.

doi:10.1186/1756-0500-4-321
Cite this article as: Lertkiatmongkol *et al.*: Homology modeling of mosquito cytochrome P450 enzymes involved in pyrethroid metabolism: insights into differences in substrate selectivity. *BMC Research Notes* 2011 **4**:321.